12-1997

An Analytical Method to Calculate Activity from Measurements Affected by Coincidence Summing

Anthony P. Popovich

Anthony P. Popovich, B.S., M.P.A.
Captain, USAF

December 1997

DEPARTMENT OF THE AIR FORCE
AIR UNIVERSITY
AIR FORCE INSTITUTE OF TECHNOLOGY

Wright-Patterson Air Force Base, Ohio

AFIT/GAP/ENP/97D-09

AN ANALYTICAL METHOD TO CALCULATE ACTIVITY FROM MEASUREMENTS AFFECTED BY COINCIDENCE SUMMING

THESIS

Presented to the Faculty of the School of Engineering
of the Air Force Institute of Technology
Air University in Partial Fulfillment of the
Requirements for the Degree of
Master of Science

Anthony P. Popovich, B.S., M.P.A.
Captain, USAF

December 1997

AFIT/GAP/ENP/97D-09

AN ANALYTICAL METHOD TO CALCULATE ACTIVITY FROM MEASUREMENTS AFFECTED BY COINCIDENCE SUMMING

THESIS

Anthony P. Popovich, Captain, USAF

AFIT/GAP/ENP/97D-09

AFIT/GAP/ENP/97D-09

AN ANALYTICAL METHOD TO CALCULATE ACTIVITY FROM MEASUREMENTS AFFECTED BY COINCIDENCE SUMMING

Anthony P. Popovich, B.S., M.P.A.
Captain, USAF

Approved:

Maj Jeffrey B. Martin, Chairman	date
Dr. Kirk A. Mathews, Committee Member	date
Dr. George John, Committee Member	date

Acknowledgments

I would like to take the opportunity here to tell all those who have helped and guided me in making this thesis thank you very much. To Maj. Jeff Martin, my thesis advisor, I truly appreciated your assistance and guidance through the whole process and, in particular, deciphering the esoteric articles on angular correlation. I thank Dr. Kirk Mathews very much for the gift of integral transformations making those Legendre polynomials something my computer could execute under a day. I also thank him and Dr. George John for asking very good questions and challenging me to understand what all the terms in Andreev's formula mean.

I appreciate and thank Capt. Nathan Wimer and Capt. Martin Keillor, my sponsors, for providing me this topic, for diligently responding to my numerous requests for information, and for funding my visit to their laboratory and my computer acquisition. I have really enjoyed working on this topic and look forward to working with AFTAC again.

I also thank Dr. Markku Koskelo, Senior Scientist at Canberra Industries, Inc., for coming to AFIT, setting up, and training me to use Canberra's prototype coincidence correction software. I am astonished and quite pleased of the timing of our efforts to solve the problem at hand and have validated solutions to give to a mutual customer.

Finally, I thank Sara, my wife, and Laura, my daughter, for letting me study in peace and for enduring the longest 18 months of our lives. I truly appreciate and bless them for their patience and consideration.

Anthony P. Popovich

Table of Contents

Acknowledgments ii

List of Figures vi

List of Tables vii

List of Symbols viii

Abstract ix

1. Introduction 1

    1.1 Customer Background 1
    1.2 Problem Background 3
    1.3 Problem and Scope 6
    1.4 Outline 8
    1.5 Benefits of Research 9

2. Nuclear Decay Phenomena 10

    2.1 Gamma-Ray Cascades 10
    2.2 Angular Correlation of Radiation 13
    2.3 Effect of Angular Correlation 22

3. An Analytical Coincidence Correction Method 34

    3.1 Determination of Summing Events from Cascades . 34
    3.2 Modification of Method for Special Cases . . . 52
    3.3 Application of Method for Mo-99 and Cs-136 . . 54
    3.4 Error Analysis of Mo-99 Results 62

4. AFTAC Experimental Data and Analysis 67

    4.1 Comparison of Mo-99 and Cs-136 Data 67
    4.2 Planchet Effect 70

5. Conclusions 73

Appendix A: Beta Particle Range. 76

Appendix B: Angular Correlation Formula 79

Appendix C: Analytical Method Code for Mo-99 86

Appendix D: Analytical Method Code for Cs-136 152

Appendix E: AFIT Experimental Data 180

Appendix F: Bibliography 183

Appendix G: Vita 185

List of Figures

Figure 1.1 Planchet Schematic 2

Figure 1.2 Detector #120 Schematic 2

Figure 2.1 Simplified Mo-99 Decay Scheme 12

Figure 2.2 Simplified Cs-136 Decay Scheme 12

Figure 2.3 Reference Angles for Correlation 16

Figure 2.4 Point Source-Solid Crystal 25

Figure 2.5 Disk Source-Solid Crystal 27

Figure 2.6 Point Source-Closed-end Coaxial Crystal . . . 28

Figure 3.1 Hypothetical Decay Scheme 35

Figure 3.2 Modified Na-22 Decay Scheme 54

List of Tables

Table 2.1 Approximation Check with Total Efficiencies for the Closed-end, Coaxial Detector with Point Source 31

Table 2.2 Correlation Coefficients for Some Mo-99 Chemical Compounds 32

Table 2.3 Calculated Normalized Angular Correlation for Mo-99 Source 10 cm above Detector 34

Table 2.4 Calculated Normalized Angular Correlation for Mo-99 Source 0 cm above Detector 34

Table 3.1 Mo-99 Nuclear Data 55

Table 3.2 Cs-136 Nuclear Data 56

Table 3.3 Detector #120 Calculated Efficiencies with Mo-99 Source at 0 cm 59

Table 3.4 Detector #120 Calculated Efficiencies with Cs-136 Source at 0 cm 60

Table 3.5 Detector #120 Calculated Probabilities of Recording a Transition per Decay of Mo-99 at 0 cm 60

Table 3.6 Detector #120 Calculated Probabilities of Recording a Transition per Decay of Cs-136 at 0 cm 61

Table 3.7 Error of Calculated Probabilities of Recording a Transition per Decay of Mo-99 at 0 cm using Detector #120 66

Table 4.1 Probabilities of Detecting Nuclear Transitions of Mo-99 Source at 0 cm 68

Table 4.2 Detector #120 Adjusted Face Peak Efficiencies with Mo-99 Source 69

Table 4.3 Detector #120 Adjusted Face Peak Efficiencies with Cs-136 Source 69

Table 4.4 Detector #120 Correction Factor with Mo-99 Source at 0 cm 70

Table E.1 AFIT Experimental Data 181

List of Symbols

S_{ik} is the probability of recording a level i to k transition.

B_i is the probability of a nucleus decaying to level i given that there are no gamma-rays detected to cause a summing-out event.

A_{ik} is the probability of the nucleus decaying from level i to k with all the gamma-rays depositing their full energy in a detector.

M_k is the probability of the nucleus decaying from level k to some lower level given that there are no gamma-rays detected to cause a summing-out event.

β_i is the probability that a parent nucleus emits a beta particle in transforming to level i of the daughter nucleus.

χ_{ik} is the probability that a nucleus de-excites from level i to k.

α_{ik} is the number of internal conversion electrons emitted per gamma-ray in the level i to k de-excitation of a nucleus.

ε_{ik}^{p} is the peak efficiency of a detector for a gamma-ray of energy E_{ik}.

ε_{ik}^{t} is the total efficiency of a detector for a gamma-ray of energy E_{ik}.

$\overline{W}$ is the normalized angular correlation factor

Abstract

An analytical method is developed and applied to find the activities of two radioisotopes based on measurements influenced by true coincidence summing. The method incorporates the solid angle subtended by the detector, the macroscopic cross sections of the materials present, the absolute peak and total efficiencies of the detector, and the modes and probabilities of decay of the radioisotope. With this information, the method corrects for both summing-in and summing-out events. Summing events affect peak counts and cause the calculated activity to differ from the true activity.

Thin disk sources of Mo-99 and Cs-136 on the face of a closed-end, coaxial high purity germanium detector have been studied. For Mo-99, the analytical method shows there is a 29% reduction in the 740 keV peak counts due to summing events. This factor adjusts the no-coincidence-assumed activity to within 4.0% of the correct value. As for Cs-136, the analytical method shows a 41% reduction in the 1048 keV peak counts. This factor corrects the simplistic activity to within 0.5% of the correct value. Hence, the results indicate that coincidence summing is the primary cause of activity discrepancies for the given configuration.

AN ANALYTICAL METHOD TO CALCULATE ACTIVITY FROM MEASUREMENTS AFFECTED BY COINCIDENCE SUMMING

1. Introduction

1.1 Customer Background

The Air Force Technical Applications Center (AFTAC) operates the Applied Chemistry Laboratory at McClellan AFB, CA. The mission of the laboratory is to determine the quantity of certain radioisotopes in samples and report the results in a timely manner. Its customers use the information to verify compliance with nuclear test ban treaties which, in turn, can have a direct impact on national policies and actions.

In performing the mission, laboratory personnel analyze samples for fission and neutron activation products. Laboratory technicians isolate the radioisotopes by element through chemical extraction, collect the precipitate on filter paper, and then mount the paper onto a planchet shown in Figure 1.1. Depending on the activity of the source on the filter paper, a technician places the planchet at a fixed distance above the detector for measurement. Because many of the sources have very low activities, they lie on

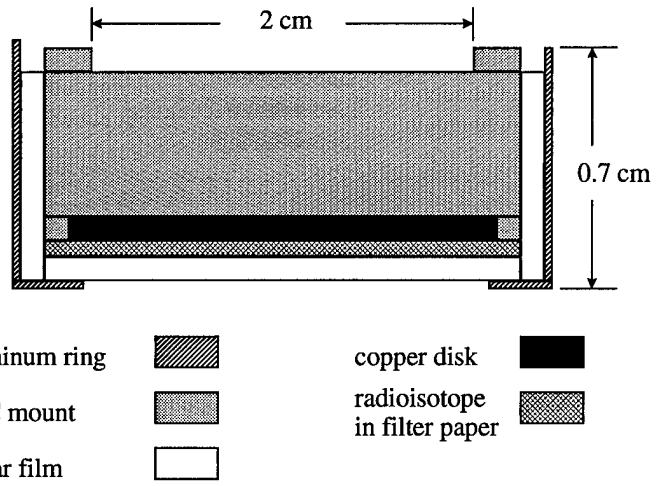

Figure 1.1 Planchet Schematic

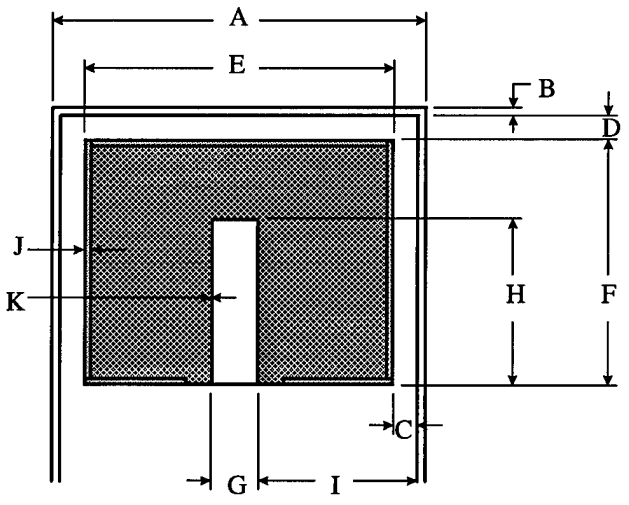

LEGEND

Item	cm
A. endcap dia.	7.6
B. thickness	0.16
C. spacing	0.64
D. spacing	0.5
E. crystal dia.	6.0
F. length	5.1
G. hole dia.	0.8
H. hole depth	3.65
I. hole to endcap	3.24
J. Li contact	0.05
K. B contact	4.E-5

Figure 1.2 Detector #120 Schematic (Canberra, 1995)

the end cap (face) of the detector. The typical detector has a closed-end, coaxial high purity germanium (HPGe) crystal enclosed by an aluminum end cap shown in Figure 1.2.

Laying the low activity (weak) source on the face of a detector maximizes the rate of registering radiation quanta (count rate) and minimizes measurement time. The measurement time depends on the total counts recorded which must be over the threshold of 10,000 counts. The laboratory uses this threshold to minimize the errors of the counts due to the statistical variation of radioactive decay. The detector may operate for as long as 1000 minutes in order to get a valid measurement.

After obtaining a reliable measurement, laboratory members determine the activity of the radioisotopes present in the sample. Then, they send the findings to Headquarters AFTAC for dissemination to the customers.

1.2 Problem Background

Before measuring the activity of a source from a collected sample, laboratory personnel calibrate the response of each detector to gamma-rays of known energies. These gamma-rays come from a source containing standard radioisotopes that predominantly emit one or two gamma-rays per decay. The standard source is usually 10 cm or more above the face of the detector. (The importance of this fact

will be made later.) A technician assigns the energies of the known gamma-rays to the corresponding peaks of counts recorded in the spectrum. With this data, the software for the detector system creates an efficiency function to calibrate the energy spectrum for future measurements.

As each radioisotope has a unique set of radiation quanta (gamma-rays in this context) with associated energy and rate of emission, laboratory members can determine the radioisotopes present and their quantity at time of formation (time zero). To find these values, laboratory technicians calculate the activity of each radioisotope based on the detector measurements. With the number of counts under a characteristic energy peak per minute, CPM, the branching ratio of the gamma-ray that caused the peak, χ, the decay constant of the radioisotope, λ, the efficiency of the detector to record the full energy of the gamma-ray (peak efficiency), ε^{peak}, the time of chemical extraction and the midpoint time of the measurement, the percent of mass yielded from chemical extraction, y, and the dilution of the sample before precipitating the solid (fraction of total volume), FTV, a technician inputs this data into a computer program (GAMANAL) and gets the activity of the radioisotope at time zero, C_0. Equation 1-1 shows the relation of the above

factors in calculating the activity at time zero (AFTAC, 1997):

$$C_0 = \frac{\text{CPM@mid\_measurement\_time}}{\text{FTV}y\chi\varepsilon^{peak}\text{Exp}[-\lambda(\text{separation\_to\_mid\_meas.\_time})]}. \qquad (1\text{-}1)$$

When they used the above equation to find the initial activities of the radioisotopes, laboratory personnel obtained reproducible results for sources that were 10 cm or more above the face of the detector. However, they observed that certain radioisotopes produced significantly different initial activities when the sources were on the face. They assumed that true coincidence summing was occurring. To correct the discrepancy between the initial activities, laboratory engineers decided to take measurements of sufficiently strong sources at 10 cm or more (where summing errors were assumed to be negligible) and then measurements of the sources on the face. Engineers adjusted the peak efficiencies for the face measurements to make the face initial activities match the upper-geometry initial activities. Consequently, the engineers made a lengthy table of adjusted peak efficiencies for each gamma-ray of each radioisotope for each detector.

1.3 Problem and Scope

Is the assumption of true coincidence summing causing the discrepancies in the initial activities correct? Is the effect of angular correlation between cascading gamma-rays augmenting the discrepancies? These are the questions AFTAC personnel want answered.

With these questions, a few more arise and must be answered: If true coincidence summing is the cause of the discrepancies, is there a method to accurately calculate the initial activity? Are there other methods to confirm the results? In addition, is the effect of angular correlation negligible for the face measurements? If not, is there a method to correct for it? In finding answers to all the questions, we will make some approximations to simplify the problem and, of course, look at the impact of those approximations.

First, with respect to the physical aspects of the problem, we will investigate only two radioisotopes of the many that AFTAC analyzes. They are molybdenum-99 (Mo-99) and cesium-136 (Cs-136). Their decay schemes are similar in complexity to those of the other radioisotopes with anomalous initial activities. Next, we will model the Mo-99 and Cs-136 sources as ideal thin disks. Lastly, the detector we will model for this effort is Canberra GC4019, Serial Number

12953567, (also known as AFTAC Detector #120) which has a closed-end, coaxial HPGe crystal shown in Figure 1.1.

Second, with respect to the method to calculate initial activity, we will develop an analytical method that can model a point or thin disk source over a detector with a cylindrical HPGe crystal. The gamma-ray backscattering from the mounting material of the planchet will be ignored in the development of the analytical method. However, the magnitude of this approximation will be addressed in Chapter 4. Next, we will assume that the diameter of the disk source is less than the diameter of the detector face and that the source is centered on the major axis of the detector. With this being true for AFTAC's application, these assumptions will simplify the equations to calculate the path length of gamma-rays from the source to the detector. Lastly, we will develop an analytical method that can model a gamma-ray emitting radioisotope including those with isomeric states and positron emission.

Third, with respect to an alternative method to accurately calculate the initial activity, we will use the Canberra, Inc. coincidence correction software to produce values for an Mo-99 source and compare them with the values generated by the analytical method developed here. The software from Canberra, Inc. is still under development and is proprietary. Because the source code has not been

released, an analysis of any differences can not be provided. The reason for using this software package is its compatibility with existing Canberra detector systems at AFTAC and AFIT.

Last, with respect to angular correlation between cascading gamma-rays, Andreev in his 1972 paper claims that its effect may be ignored when determining the true activity of a source for near geometries. We will investigate this claim. If true, we will not include angular correlation in the development of the analytical method. Unfortunately, we will not investigate those cases where the source is at some intermediate distance above the detector in which angular correlation and true coincidence summing may produce a maximum discrepancy effect. The laboratory has manufactured source stands for each detector with fixed positions at 0, 5, 10, and 15 cm above the face. Laboratory personnel did not observe any significant discrepancies in initial activities for Mo-99 sources down to the 5 cm position. Because of the laboratory's set measurement configuration, we will not investigate where correlation and summing effects create a maximum.

1.4 Outline

To start the investigation, Chapter 2 reviews the relevant fundamentals of cascading radiation, true

coincidence summing, and angular correlation. Next, Chapter 3 presents an analytical method to correct for summing events and its results for Mo-99 and Cs-136. Then, Chapter 4 compares the analytical results with those of the Canberra, Inc. program. Lastly, Chapter 5 provides some conclusions.

1.5 Benefits of Research

With the results from the analytical and Canberra, Inc. methods, we will be able to answer AFTAC's questions and show if gamma-ray cascades cause the anomalous activities for the face geometry. In addition, as the laboratory transitions from planchets to vials containing the radioisotopes in solution, this thesis can serve as the starting point for a follow-on investigation into the added complications of self-attenuation and scattering that a voluminous source presents.

2. Nuclear Decay Phenomena

To understand why a detector has a problem in accurately recording gamma-rays, we need to review what the nucleus is doing as it decays and emits radiation. In particular, we will look at the decay data on Mo-99 and Cs-136. Then, we will review concepts of angular correlation and the magnitude of its effect for Mo-99 and Cs-136.

2.1 Gamma-Ray Cascades

The origin of the observed discrepancy in the activity of a radioisotope is its inherent decay mechanisms. A nucleus that rapidly emits gamma-rays in series causes counting errors due to the finite resolution time of a detector in discerning one emission from the next.

Gamma-rays are photons ejected from the nucleus as it de-excites to a state of lower energy. Depending on the radioisotope, a nucleus may de-excite through a number of intermediate energy levels emitting gamma-rays with corresponding energy. A serial emission of radiation is called a cascade. If an intermediate energy level is not meta-stable, i.e., not relatively long-lasting, the nucleus may exist for typically 10^{-20} to 10^{-10} seconds before de-exciting to the next level (Peker, 1994). The typical high-purity germanium (HPGe) detector needs time on the order of 10^{-7} seconds (Knoll, 1989) to collect the energy deposited by

a gamma-ray. Then there is a system dead time of about 5×10^{-6} seconds (Canberra, 1992) for the counting system to process the resulting charge pulse and re-establish itself to receive the next one.

In addition to the problem of a finite response time, cascading gamma-rays may deposit some or all of their energy in the detector and cause a count related to the summed energies. If the sum of the energy deposited approximates the energy of an emitted gamma-ray, the event causes a summing-in count for that gamma. Even if the summed energies do not tally a count for an existing gamma-ray, the event still causes a summing-out situation that suppresses counts for the constituent gamma-ray peaks.

To illustrate these summing-in and -out events, first, we observe the energy levels of and gamma-rays emitted from Mo-99 and Cs-136 shown in Figures 2.1 and 2.2. The decay schemes show the most prominent energy levels and radiation quanta. (Note the 6 hour meta-stable state of Mo-99 essentially breaks the 777 keV and 411-366 keV cascades.) For an example of a summing-in event, if both the 411 and 366 keV gamma-rays from Mo-99 deposit their full energy in a

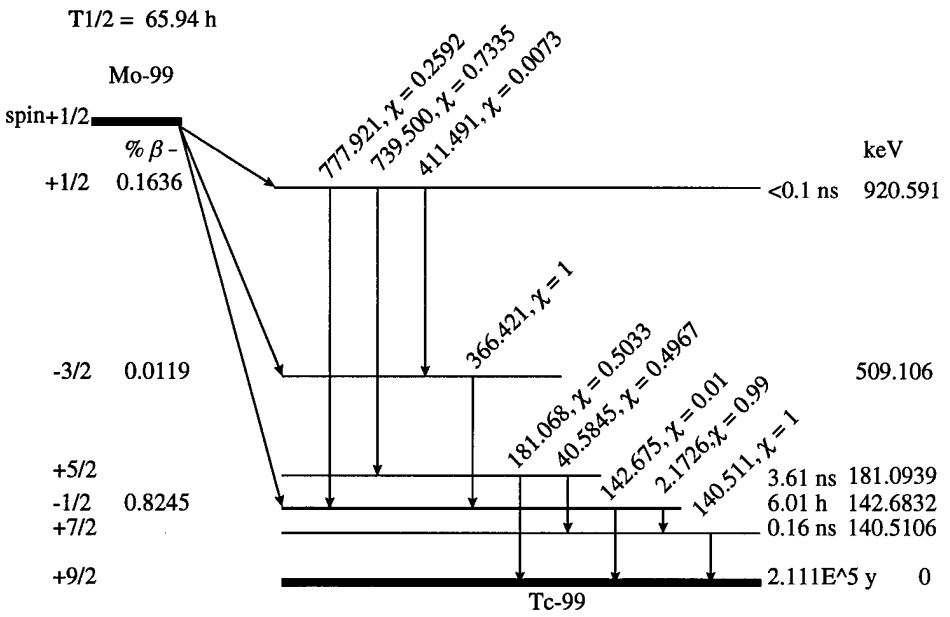

Figure 2.1 Simplified Mo-99 Decay Scheme (Peker, 1994)

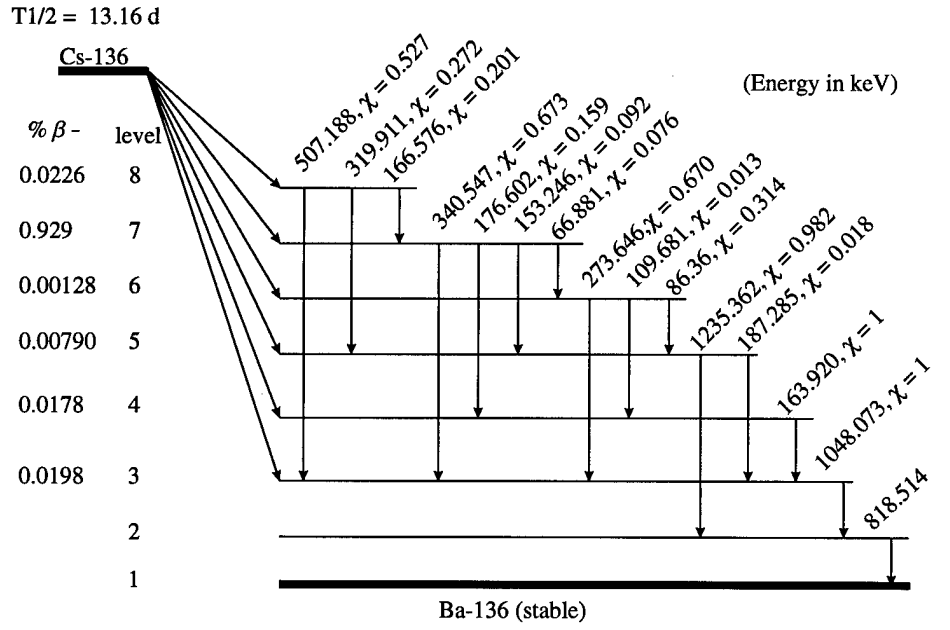

Figure 2.2 Simplified Cs-136 Decay Scheme (Tuli, 1987)

detector within its charge collection time, the sum, 777 keV, will register a count for the 777 keV gamma-ray. For an example of a summing-out event, if the 411 keV gamma-ray deposits its full energy and the 366 keV gamma-ray deposits some portion of its energy, the sum will register a count in the energy spectrum above, i.e., out of, the 411 keV peak.

As a further contribution to the activity discrepancy, the solid angle subtended at the face of the detector allows more summing-in and -out events to occur. This comes from the cascading gamma-rays having a greater probability to interact and deposit their energy in the detector crystal. For radioisotopes with significant gamma-ray cascading, summing events may cause substantial deviation which we will investigate in the next chapter.

2.2 Angular Correlation of Radiation

In most applications, we assume a de-exciting nucleus emits gamma-rays isotropically. However, when the nucleus emits a cascade of gamma-rays, a correlation among the directions of the gamma-rays appears. What causes this correlation, and how much can it enhance true coincidence summing?

First, the angular momentum (spin state) of the nucleus is the primary influence on this correlation of directions.

A nucleus has a particular spin state for each of its energy levels. When a nucleus emits a gamma-ray and loses energy, its spin state changes. The direction of the gamma-ray is related to the initial spin state (Evans, 1967). When there is a cascade, the quantum mechanical behavior of the nucleus as it de-excites imparts a correlation on the directions of the gamma-rays. In his 1965 book, Ferguson uses wave equations to show how the correlation arises and how to determine its magnitude. Because the presentation of the details is very lengthy, please refer to his book for further inquiry.

Second, the magnetic and electric quadrupole moments of the nucleus may perturb the correlation if the nucleus exists at one energy level for more than 10^{-11} seconds (Friedlander and others, 1981). A case in point is Mo-99. See Figure 2.1 for its energy level lifetimes. Unfortunately, in their presentations, Friedlander (1981) and Ferguson (1965) do not explain and show how the quadrupole moments affect the correlation. Only Gardulski and Wiedenbeck (1974) in their paper provide some experimental results on the magnitude of this effect for Mo-99. We will look at the data later.

In a related matter, even though there is correlation between beta particles and a cascade of gamma-rays, we will only consider the gamma-gamma correlation when we analyze Mo-

99 and Cs-136. The energies of the beta particles from these isotopes are not high enough to let the beta particles penetrate the mounting structure (aluminum end cap) of a detector to make a substantial difference in the counts. Appendix A shows the ranges of the highest energy Mo-99 and Cs-136 beta particles in aluminum and the weak bremsstrahlung radiation created.

With the cause identified, we will now define angular correlation in terms of probability. To begin, we need to define the angles that describe the directions of the gamma-rays. We assume a source emits a gamma-ray, γ_a, in the direction of Ω_a with polar angle α_a and azimuthal angle ω_a as shown in Figure 2.3. Then, we assume the source emits a second gamma-ray, γ_b, in the direction of Ω_b with polar angle α_b and azimuthal angle ω_b. Let the azimuthal angle between the paths of the two gamma-rays be $\Delta\omega$. Also, let the angle between the paths of the two gamma-rays in the plane defined by those paths be θ.

Hence, let the angular correlation, $W(\Omega_a,\Omega_b)$, be the probability per steradian squared that the nucleus emits γ_a and γ_b in directions Ω_a and Ω_b, respectively.

As a consequence, when we include the detector in the situation, we introduce another probability—that of registering γ_a and γ_b. So, let $\varepsilon(\Omega_a)$ be the probability of detecting γ_a given the nucleus emits γ_a in the direction of Ω_a. Likewise, let $\varepsilon(\Omega_b)$ be the probability of detecting γ_b given the nucleus emits γ_b in the direction of Ω_b. Then the probability of detecting both γ_a and γ_b given the same nucleus emits them is , $\tilde{W}$, the integral of the probability

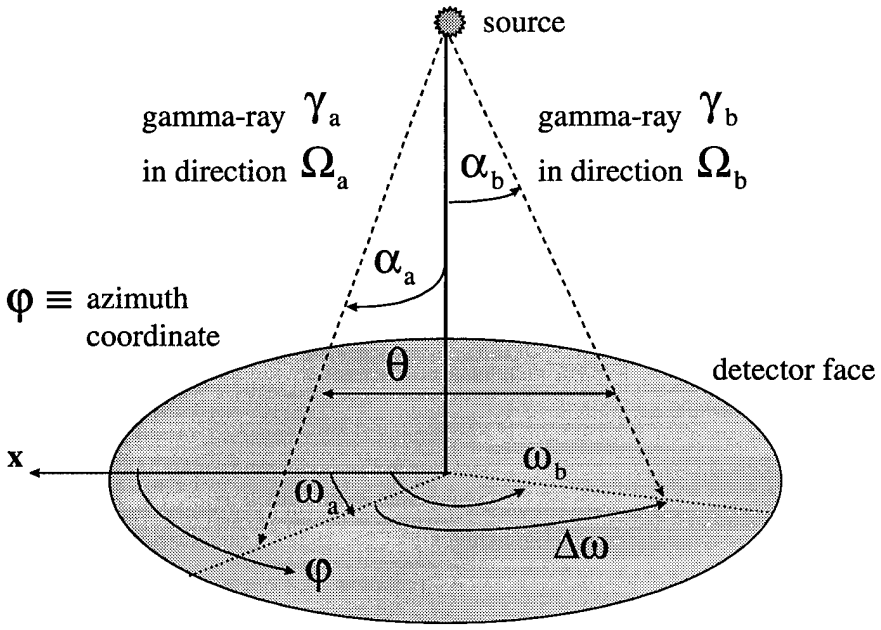

Figure 2.3 Reference Angles for Correlation

of detecting γ_a over all directions multiplied by the probability of detecting γ_b over all directions multiplied by the angular correlation between γ_a and γ_b as shown in Equation 2-1:

$$\tilde{W} = \iint \varepsilon(\Omega_a)\varepsilon(\Omega_b)W(\Omega_a,\Omega_b)\frac{d\Omega_a}{4\pi}\frac{d\Omega_b}{4\pi}. \qquad (2\text{-}1)$$

Next, to find how much of an effect angular correlation has on the probability of detecting γ_a and γ_b, we will normalize Equation 2-1 with respect to the probability of detecting γ_a and γ_b assuming the nucleus emits them isotropically which Equation 2-2 expresses. If there is no angular correlation between γ_a and γ_b, then the normalized angular correlation, $\overline{W}$, will equal one:

$$\overline{W} = \frac{\iint \varepsilon(\Omega_a)\varepsilon(\Omega_b)W(\Omega_a,\Omega_b)\frac{d\Omega_a}{4\pi}\frac{d\Omega_b}{4\pi}}{\iint \varepsilon(\Omega_a)\varepsilon(\Omega_b)\frac{d\Omega_a}{4\pi}\frac{d\Omega_b}{4\pi}}. \qquad (2\text{-}2)$$

Now, we take a closer look at $W(\Omega_a,\Omega_b)$. Due to the spherical harmonics of Legendre polynomials, we express the

function W in terms of an infinite series of these polynomials, P_k, which operate on the cosine of the angle between γ_a and γ_b, that is, θ, with their coefficients, A_k, as weights which Equation 2-3 shows:

$$W(\theta) = 1 + \sum_{k=2,4,6,\ldots}^{\infty} A_k P_k(\cos\theta). \qquad (2\text{-}3)$$

The magnitude of A_k comes from the relations of the wave equations of the nucleus as it de-excites from one energy level with its electric and magnetic moments to the next **(Ferguson, 1965)**.

As a reminder, Equation 2-4 shows the relation between θ and the components of Ω for γ_a and γ_b, i.e., α and ω shown in Figure 2.3:

$$\cos\theta = \cos\alpha_a \cos\alpha_b + \sin\alpha_a \sin\alpha_b \cos\Delta\omega. \qquad (2\text{-}4)$$

Employing a widely accept approximation, we reduce the infinite series of Equation 2-3 to the first two terms because experimental data has shown that the higher order terms are negligible. Thus, Equation 2-5 approximates the function W:

$$W(\theta) \cong 1 + A_2 P_2(\cos\theta) + A_4 P_4(\cos\theta). \qquad (2\text{-}5)$$

Next, as a brief review, Equations 2-6 and 2-7 show the second and fourth order Legendre polynomials used in Equation 2-5:

$$P_2(\cos\theta) = \frac{1}{2}(3\cos^2\theta - 1) \qquad (2\text{-}6)$$

$$P_4(\cos\theta) = \frac{1}{8}(35\cos^4\theta - 30\cos^2\theta + 3). \qquad (2\text{-}7)$$

In executing Equation 2-2 to find $\overline{W}$, Camp and Van Lehn (1969) present in their paper a set of equations that computes $\overline{W}$ in a more efficient manner. (Appendix B shows some of the key steps in transforming Equation 2-2 to Camp and Van Lehn's equations.) They incorporate the A_2 and A_4 coefficients as well as the integration and normalization into the A_2^{exp} and A_4^{exp} terms shown in Equation 2-8. In particular, they incorporate the integration and normalization into the Q_k term shown in Equation 2-9:

$$\overline{W} = 1 + A_2^{exp} + A_4^{exp} \qquad (2\text{-}8)$$

$$A_k^{exp} = A_k Q_k. \tag{2-9}$$

In the next step, they separate the variables for γ_a and γ_b, i.e., the angles that define the directions of the gamma-rays, into the J functions as Equation 2-10 shows:

$$Q_k = \frac{J_k(\gamma_a)J_k(\gamma_b)}{J_0(\gamma_a)J_0(\gamma_b)}. \tag{2-10}$$

The J function is an integral of the probability of a gamma-ray interacting with the detector and of the Legendre polynomial of order k operating on the cosine of the angle between γ_a and γ_b, θ. First, the probability of interaction is a function of the energy of the gamma-ray, E_γ, and the macroscopic cross section of the target material, Σ_{Ge}, in this case germanium. However, in the detector of Figure 1.2, there are the aluminum end cap and lithium contact which may attenuate the gamma-rays. So, we will incorporate their macroscopic cross sections as well, Σ_{Al} and Σ_{Li}.

In addition, the probability of interaction is a function of the path length of the gamma-ray through the

detector. Let $x_{Al}(\alpha)$ be the path length of a gamma-ray through the end cap at the polar angle, α, from the source to the detector. Let $x_{Li}(\alpha)$ be the path length of a gamma-ray through the lithium contact for the same angle α. Lastly, let $x_{Ge}(\alpha)$ be the path length of the gamma-ray through the detector crystal at angle, α. As we explain in the next section, if the detector is divided into zones for ease to mathematically describe the path length of a gamma-ray, then we introduce upper and lower limits of the zones for integration. Let $A(\alpha)$ be the lower limit angle defining a zone while $B(\alpha)$ be the upper limit angle.

Finally, incorporating all the cross sections, path lengths, and Legendre polynomials, Equation 2-11 shows that the J function is an integral of the probability of the gamma-rays interacting with the detector with attenuation by the end cap and lithium contact and weighted by a modified correlation factor, $P_k(\cos\theta)$:

$$J_k(E_\gamma) = \sum_{i=1}^{Nzones} \int_{A(\alpha)_i}^{B(\alpha)_i} P_k(\cos\theta)\left[1 - \mathrm{Exp}[-\Sigma_{Ge}(E\gamma)x_{Ge}(\alpha)_i]\right]\times$$

$$\left[\mathrm{Exp}[-\Sigma_{Al}(E\gamma)x_{Al}(\alpha)_i - \Sigma_{Li}(E\gamma)x_{Li}(\alpha)_i]\right]\sin(\alpha)_i d(\alpha)_i. \qquad (2\text{-}11)$$

There are some assumptions in using Equation 2-11. One is the aluminum end cap and lithium contact that cover the detector crystal attenuate the gamma-rays via any interaction. This means the interacted gamma-rays can not deposit their full, initial energy. Also, no scattered radiation returns to the crystal which would add to the total detection efficiency. The impact of this assumption will be reviewed in Chapter 4.

2.3 Effect of Angular Correlation

With Equations 2-8 through 2-11, we now have a way to approximate angular correlation. The terms that remain for us to determine are the macroscopic absorption cross sections and the path lengths of the gamma-rays going through the detector. First, the macroscopic cross sections are dependent on the atom density of the material and the energy of the incident gamma-ray. The densities of aluminum, lithium, and germanium with their natural abundance of constituent isotopes are widely published. The most recent values for the energy dependent microscopic absorption cross sections (Compton scattering, photoelectric, and pair production) are listed in the Brookhaven National Laboratory website (Brookhaven, 1997). Pages 90 through 93 in Appendix C have the densities and cross sections listed. (Appendix C

is the source code for the Mathematica program to perform the calculations needed.)

Second, to find the path lengths of the gamma-rays, we need the dimensions of the configuration of the source and detector. We already have the dimensions of Detector #120 shown in Figure 1.2, and AFTAC has provided the area of the source whose radius is 0.9974 cm on the filter paper. The disk source is centered on the major axis of and parallel to the detector.

The task is to represent the path lengths of the gamma-rays from any point on the source through any portion of the detector in mathematical equations. Then, using Equations 2-8 through 2-11, we will find the angular correlation. However, when we look at the trigonometry and integration to find the J functions, we see that the disk source and closed-end, coaxial detector will lead to a long set of complicated piece-wise functions and integrals. This is due to the loss of symmetry when the source point is off of the major axis.

To avoid this difficulty, there are two main techniques to approximate the integration. We may use a Monte Carlo program, tally the results of many gamma-ray histories, and determine a value for the J functions. On the other hand, we may use the J function values of other, simpler

configurations and proportion them to find an approximate value for the actual configuration. One difficulty with the Monte Carlo technique is inserting a correlation into gamma-ray histories. Another difficulty is modeling the varying electric field in the detector crystal which determines the charge collection and peak efficiency (McCallum and Coote, 1975).

Due to these difficulties with the Monte Carlo technique, we will proportion the results from the configurations of (1) a point source centered over a solid cylindrical detector, Figure 2.4, (2) a disk source centered over a solid cylindrical detector, Figure 2.5, and (3) a point source centered over a bored cylindrical detector, Figure 2.6. Heath (1964) and Camp and Van Lehn (1969) have published formulas similar to Equations 2-12 through 2-14 for the total efficiency of a detector. When we include the $P_k(\cos\theta)$ term into their formulas, we obtain the necessary J functions.

The first configuration, Figure 2.4, is for the point source (ps) with the three sided (3s) cylindrical detector (two circular faces plus one side). The detector is divided into two zones to compute the necessary J function, $J_k ps3s$: The first one is for the truncated inner cone. The second is for the convoluted outer wedge. In Equations 2-12 through 2-

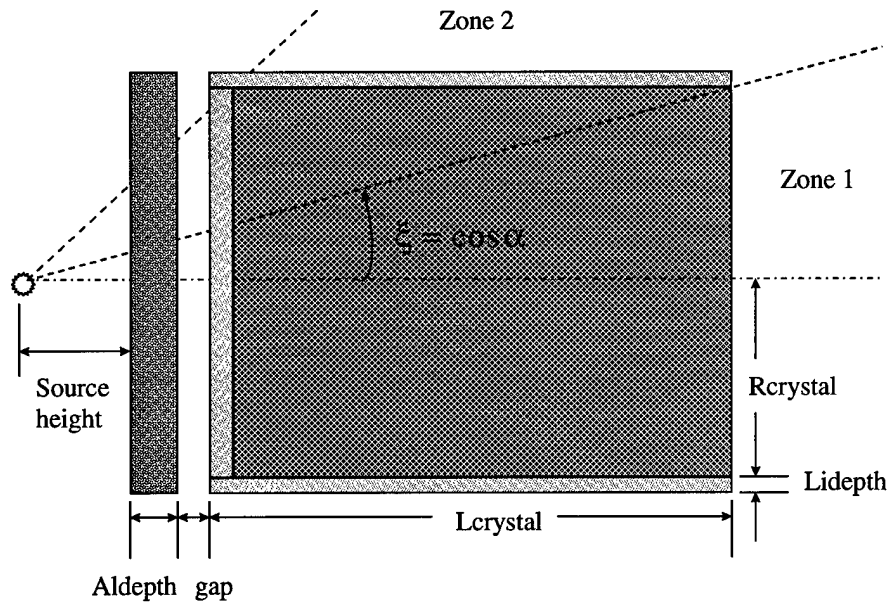

Figure 2.4 Point Source-Solid Crystal (Heath, 1964)

14, the cosine of the polar angle is used to reduce the computation time with the Mathematica program:

$$J_k ps3s(E_\gamma) = \frac{1}{2}\sum_{i=1}^{2}\int_{Aps3s(i)}^{Bps3s(i)} P_k(\xi)\{1 - Exp[-\Sigma_{Ge}(E_\gamma)xps3s_i(\xi)]\} \qquad (2\text{-}12)$$

$$\times \{Exp[-\Sigma_{Al}(E_\gamma)xAl(\xi) - \Sigma_{Li}(E_\gamma)xLi(\xi)]\}d\xi \quad \text{where}$$

$$P_0(\xi) = 1,$$

$$P_2(\xi) = \frac{3}{2}\xi^2 - \frac{1}{2},$$

$$P_4(\xi) = \frac{35}{8}\xi^4 - \frac{30}{8}\xi^2 + \frac{3}{8},$$

$$Aps3s(1) = 1,$$

$$Bps3s(1) = \cos\left(\arctan\left(\frac{Rcrystal}{sourceheight + Aldepth + gap + Lidepth + Lcrystal}\right)\right),$$

$$Aps3s(2) = \cos\left(\arctan\left(\frac{Rcrystal}{sourceheight + Aldepth + gap + Lidepth + Lcrystal}\right)\right),$$

$$Bps3s(2) = \cos\left(\arctan\left(\frac{Rcrystal}{sourceheight + Aldepth + gap + Lidepth}\right)\right),$$

$$xps3s_1 = Lcrystal / \xi,$$

$$xps3s_2 = \frac{Rcrystal}{\sqrt{1-\xi^2}} - \frac{sourceheight + Aldepth + gap + Lidepth}{\xi},$$

$$xAl = Aldepth / \xi, \text{ and}$$

$$xLi = Lidepth / \xi.$$

The second configuration, Figure 2.5, is for the disk source (ds) with the three sided (3s). The detector is again divided into two zones to compute the necessary J function, $J_k ds3s$: The first one is for the truncated inner cone. The second is for the convoluted outer wedge. The limits of integration in Equation 2-13 show the increased complexity of determining the gamma-ray path lengths when modeling a source point that is away from the central axis:

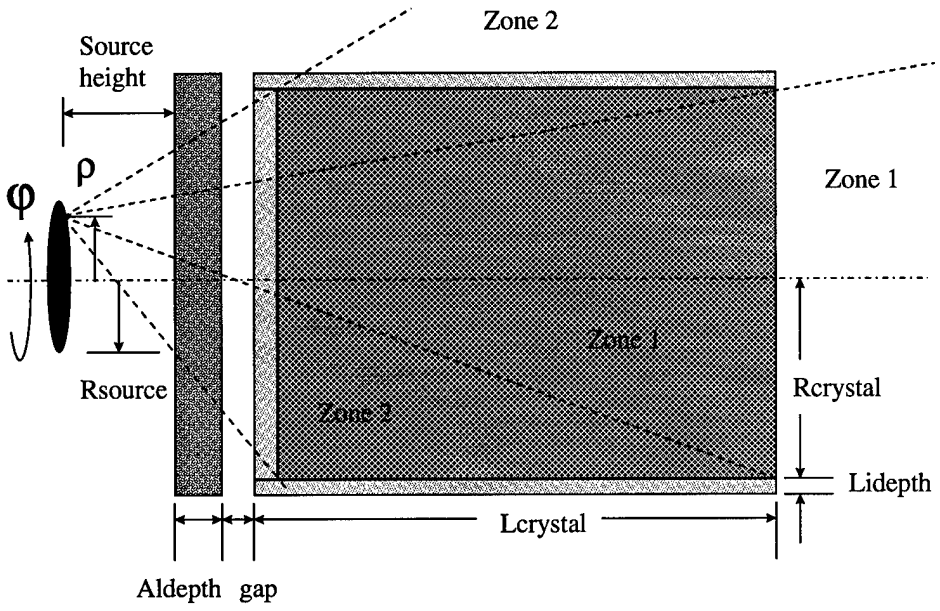

Figure 2.5 Disk Source-Solid Crystal (Heath, 1964)

$$J_k ds3s(E_\gamma) = \frac{1}{\pi Rcrystal^2} \sum_{i=1}^{2} \int_0^{Rsource} \rho d\rho \int_{-\pi/2}^{\pi/2} d\varphi \int_{Ads3s(i)}^{Bds3s(i)} P_k(\xi)\{1 - Exp[-\Sigma_{Ge}(E_\gamma) x ds3s_i(\xi)]\}$$

$$\times \{Exp[-\Sigma_{Al}(E_\gamma) x Al(\xi) - \Sigma_{Li}(E_\gamma) x Li(\xi)]\} d\xi \qquad (2\text{-}13)$$

where $Ads3s(1) = 1$,

$$Bds3s(1) = Cos(Arc\tan(\frac{-\rho \sin\varphi + \sqrt{\rho^2 \sin^2\varphi - \rho^2 + Rcrystal^2}}{sourceheight + Aldepth + gap + Lidepth + Lcrystal})),$$

$$Ads3s(2) = Cos(Arc\tan(\frac{-\rho \sin\varphi + \sqrt{\rho^2 \sin^2\varphi - \rho^2 + Rcrystal^2}}{sourceheight + Aldepth + gap + Lidepth + Lcrystal})),$$

$$Bds3s(2) = Cos(Arc\tan(\frac{-\rho \sin\varphi + \sqrt{\rho^2 \sin^2\varphi - \rho^2 + Rcrystal^2}}{sourceheight + Aldepth + gap + Lidepth})),$$

$$xds3s_1 = Lcrystal / \xi, \text{ and}$$

$$xds3s_2 = \frac{-\rho\sin\varphi + \sqrt{\rho^2\sin^2\varphi - \rho^2 + Rcrystal^2}}{\sqrt{1-\xi^2}} - \frac{sourceheight + Aldepth + gap + Lidepth}{\xi}.$$

The third configuration, Figure 2.6, is for the point source (ps) with the five sided (5s) cylindrical detector (two circular faces, one annular face, plus two sides). The detector is divided into four zones to compute the J function, $J_k ps5s$: The first one is for the truncated inner cone. The next three are for the convoluted outer wedges:

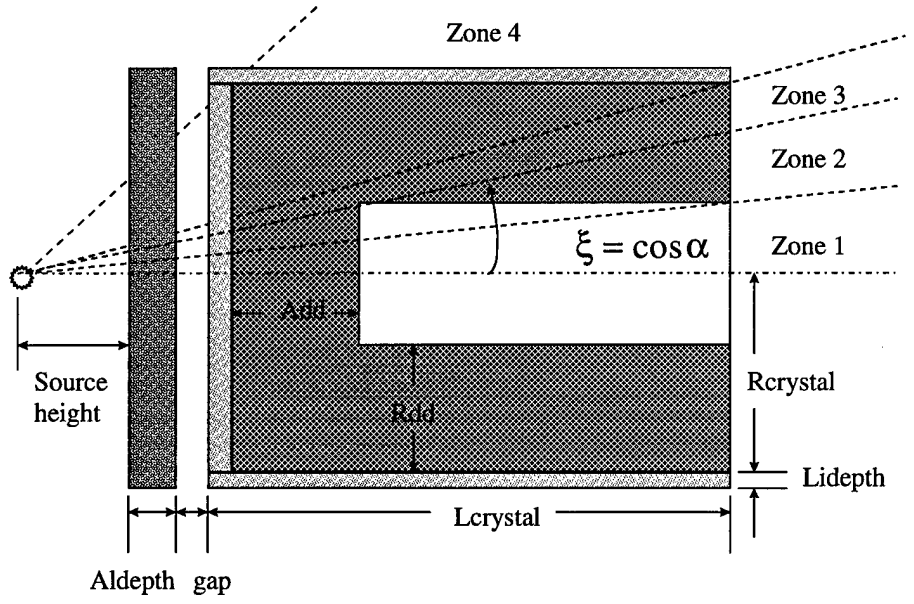

Figure 2.6 Point Source-Closed-end Coaxial Crystal (Camp and Van Lehn, 1969)

$$J_k ps5s(E_\gamma) = \frac{1}{2}\sum_{i=1}^{4}\int_{Aps5s(i)}^{Bps5s(i)} P_k(\xi)\{1 - Exp[-\Sigma_{Ge}(E_\gamma)xps5s_i(\xi)]\} \qquad (2\text{-}14)$$

$$\times \{Exp[-\Sigma_{Al}(E_\gamma)xAl(\xi) - \Sigma_{Li}(E_\gamma)xLi(\xi)]\}d\xi \quad \text{where}$$

$$Aps5s(1) = 1,$$

$$Bps5s(1) = Cos(Arc\tan(\frac{Rcrystal - Rdd}{sourceheight + Aldepth + gap + Lidepth + Lcrystal})),$$

$$Aps5s(2) = Cos(Arc\tan(\frac{Rcrystal - Rdd}{sourceheight + Aldepth + gap + Lidepth + Lcrystal})),$$

$$Bps5s(2) = Cos(Arc\tan(\frac{Rcrystal - Rdd}{sourceheight + Aldepth + gap + Lidepth + Add})),$$

$$Aps5s(3) = Cos(Arc\tan(\frac{Rcrystal - Rdd}{sourceheight + Aldepth + gap + Lidepth + Add})),$$

$$Bps5s(3) = Cos(Arc\tan(\frac{Rcrystal}{sourceheight + Aldepth + gap + Lidepth + Lcrystal})),$$

$$Aps5s(4) = Cos(Arc\tan(\frac{Rcrystal}{sourceheight + Aldepth + gap + Lidepth + Lcrystal})),$$

$$Bps5s(4) = Cos(Arc\tan(\frac{Rcrystal}{sourceheight + Aldepth + gap + Lidepth})),$$

$$xps5s_1 = Add / \xi,$$

$$xps5s_2 = \frac{sourceheight + Aldepth + gap + Lidepth + Lcrystal + Add}{\xi} - \frac{Rcrystal - Rdd}{\sqrt{1-\xi^2}},$$

$$xps5s_3 = Lcrystal / \xi, \quad \text{and}$$

$$xds5s_4 = \frac{Rcrystal}{\sqrt{1-\xi^2}} - \frac{sourceheight + Aldepth + gap + Lidepth}{\xi}.$$

Thus, with Equations 2-12 through 2-14, the dimensions of the source and detector, and the energy-dependent macroscopic absorption cross sections, we can calculate the J function values for the Mo-99 gamma-rays that have correlation data. Then we proportion those values according to Equation 2-15 to find an approximation for the J function of the actual source and detector geometry, $J_k ds5s$:

$$J_k ds5s = J_k ds3s \frac{J_k ps5s}{J_k ps3s}. \qquad (2\text{-}15)$$

To get some confidence in using this approximation based on the results from the simple configurations, we compare the total efficiencies for the Mo-99 gamma-rays using the point-source-five-sided-detector (ps5s) to those of the point-source-three-sided-detector with the contribution from the inner core (equivalent to the hole in the ps5s detector) removed. In this instance, we will compare the total efficiencies with the Mo-99 source 10 cm above the face using Equations 2-11 through 2-14 and deleting the $P_k(\xi)$ term. Pages 7 through 10 in Appendix C show the equations in Mathematica code. Table 2.1 below displays the nearly equal results between the two cases.

Table 2.1 Approximation Check with Total Efficiencies for the Closed-end, Coaxial Detector with Point Source

Gamma-Ray (keV)	ps5s Total Efficiency	Delta ps3s Total Efficiency
778	0.01144	0.01143
740	0.01157	0.01156
411	0.01289	0.01288
366	0.01313	0.01311
181	0.01553	0.01552
142	0.01625	0.01624
140	0.01633	0.01632
40	0.01517	0.01517

To bring to attention a special note about the correlation data of Mo-99 gamma-rays, the relatively long lifetimes of the energy levels allows the angular correlation to be perturbed by the electric and magnetic quadrupole moments. This results in the chemical state of Mo-99 affecting the angular correlation of a nuclear event! The A_k coefficients can differ by a factor of two between pure Mo in a cubic crystal and Mo as a powder in the compound MoO_3 / Mo_2O_5 (Gardulski and Wiedenbeck, 1974) (Bailar and others, 1973). Table 2.2 displays the range of values the coefficients may have depending on the chemical form. For our purposes, the Mo-99 source is in the form of MoO_3 / Mo_2O_5 (AFTAC, 1997).

Table 2.2 Correlation Coefficients for Some Mo-99 Chemical Compounds (Gardulski and Wiedenbeck, 1974)

Cascade (keV)	A_2	A_4	Source Form
740-181	0.126 ± 0.004	-0.005 ± 0.006	Metal
740-181	0.061 ± 0.003	-0.004 ± 0.005	MoO_3 powder
740-40-140	-0.184 ± 0.004	0.001 ± 0.005	Metal
740-40-140	-0.083 ± 0.009	0.007 ± 0.012	MoO_3 powder

Finally, to get the results, we enter Equations 2-11 through 2-15 and the necessary data into the Mathematica program with the code shown on pages 19 through 30 of Appendix C. The Mo-99 gamma-rays that have correlation data are the 740, 181, 40, and 140 keV ones shown in Figure 2.1. The program computes the normalized angular correlation, $\overline{W}$, for the two cases where the source is 10 cm or 0 cm above the face. Table 2.3 shows the values of $\overline{W}$ for the 10 cm case, and Table 2.4 shows the values for the 0 cm case.

Table 2.3 Calculated Normalized Angular Correlation for Mo-99 Source 10 cm above Detector

Cascade (keV)	$\overline{W}$ (ps3s)	$\overline{W}$ (ps5s)	$\overline{W}$ (ds3s)	$\overline{W}$ (ds5s)
740-181	1.053	1.052	1.052	1.052
740-40	0.918	0.918	0.919	0.919
740-140	0.930	0.930	0.930	0.930
140-40	1.104	1.104	1.103	1.103

Table 2.4 Calculated Normalized Angular Correlation for Mo-99 Source 0 cm above Detector

Cascade (keV)	$\overline{W}$ (ps3s)	$\overline{W}$ (ps5s)	$\overline{W}$ (ds3s)	$\overline{W}$ (ds5s)
740-181	1.004	1.004	1.004	1.004
740-40	0.994	0.995	0.994	0.994
740-140	0.995	0.995	0.995	0.995
140-40	1.005	1.005	1.005	1.005

Hence, we see for all configurations the normalized angular correlation, $\overline{W}$, approaches unity as the source moves closer to the detector as Andreev (1972) claimed. The correlation effect diminishes as the solid angle subtended by the detector increases. The probability of detecting two correlated gamma-rays approaches the probability of detecting two isotropically emitted gamma-rays. Therefore, in view of the roughly 0.5% effect for the face geometry, we will make another approximation in our analytical method by not considering the effect of angular correlation.

3. An Analytical Coincidence Correction Method

We now begin the development of an analytical method to estimate the true activity of a source based on measurements affected by coincidence summing. The analytical method will use the dimensions, materials, and nuclear properties of the source and detector to determine the probability of gamma-rays being individually recorded or summed with others. As stated in the previous chapters, we will use the approximations of (1) modeling the source as a thin disk, (2) ignoring beta particles and scattered gamma-rays that may enter the detector crystal in coincidence with other gamma-rays, and (3) ignoring the effect of angular correlation between gamma-rays in cascade. Then given the duration of the measurement, the peak counts, and the probability of recording the nuclear events, we can obtain an accurate estimate of the initial activity.

3.1 Determination of Summing Events from Cascades

In order to determine the extent of summing-in and -out events from cascades, we need to investigate a radioisotope's decay scheme to see the relationships between all the existing gamma-rays, the frequency of each emission, the presence of meta-stable states, and the presence of positron emission. Also, based on the energy of the gamma-ray, the

absolute peak and total efficiencies will affect the recording of the counts.

First, we will look at a simple, hypothetical decay scheme with only β^- decay from parent to daughter nuclei and de-excitation by gamma-ray emission with no meta-stable states as shown in Figure 3.1. In this example, we will include the ratio of internal conversion electrons being emitted per gamma-ray, α. However, we will assume these electrons will not penetrate the aluminum end cap and thereby not deposit any energy in the detector crystal.

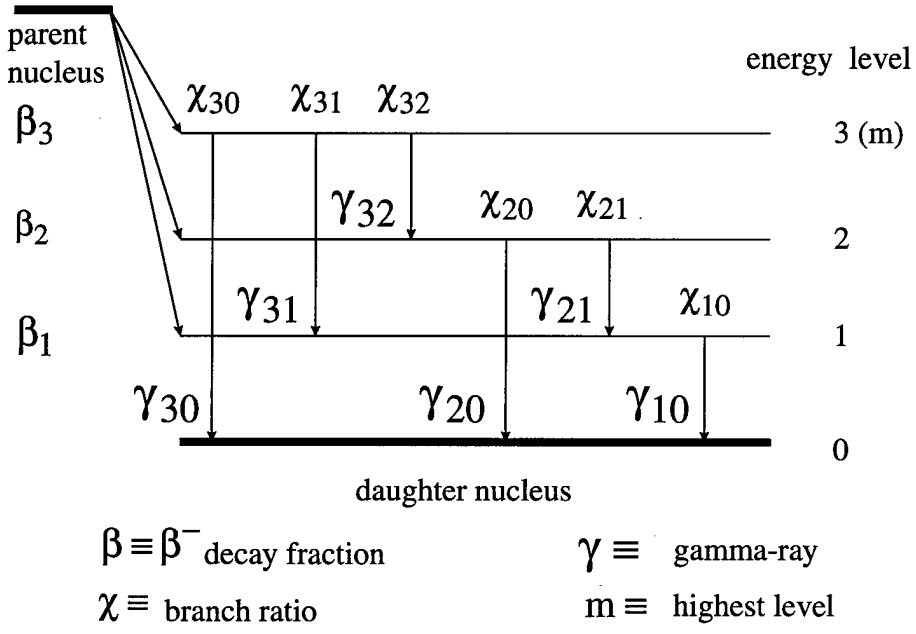

Figure 3.1 Hypothetical Decay Scheme

Let us look at the probability of a detector recording the transition from level 3 to level 0 per decay. There are

four paths or chains of gamma-rays emitted in this transition: (1) γ_{30}; (2) γ_{31} and γ_{10}; (3) γ_{32} and γ_{20}; and, (4) γ_{32}, γ_{21}, and γ_{10}. The last three chains are the ones that cause summing-in events. During its resolution time, the detector collects all the deposited energies of the constituent gamma-rays and registers a count for the sum—in this case, a count for γ_{30}.

First, the probability of the detector recording chain 1 is the probability of γ_{30} depositing its full energy (peak efficiency), ε_{30}^{p}, given the probability that the parent nucleus decays to level 3, β_3, the probability that the daughter nucleus de-excites to level 0, χ_{30}, and the probability that the daughter nucleus emits a gamma-ray vice an internal conversion electron, $\frac{1}{1+\alpha_{30}}$. Thus, the probability for recording chain 1 is $\beta_3 \frac{\chi_{30}\varepsilon_{30}^{p}}{1+\alpha_{30}}$.

Next, the probability of the detector recording chain 2 is the probability of γ_{31} and γ_{10} depositing their full energy, $\varepsilon_{31}^{p}\varepsilon_{10}^{p}$, given the probability that the parent nucleus decays to level 3, β_3, the probability that the daughter nucleus de-excites to level 1 and then to level 0, $\chi_{31}\chi_{10}$,

and the probability that the daughter nucleus emits gamma-rays vice internal conversion electrons, $\frac{1}{1+\alpha_{31}}\frac{1}{1+\alpha_{10}}$. The probability for recording chain 2 is $\beta_3\frac{\chi_{31}\varepsilon_{31}^{p}}{1+\alpha_{31}}\frac{\chi_{10}\varepsilon_{10}^{p}}{1+\alpha_{10}}$.

The probability of the detector recording chain 3 is the probability of γ_{32} and γ_{20} depositing their full energy, $\varepsilon_{32}^{p}\varepsilon_{20}^{p}$, given the probability that the parent nucleus decays to level 3, β_3, the probability that the daughter nucleus de-excites to level 2 and then to level 0, $\chi_{32}\chi_{20}$, and the probability that the daughter nucleus emits gamma-rays vice internal conversion electrons, $\frac{1}{1+\alpha_{32}}\frac{1}{1+\alpha_{20}}$. Therefore, the probability for recording chain 3 is $\beta_3\frac{\chi_{32}\varepsilon_{32}^{p}}{1+\alpha_{32}}\frac{\chi_{20}\varepsilon_{20}^{p}}{1+\alpha_{20}}$.

At last, the probability of the detector recording chain 4 is the probability of γ_{32}, γ_{21}, and γ_{10} depositing their full energy, $\varepsilon_{32}^{p}\varepsilon_{21}^{p}\varepsilon_{10}^{p}$, given the probability that the parent nucleus decays to level 3, β_3, the probability that the daughter nucleus de-excites to level 2, to level 1, and then to level 0, $\chi_{32}\chi_{21}\chi_{10}$, and the probability that the daughter nucleus emits gamma-rays vice internal conversion

electrons, $\frac{1}{1+\alpha_{32}}\frac{1}{1+\alpha_{21}}\frac{1}{1+\alpha_{10}}$. Thus, the probability for recording chain 4 is $\beta_3\frac{\chi_{32}\varepsilon^p_{32}}{1+\alpha_{32}}\frac{\chi_{20}\varepsilon^p_{20}}{1+\alpha_{20}}\frac{\chi_{10}\varepsilon^p_{10}}{1+\alpha_{10}}$.

Because the parent nucleus will decay only once through one of the chains, the probabilities of recording the chains are independent. As such, the probability of recording a level 3 to 0 transition is the sum of the probabilities, S_{30}, of the chains as Equation 3-1 shows:

$$S_{30} = \{\beta_3\}\{\frac{\chi_{30}\varepsilon^p_{30}}{1+\alpha_{30}} + \frac{\chi_{31}\varepsilon^p_{31}}{1+\alpha_{31}}(\frac{\chi_{10}\varepsilon^p_{10}}{1+\alpha_{10}}) + \frac{\chi_{32}\varepsilon^p_{32}}{1+\alpha_{32}}(\frac{\chi_{20}\varepsilon^p_{20}}{1+\alpha_{20}} + \frac{\chi_{21}\varepsilon^p_{21}}{1+\alpha_{21}}(\frac{\chi_{10}\varepsilon^p_{10}}{1+\alpha_{10}}))\}. \quad (3\text{-}1)$$

We now proceed to find the probability of a detector recording the transition from level 3 to level 1 per decay. There are two chains of gamma-rays in this transition: (1) γ_{31} and γ_{10}; and, (2) γ_{32}, γ_{21}, γ_{10}. The probability of the detector recording chain 1 is the probability of γ_{31} depositing its full energy (peak efficiency), ε^p_{31}, given the probability that the parent nucleus decays to level 3, β_3, the probability that the daughter nucleus de-excites to level 1, χ_{31}, the probability that the daughter nucleus emits a gamma-ray vice an internal conversion electron, $\frac{1}{1+\alpha_{31}}$, and,

however, the probability that the γ_{10} gamma-ray emitted in cascade does not deposit any energy (total efficiency), ε_{10}^{t}. The last probability accounts for the summing-out event from coincident detection of the γ_{31} and γ_{10} gamma-rays. Thus, the probability for recording chain 1 is $\beta_3 \frac{\chi_{31}\varepsilon_{31}^{p}}{1+\alpha_{31}}\chi_{10}(1-\frac{\varepsilon_{10}^{t}}{1+\alpha_{10}})$.

Next, the probability of a detector recording chain 2 is the probability of γ_{32} and γ_{21} depositing their full energy, $\varepsilon_{32}^{p}\varepsilon_{21}^{p}$, given the probability that the parent nucleus decays to level 3, β_3, the probability that the daughter nucleus de-excites to level 2 and then level 1, $\chi_{32}\chi_{21}$, the probability that the daughter nucleus emits gamma-rays vice internal conversion electrons, $\frac{1}{1+\alpha_{32}}\frac{1}{1+\alpha_{21}}$, and the probability that the γ_{10} gamma-ray emitted in cascade does not deposit any energy, ε_{10}^{t}. Thus, the probability for recording chain 2 is $\beta_3 \frac{\chi_{32}\varepsilon_{32}^{p}}{1+\alpha_{32}}\frac{\chi_{21}\varepsilon_{21}^{p}}{1+\alpha_{21}}\chi_{10}(1-\frac{\varepsilon_{10}^{t}}{1+\alpha_{10}})$.

Hence, the probability of recording a level 3 to 1 transition is the sum of the probabilities, S_{31}, of the chains from above as Equation 3-2 shows:

$$S_{31} = \{\beta_3\}\{\frac{\chi_{31}\varepsilon_{31}^{p}}{1+\alpha_{31}} + \frac{\chi_{32}\varepsilon_{32}^{p}}{1+\alpha_{32}}(\frac{\chi_{21}\varepsilon_{21}^{p}}{1+\alpha_{21}})\}\{\chi_{10}(1-\frac{\varepsilon_{10}^{t}}{1+\alpha_{10}})\} . \qquad (3\text{-}2)$$

Next, we determine the probability of a detector recording the transition from level 3 to level 2 per decay. There are two chains in this transition: (1) γ_{32} and γ_{20}; and (2) γ_{32}, γ_{21}, and γ_{10}. There is the probability of summing-out events due to coincident detection of γ_{32} with γ_{20} from chain 1 and with γ_{21} or γ_{10} from chain 2.

First, the probability of the detector recording chain 1 is the probability of γ_{32} depositing its full energy, ε_{32}^{p}, given the probability that the parent nucleus decays to level 3, β_3, the probability that the daughter nucleus de-excites to level 2, χ_{32}, the probability that the daughter nucleus emits a gamma-ray vice an internal conversion electron, $\frac{1}{1+\alpha_{32}}$, and the probability that the γ_{20} emitted in cascade does not deposit any energy, ε_{20}^{t}. The probability of recording chain 1 is $\beta_3(\frac{\chi_{32}\varepsilon_{32}^{p}}{1+\alpha_{32}})\chi_{20}(1-\frac{\varepsilon_{20}^{t}}{1+\alpha_{20}})$.

Second, the probability of the detector recording chain 2 is the probability of γ_{32} depositing its full energy, ε_{32}^{p},

given the probability that the parent nucleus decays to level 3, β_3, the probability that the daughter nucleus de-excites to level 2, χ_{32}, the probability that the daughter nucleus emits a gamma-ray vice an internal conversion electron, $\frac{1}{1+\alpha_{32}}$, and the probability that the γ_{21} and γ_{10} gamma-rays emitted in cascade do not deposit any energy, ε_{21}^{t} and ε_{10}^{t}. The probability of recording chain 2 is

$$\beta_3\left(\frac{\chi_{32}\varepsilon_{32}^{p}}{1+\alpha_{32}}\right)\chi_{21}\left(1-\frac{\varepsilon_{21}^{t}}{1+\alpha_{21}}\right)\chi_{10}\left(1-\frac{\varepsilon_{10}^{t}}{1+\alpha_{10}}\right).$$

Putting it all together, Equation 3-3 shows the probability of recording the level 3 to 2 transition:

$$S_{32} = \{\beta_3\}\left\{\frac{\chi_{32}\varepsilon_{32}^{p}}{1+\alpha_{32}}\right\}\left\{\chi_{20}\left(1-\frac{\varepsilon_{20}^{t}}{1+\alpha_{20}}\right)+\chi_{21}\left(1-\frac{\varepsilon_{21}^{t}}{1+\alpha_{21}}\right)\left(\chi_{10}\left(1-\frac{\varepsilon_{10}^{t}}{1+\alpha_{10}}\right)\right)\right\}. \quad (3\text{-}3)$$

Moving to the next transition, we will determine the probability of a detector recording the de-excitation from level 2 to level 0 per decay. There are four chains involved in this transition: (1) γ_{20}; (2) γ_{21} and γ_{10}; (3) γ_{32} and γ_{20}; and, (4) γ_{32}, γ_{21}, and γ_{10}. For this transition, there is the probability of summing-out events due to coincident recording of γ_{32} at the beginning of the chain 3. Also,

there is the probability of summing-in events from the γ_{21} and γ_{10} cascade.

First, the probability of recording chain 1 is the probability of γ_{20} depositing its full energy, ε_{20}^{p}, given the probability that the parent nucleus decays to level 2, β_2, the probability that the daughter nucleus de-excites to level 0, χ_{20}, and the probability that the daughter nucleus emits a gamma-ray vice an internal conversion electron, $\frac{1}{1+\alpha_{20}}$. Thus the probability for chain 1 is $\beta_2 \frac{\chi_{20}\varepsilon_{20}^{p}}{1+\alpha_{20}}$.

Because the gamma-rays of chain 1 are a subset of chain 3, we only need to include the probability that the nucleus decays to level 3, β_3, de-excites to level 2, χ_{32}, and emits a gamma-ray, γ_{32}, vice an internal conversion electron, $\frac{1}{1+\alpha_{32}}$, without the detector receiving any energy from γ_{32}, ε_{32}^{t} (thereby increasing the occurrence of the γ_{20} and γ_{21}-γ_{10} cascades). The resulting probability for chain 3 is

$$\beta_3\chi_{32}(1-\frac{\varepsilon_{32}^{t}}{1+\alpha_{32}})(\frac{\chi_{20}\varepsilon_{20}^{p}}{1+\alpha_{20}}).$$

Next, the probability of recording chain 2 is the probability of γ_{21} and γ_{10} depositing their full energy,

$\varepsilon_{21}^{p}\varepsilon_{10}^{p}$, given the probability that the parent nucleus decays to level 2, β_2, the probability that the daughter nucleus de-excites to level 1 and then level 0, $\chi_{21}\chi_{10}$, and the probability that the daughter nucleus emits gamma-rays vice internal conversion electrons, $\frac{1}{1+\alpha_{21}}\frac{1}{1+\alpha_{10}}$. The probability of recording chain 2 is $\beta_2(\frac{\chi_{21}\varepsilon_{21}^{p}}{1+\alpha_{21}})(\frac{\chi_{10}\varepsilon_{10}^{p}}{1+\alpha_{10}})$.

Again, because the gamma-rays of chain 2 are a subset of chain 4, we only need to include the probability that the nucleus decays to level 3, β_3, de-excites to level 2, χ_{32}, and emits a gamma-ray, γ_{32}, vice an internal conversion electron, $\frac{1}{1+\alpha_{32}}$, without the detector receiving any energy from γ_{32}, ε_{32}^{t}. The resulting probability for chain 4 is

$\beta_3\chi_{32}(1-\frac{\varepsilon_{32}^{t}}{1+\alpha_{32}})(\frac{\chi_{21}\varepsilon_{21}^{p}}{1+\alpha_{21}})(\frac{\chi_{10}\varepsilon_{10}^{p}}{1+\alpha_{10}})$.

Ergo, the probability of recording a level 2 to 0 transition is the sum of the probabilities, S_{20}, of the four chains as Equation 3-4 shows:

$$S_{20} = \{\beta_2 + \beta_3\chi_{32}(1-\frac{\varepsilon_{32}^{t}}{1+\alpha_{32}})\}\{\frac{\chi_{20}\varepsilon_{20}^{p}}{1+\alpha_{20}} + \frac{\chi_{21}\varepsilon_{21}^{p}}{1+\alpha_{21}}(\frac{\chi_{10}\varepsilon_{10}^{p}}{1+\alpha_{10}})\}. \qquad (3-4)$$

Moving along, we look at the probability of recording the transition from level 2 to level 1 per decay. There are two chains involved with this transition: (1) γ_{21} and γ_{10}; and (2) γ_{32}, γ_{21}, and γ_{10}. Once more, there is the probability of summing-out events for γ_{21} due to coincident detection with γ_{32} from the chain 2 cascade and detection with γ_{10} later in the cascades. As for summing-in events, there are none because the nucleus emits no other gamma-rays from level 2 to 1.

So, the probability of the detector recording chain 1 is the probability of γ_{21} depositing its full energy, ε_{21}^{p}, given the probability that the parent nucleus decays to level 2, β_2, the probability that the daughter nucleus de-excites to level 1, χ_{21}, the probability that the daughter nucleus emits a gamma-ray vice an internal conversion electron, $\frac{1}{1+\alpha_{21}}$, and the probability that γ_{10} emitted in cascade does not deposit any energy, ε_{10}^{t}. The probability of recording chain 1 is $\beta_2(\frac{\chi_{21}\varepsilon_{21}^{p}}{1+\alpha_{21}})(\chi_{10}(1-\frac{\varepsilon_{10}^{t}}{1+\alpha_{10}}))$.

Next, due to the fact that the gamma-rays of chain 1 are a subset of chain 2, we just include the probability that

the nucleus decays to level 3, β_3, de-excites to level 2, χ_{32}, and emits a gamma-ray, γ_{32}, vice an internal conversion electron, $\frac{1}{1+\alpha_{32}}$, without the detector receiving any energy from γ_{32}, ε_{32}^{t}. The resulting probability for chain 2 is

$$\beta_3\chi_{32}(1-\frac{\varepsilon_{32}^{t}}{1+\alpha_{32}})(\frac{\chi_{21}\varepsilon_{21}^{p}}{1+\alpha_{21}})(\chi_{10}(1-\frac{\varepsilon_{10}^{t}}{1+\alpha_{10}}) .$$

The probability of recording a level 2 to 1 transition is the sum of the probabilities, S_{21}, of the two chains as Equation 3-5 shows:

$$S_{21} = \{\beta_2 + \beta_3\chi_{32}(1-\frac{\varepsilon_{32}^{t}}{1+\alpha_{32}})\}\{\frac{\chi_{21}\varepsilon_{21}^{p}}{1+\alpha_{21}}\}\{\chi_{10}(1-\frac{\varepsilon_{10}^{t}}{1+\alpha_{10}})\} . \qquad (3-5)$$

At last, we look at the probability of the detector recording the level 1 to 0 transition. There are four chains of concern with this process: (1) γ_{10}; (2) γ_{21} and γ_{10}; (3) γ_{31} and γ_{10}; and, (4) γ_{32}, γ_{21}, and γ_{10}. Again, there are probabilities of summing-out with γ_{21} in chains 2 and 3, with γ_{31} in chain 4, and with γ_{32} in chain 3.

First, the probability of the detector recording chain 1 is the probability of γ_{10} depositing its full energy, ε_{10}^{p}, given the probability that the parent nucleus decays to level

1, β_1, the probability that the daughter nucleus de-excites to level 0, χ_{10}, and the probability that the daughter nucleus emits a gamma-ray vice an internal conversion electron, $\frac{1}{1+\alpha_{10}}$. Thus, the probability for recording chain 1 is $\beta_1 \frac{\chi_{10}\varepsilon_{10}^{p}}{1+\alpha_{10}}$.

Next, the gamma-ray of chain 1 is a subset of chain 2, we include the probability that the nucleus decays to level 2, β_2, de-excites to level 1, χ_{21}, and emits a gamma-ray, γ_{21}, vice an internal conversion electron, $\frac{1}{1+\alpha_{21}}$, without the detector receiving any energy from γ_{21}, ε_{21}^{t}. The resulting probability for chain 2 is $\beta_2\chi_{21}(1-\frac{\varepsilon_{21}^{t}}{1+\alpha_{21}})(\frac{\chi_{10}\varepsilon_{10}^{p}}{1+\alpha_{10}})$.

Once more, the gamma-ray of chain 1 is a subset of chain 3, we include the probability that the nucleus decays to level 3, β_3, de-excites to level 1, χ_{31}, and emits a gamma-ray, γ_{31}, vice an internal conversion electron, $\frac{1}{1+\alpha_{31}}$, without the detector receiving any energy from γ_{31}, ε_{31}^{t}. The resulting probability for chain 3 is $\beta_3\chi_{31}(1-\frac{\varepsilon_{31}^{t}}{1+\alpha_{31}})(\frac{\chi_{10}\varepsilon_{10}^{p}}{1+\alpha_{10}})$.

Finally, the probability of the detector recording chain 4 is the probability of γ_{10} depositing its full energy, ε_{10}^{p}, and the probability that the daughter nucleus emits a gamma-ray vice an internal conversion electron, $\frac{1}{1+\alpha_{10}}$, given that the parent nucleus decays to level 3, β_3, the probability that the daughter nucleus de-excites to level 2, χ_{32}, the probability that the daughter nucleus emits γ_{32} without detection, the probability that the nucleus de-excites to level 1, χ_{21}, and the probability that the nucleus emits γ_{21} without detection. Thus, the probability for recording chain 4 is $\beta_3\chi_{32}(1-\frac{\varepsilon_{32}^{t}}{1+\alpha_{32}})\chi_{21}(1-\frac{\varepsilon_{21}^{t}}{1+\alpha_{21}})\frac{\chi_{10}\varepsilon_{10}^{p}}{1+\alpha_{10}}$.

The probability of recording a level 1 to 0 transition is the sum of the probabilities, S_{10}, of the four chains as Equation 3-6 shows:

$$S_{10} = \{\beta_1 + [\beta_2 + \beta_3\chi_{32}(1-\frac{\varepsilon_{32}^{t}}{1+\alpha_{32}})]\chi_{21}(1-\frac{\varepsilon_{21}^{t}}{1+\alpha_{21}}) + \beta_3\chi_{31}(1-\frac{\varepsilon_{31}^{t}}{1+\alpha_{31}})\}\{\frac{\chi_{10}\varepsilon_{10}^{p}}{1+\alpha_{10}}\}. \quad (3-6)$$

From the analysis of this simple, hypothetical decay scheme, a pattern emerges in accounting for (1) the

probability of gamma-rays preceding the transition of interest that cause summing-out events, (2) the probability of gamma-rays in the transition of interest that deposit their full energy into the detector that cause summing-in events, and (3) the probability of gamma-rays that follow the transition of interest that cause summing-out events. This pattern holds for decay schemes with more energy levels, such as for Mo-99 and Cs-136, providing that there is no angular correlation terms to include. Due to the large number of terms, we will not present the equations for probabilities of recording the energy level transitions.

Fortunately, Andreev and others (1972) noted this pattern and developed a recursion relation—a major portion of the analytical method we seek. Their formula produces the terms of the probability equations, again, providing there is no angular correlation to include. Their recursion relation consists of three main factors. As alluded to above, the first factor, B_i, accounts for the probability of gamma-rays preceding the transition of interest, which begins with level i, that cause summing-out events as Equation 3-7 shows:

$$B_i = \beta_i + \sum_{n=i+1}^{m} B_n \chi_{ni} \left(1 - \frac{\varepsilon_{ni}^t}{1+\alpha_{ni}}\right). \qquad (3\text{-}7)$$

The second factor, A_{ik}, accounts for the probability of gamma-rays in the transition of interest (level i to k) that deposit their full energy into the detector that cause summing-in events as Equation 3-8 shows:

$$A_{ik} = \chi_{ik}\left(\frac{\varepsilon_{ik}^{p}}{1+\alpha_{ik}}\right) + \sum_{j=k+1}^{i-1} \chi_{ij}\left(\frac{\varepsilon_{ij}^{p}}{1+\alpha_{ij}}\right)A_{jk} \,. \qquad (3\text{-}8)$$

The third factor, M_k, accounts for the probability of gamma-rays that follow the transition of interest, which ends at level k, that cause summing-out events as Equation 3-9 shows. Because there are no gamma-rays emitted in coincidence below level 0, $M_0 = 1$:

$$M_k = \sum_{j=0}^{k-1} M_j \chi_{kj}\left(1-\frac{\varepsilon_{kj}^{t}}{1+\alpha_{kj}}\right) . \qquad (3\text{-}9)$$

The product of these three factors yields the equation for the probability of the detector recording a level i to k transition, S_{ik}, as Equation 3-10 displays:

$$S_{ik} = B_i A_{ik} M_k \,. \qquad (3\text{-}10)$$

In the present form, the Equation 3-10 does not include the number of decays that occurred during the measurement or the number of counts recorded in the energy peak, E_{ik}, i.e., the energy released in the level i to k transition. To include this data into the equation, we introduce the factor N to account for the number of decays and $\overline{S}_{ik}$ to be the number of peak counts.

With respect to N, we wish to determine the number of decays events that happened during the time of the measurement correcting for any decrease in the activity of the source. We will not account for activation or production of parent nuclei during the measurement as the case does not apply to AFTAC. With that stated, Equation 3-11 determines the number of decay events, N, that occurred during a measurement from time t_1 to time t_2 given the true initial activity, C_0, of the source and the radioisotope's decay constant, λ:

$$N = \frac{C_0}{\lambda}(\mathrm{Exp}[-\lambda t_1] - \mathrm{Exp}[-\lambda t_2]) \,. \qquad (3\text{-}11)$$

However, if λ is small compared to $\frac{1}{t_2 - t_1}$ or what we will call $\frac{1}{\Delta t}$, then Equation 3-11 is poorly conditioned. To remedy this, we will use a series expansion. First, we convert Equation 3-11 to a different form:

$$N = C_0(\Delta t)\mathrm{Exp}[-\lambda t_1]\{\frac{1-\mathrm{Exp}[-\lambda\Delta t]}{\lambda\Delta t}\}, \qquad (3\text{-}12)$$

where $C_0(\Delta t)\mathrm{Exp}[-\lambda t_1]$ would be the counts if the initial activity were maintained and $\{\frac{1-\mathrm{Exp}[-\lambda\Delta t]}{\lambda\Delta t}\}$ is the correction factor accounting for the decrease in the activity during the measurement. On the latter term, we apply the series expansion:

$$\{\frac{1-\mathrm{Exp}[-\lambda\Delta t]}{\lambda\Delta t}\} = \frac{1-\sum_{h=0}^{\infty}\frac{(-\lambda\Delta t)^h}{h!}}{\lambda\Delta t} = \sum_{h=1}^{\infty}\frac{(-1)^{h-1}(\lambda\Delta t)^{h-1}}{h!} = \sum_{h=0}^{\infty}\frac{(-\lambda\Delta t)^h}{(h+1)!}, \qquad (3\text{-}13)$$

where we would use a few terms if $0 < \lambda\Delta t << 1$. Thus, Equation 3-12 takes on the new form:

$$N = C_0(\Delta t)\mathrm{Exp}[-\lambda t_1]\sum_{h=0}^{\infty}\frac{(-\lambda\Delta t)^h}{(h+1)!}\,. \qquad (3\text{-}14)$$

Hence with the product of the probability of recording the level i to k transition, S_{ik}, and the number of decays that occurred during the measurement, N, we find the number of counts in the E_{ik} energy peak, i.e., $\overline{S}_{ik}$:

$$\overline{S}_{ik} = B_i A_{ik} M_k N\,. \qquad (3\text{-}15)$$

By rearranging the terms in Equation 3-15, we find the analytical method that determines the true initial activity of a source:

$$C_0 = \frac{\overline{S}_{ik}}{B_i A_{ik} M_k (\Delta t)\mathrm{Exp}[-\lambda t_1]\sum_{h=0}^{\infty}\frac{(-\lambda\Delta t)^h}{(h+1)!}}\,. \qquad (3\text{-}16)$$

3.2 Modification of Method for Special Cases

In the above form, the analytical method can be applied to the most complex β^- and γ decay scheme. However, if a radioisotope has meta-stable states or β^+ emission in its decay, the method needs modification.

A meta-stable state interrupts the coincidence of a cascade if the state has a half-life that is long relative to the resolving time of the detector. It is possible that the meta-stable state may decay quickly enough to emit the next gamma-ray in the cascade within the resolving time. Therefore, the summing-in and -out events are greatly reduced when the nucleus reaches this state. Of course, there may be more summing events if a cascade continues after this meta-stable state.

The analytical formula presumes there are no breaks in a cascade. To remedy this problem, a solution is to de-couple the cascades, adjust/check B_i to correctly estimate the production of each gamma-ray, execute the equations for each chain, and then sum the results.

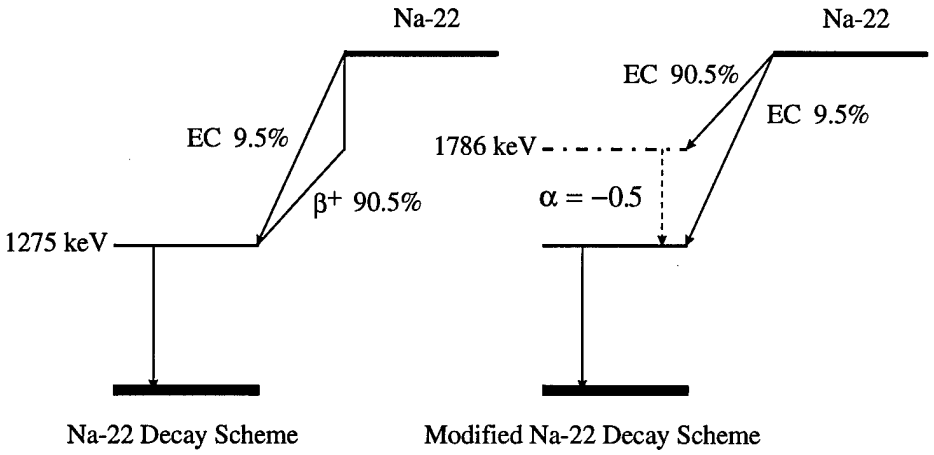

Figure 3.2 Modified Na-22 Decay Scheme

(McCallum and Coote, 1975)

For β^+ emission, McCallum and Coote (1975) modified Andreev's method by representing the β^+ branch with a pseudo β^- branch that decays to a level 511 keV higher than the actual energy state and has an internal conversion coefficient $\alpha = -0.5$ as shown in Figure 3.2. This fix provides for the two 511 keV photons that are not measured in coincidence (McCallum and Coote, 1975).

3.3 Application of Method for Mo-99 and Cs-136

With the analytical method determined, we will now apply it to find the probabilities of recording the

Table 3.1 Mo-99 Nuclear Data (Peker, 1994)

Energy (keV)	β^- Decay Fraction	Branch Ratio	Internal Conversion	Int. Conv. Error	Intensity %	Intensity Error
778	0.164	0.260	0.00059	0.00008	35.1	0.4
740	0.164	0.739	0.0016	0.0004	100	1
411	0.164	0.001	0.003	0.001	0.120	0.005
366	0.012	1	0.0076	0.0010	9.82	0.11
181	0	0.579	0.126	0.007	49.4	0.6
142	0.824	0.01	29	3	0.021	0.002
140	0	1	0.119	0.003	37.3	1.9
40	0	0.421	3.2	0.2	8.68	0.27

transitions in the decay of Mo-99 and Cs-136. Because these probabilities are the key part of obtaining the true initial activity, we will concentrate on calculating their values for the two radioisotopes. We will put aside the number of decays, N, and recorded counts, $\bar{S}_{ik}$, which can easily be found after a measurement.

To start, we note the eight prominent gamma-rays and six levels of Mo-99 in Figure 2.1 and the fifteen gamma-rays and eight levels of Cs-136 in Figure 2.2. Their nuclear data is listed in Tables 3.1 and 3.2:

Table 3.2 Cs-136 Nuclear Data (Tuli, 1987)

Energy (keV)	β^- Decay Ratio	Branch Ratio	Internal Conversion
1235	0.00790	0.982	0
1048	0.0198	1	0
818	0	1	0.00282
507	0.0226	0.527	0.0112
340	0.929	0.673	0.0305
320	0.0226	0.272	0.0393
273	0.00128	0.670	0.016
187	0.00790	0.018	0.190
176	0.929	0.159	0.094
166	0.0226	0.201	0.245
164	0.0178	1	2.26
153	0.929	0.092	0.433
109	0.00128	0.013	1.47
86	0.00128	0.314	0.343
67	0.929	0.076	0.694

The next piece of information we need is data to characterize the peak efficiency of the model detector. AFTAC has measured the peak efficiency of Detector #120 using a source of standard radioisotopes 10 cm above the face. The program that calibrates the energy response of the detector to the known gamma-ray energies has produced a function of the peak efficiency, ε^{p}_{10cm}, for a source at 10 cm above the face for a gamma-ray with energy, E_γ:

$$\varepsilon^{p}_{10cm}(E_\gamma) = \mathrm{Exp}[-5.927 - 0.8438\mathrm{Ln}[E_\gamma] - 0.02031(\mathrm{Ln}[E_\gamma])^2 - \qquad (3\text{-}17)$$

$$0.00007080(\mathrm{Ln}[E_\gamma])^3 + 0.02496(\mathrm{Ln}[E_\gamma])^4 + 0.01560(\mathrm{Ln}[E_\gamma])^5] .$$

With (1) the nuclear data on Mo-99 and Cs-136, (2) the macroscopic absorption cross sections for aluminum, lithium, and germanium for Mo-99 gamma-rays (page 7, Appendix C) and for Cs-136 gamma-rays (page 8, Appendix D), and (3) a means to determine the peak efficiency of the detector at a reference height, we can now determine the total efficiency at 10 cm, the peak-to-total ratio, and the efficiencies at the face. As we previously have done in Chapter 2.3, we transform Equations 2-12 through 2-14 with the same definitions for the terms to find the total efficiency, ε^t, for the three simple configurations by removing the Legendre polynomials:

$$\varepsilon^t ps3s(E_\gamma) = \frac{1}{2}\sum_{i=1}^{2} \int_{Aps3s(i)}^{Bps3s(i)} \{1 - \mathrm{Exp}[-\Sigma_{Ge}(E_\gamma) x ps3s_i(\xi)]\} \qquad (3\text{-}18)$$

$$\times \{\mathrm{Exp}[-\Sigma_{Al}(E_\gamma) x Al(\xi) - \Sigma_{Li}(E_\gamma) x Li(\xi)]\} d\xi ,$$

$$\varepsilon^t ds3s(E_\gamma) = \frac{1}{\pi Rcrystal^2}\sum_{i=1}^{2} \int_0^{Rsource} \rho d\rho \int_{-\pi/2}^{\pi/2} d\varphi \int_{Ads3s(i)}^{Bds3s(i)} \{1 - \mathrm{Exp}[-\Sigma_{Ge}(E_\gamma) x ds3s_i(\xi)]\}$$

$$\times \{\mathrm{Exp}[-\Sigma_{Al}(E_\gamma) x Al(\xi) - \Sigma_{Li}(E_\gamma) x Li(\xi)]\} d\xi , \text{ and} \qquad (3\text{-}19)$$

$$\varepsilon^{t}ps5s(E_{\gamma}) = \frac{1}{2}\sum_{i=1}^{4}\int_{Aps5s(i)}^{Bps5s(i)}\{1-Exp[-\Sigma_{Ge}(E_{\gamma})xps5s_{i}(\xi)]\} \qquad (3\text{-}20)$$

$$\times\{Exp[-\Sigma_{Al}(E_{\gamma})xAl(\xi)-\Sigma_{Li}(E_{\gamma})xLi(\xi)]\}d\xi\ .$$

Then, using the approximation of proportioning the total efficiencies from the three simple configurations, we modify Equation 2-15 to find the total efficiency for the model configuration of a thin disk source and closed-end, coaxial detector:

$$\varepsilon^{t}ds5s = \varepsilon^{t}ds3s\frac{\varepsilon^{t}ps5s}{\varepsilon^{t}ps3s}. \qquad (3\text{-}21)$$

After finding the total efficiency of the model configuration with the source at 10 cm above the face with Equations 3-18 through 3-21 and then finding the peak efficiency for each gamma-ray of Mo-99 and Cs-136 with Equation 3-17, we determine the peak-to-total (P/T) efficiency ratios which we assume are sufficiently independent of the distance between source and detector (McCallum and Coote, 1975). Then we find the total efficiencies for all the Mo-99 and Cs-136 gamma-rays with the sources on the face. Finally, we multiply the P/T ratios with the face total efficiencies to obtain the face peak

efficiencies for all the gamma-rays. Tables 3.3 and 3.4 show the efficiencies and P/T ratios for the Mo-99 and Cs-136 sources on the face. For Mo-99, pages 13 through 17 in Appendix C show the calculations, and, for Cs-136, pages 13 through 18 in Appendix D show the calculations.

Table 3.3 Detector #120 Calculated Efficiencies with Mo-99 Source at 0 cm

Gamma-Ray (keV)	Total Efficiency	Peak Efficiency	P/T Ratio
778	0.2002	0.0578	0.2887
740	0.2028	0.0604	0.2978
411	0.2302	0.1003	0.4357
366	0.2354	0.1108	0.4707
181	0.2941	0.1994	0.6780
142	0.3113	0.2277	0.7314
140	0.3130	0.2291	0.7319
40	0.2566	0.0394	0.1535

Table 3.4 Detector #120 Calculated Efficiencies with Cs-136 Source at 0 cm

Gamma-Ray (keV)	Total Efficiency	Peak Efficiency	P/T Ratio
1235	0.1767	0.0386	0.2184
1048	0.1851	0.0446	0.2410
818	0.1975	0.0553	0.2800
507	0.2203	0.0837	0.3799
340	0.2391	0.1181	0.4939
320	0.2427	0.1246	0.5134
273	0.2734	0.1455	0.5322
187	0.2912	0.1947	0.6686
176	0.2951	0.2026	0.6865
166	0.2958	0.2095	0.7082
164	0.2957	0.2113	0.7146
153	0.2955	0.2184	0.7391
109	0.3156	0.2392	0.7579
86	0.3180	0.2210	0.6950
67	0.3129	0.1680	0.5369

At this point, all the data is present to employ the analytical method, Equations 3-7 through 3-10, to calculate the probabilities of recording the transitions in Mo-99 and Cs-136. In addition, we can compare the probabilities with those of the no-coincidence-assumed formula, i.e., Equations

Table 3.5 Detector #120 Calculated Probabilities of Recording a Transition per Decay of Mo-99 at 0 cm

Gamma-Ray (keV)	No-Summing Method	Analytical Method	Ratio
778	2.464E-3	2.467E-3	0.9989
740	7.312E-3	5.206E-3	0.7120
411	1.640E-5	1.257E-5	0.7665
366	1.338E-3	1.334E-3	0.9970
181	1.243E-2	9.979E-3	0.8028
142	6.669E-5	6.667E-5	0.9997
140	1.885E-1	1.859E-1	0.9862
40	4.789E-4	2.750E-4	0.5742

3-7 through 3-10 with the terms accounting for summing-in and -out events deleted. Tables 3.5 and 3.6 show the comparison for Mo-99 and Cs-136. For Mo-99, pages 31 through 37 in Appendix C show the calculations, and, for Cs-136, pages 20 through 25 in Appendix D show the calculations.

From the information in Tables 3.5 and 3.6, we notice the extent that summing events have on measuring Mo-99 and Cs-136 sources on the face of the detector. For Mo-99, the probability of recording a count for the 740 keV gamma-ray per decay is reduced by nearly 29% from what the simplistic, no-coincidence-assumed formula produces. Lastly, for the 40 keV gamma-ray, its probability is reduced by almost 43%. In the case of Cs-136, the smallest reduction is 30% for the 507

Table 3.6 Detector #120 Calculated Probabilities of Recording a Transition per Decay of Cs-136 at 0 cm

Gamma-Ray (keV)	No-Summing Method	Analytical Method	Ratio
1235	1.118E-2	6.907E-3	0.6178
1048	3.062E-2	1.804E-2	0.5892
818	5.384E-2	3.273E-2	0.6079
507	4.051E-2	2.821E-2	0.6964
340	1.450E-2	7.499E-3	0.5172
320	3.030E-2	2.024E-2	0.6680
273	2.132E-3	1.059E-3	0.4967
187	8.683E-4	4.356E-4	0.5017
176	5.536E-3	2.518E-3	0.4548
166	3.142E-2	1.526E-2	0.4857
164	1.958E-3	7.161E-4	0.3657
153	2.636E-3	1.362E-3	0.5167
109	3.008E-5	1.355E-5	0.4505
86	1.150E-3	5.731E-4	0.4983
67	1.417E-3	5.268E-4	0.3718

keV gamma-ray, and the largest reduction is 63% for the 164 keV gamma-ray. Overall, the importance of correcting for summing events is clear with these two radioisotopes.

3.4 Error Analysis of Mo-99 Results

Given the results from the analytical method, we now need to perform an error analysis and gauge some confidence in the calculated probabilities. Unfortunately, there is insufficient error data for the decay fractions, branching ratios, and internal conversion factors of Cs-136. For Mo-99, there is error data on the intensity and internal conversion factors shown in Table 3.1. However, we will need to make some approximations to perform the error analysis.

To begin, we note the equations used in calculating the probabilities, i.e., Equations 3-7 through 3-10:

$$B_i = \beta_i + \sum_{n=i+1}^{m} B_n \chi_{ni} \left(1 - \frac{\varepsilon_{ni}^t}{1+\alpha_{ni}}\right) . \qquad (3\text{-}7)$$

$$A_{ik} = \chi_{ik} \left(\frac{\varepsilon_{ik}^p}{1+\alpha_{ik}}\right) + \sum_{j=k+1}^{i-1} \chi_{ij} \left(\frac{\varepsilon_{ij}^p}{1+\alpha_{ij}}\right) A_{jk} . \qquad (3\text{-}8)$$

$$M_k = \sum_{j=0}^{k-1} M_j \chi_{kj} \left(1 - \frac{\varepsilon_{kj}^t}{1+\alpha_{kj}}\right) . \qquad (3\text{-}9)$$

$$S_{ik} = B_i A_{ik} M_k . \qquad (3\text{-}10)$$

Next, we apply Equation 3-22 to the above equations to determine the error propagation from the terms with measured (x, y, and z) data and the errors (σ_x, σ_y, and σ_z) to the resulting error (σ_u) in the probability (u) (Knoll, 1989).

$$\sigma_u^2 = (\frac{\partial u}{\partial x})^2\sigma_x^2 + (\frac{\partial u}{\partial y})^2\sigma_y^2 + (\frac{\partial u}{\partial z})^2\sigma_z^2 + \ldots \qquad (3\text{-}22)$$

To make the error propagation manageable, we perform the differentiation on the top level equation first, Equation 3-10, and proceed down:

$$\sigma_S = [(\frac{\partial S}{\partial B})^2\sigma_B^2 + (\frac{\partial S}{\partial A})^2\sigma_A^2 + (\frac{\partial S}{\partial M})^2\sigma_M^2]^{1/2} \quad \text{and} \qquad (3\text{-}23)$$

$$\sigma_S = [(AM)^2\sigma_B^2 + (BM)^2\sigma_A^2 + (BA)^2\sigma_M^2]^{1/2} . \qquad (3\text{-}24)$$

To find the errors σ_B, σ_A, and σ_M, we continue the differentiation with respect to the constituent terms of Equations 3-7 through 3-9:

$$\sigma_B = [(\frac{\partial B}{\partial \beta})^2\sigma_\beta^2 + (\frac{\partial B}{\partial \chi})^2\sigma_\chi^2 + (\frac{\partial B}{\partial \alpha})^2\sigma_\alpha^2 + (\frac{\partial B}{\partial \varepsilon^t})^2\sigma_{\varepsilon^t}^2]^{1/2} , \qquad (3\text{-}25)$$

$$\sigma_A = [(\frac{\partial A}{\partial \chi})^2 \sigma_\chi^2 + (\frac{\partial A}{\partial \alpha})^2 \sigma_\alpha^2 + (\frac{\partial A}{\partial \varepsilon^P})^2 \sigma_{\varepsilon^P}^2]^{1/2}, \text{ and} \quad (3\text{-}26)$$

$$\sigma_M = [(\frac{\partial M}{\partial \chi})^2 \sigma_\chi^2 + (\frac{\partial M}{\partial \alpha})^2 \sigma_\alpha^2 + (\frac{\partial M}{\partial \varepsilon^t})^2 \sigma_{\varepsilon^t}^2]^{1/2}. \quad (3\text{-}27)$$

Due to the absence of error data for the decay fraction β and the branch ratio χ, we will make an approximation and assume that β and α are constants with no errors in the equation to determine the intensity of a gamma-ray:

$$I = \frac{\beta\chi}{1+\alpha}, \quad (3\text{-}28)$$

$$\sigma_I^2 = (\frac{\partial I}{\partial \chi})^2 \sigma_\chi^2, \quad (3\text{-}29)$$

$$\left|\sigma_I\right| = \left|\frac{\beta}{1+\alpha}\right| \left|\sigma_\chi\right|, \quad (3\text{-}30)$$

$$\left|\sigma_I\right| = \left|\frac{I}{\chi}\right| \left|\sigma_\chi\right|, \text{ and} \quad (3\text{-}31)$$

$$\left|\sigma_\chi\right| = \left|\sigma_I \frac{\chi}{I}\right|. \quad (3\text{-}31)$$

In addition, to these approximations for errors, we will make an approximation for the error in the peak and total efficiencies. There is a worst case error of 1.5% in the peak efficiencies for the sources at 10 cm (AFTAC, 1997).

Also, there is rough estimate of 3% in the total efficiency at 10 cm (Canberra, 1995). To propagate the error from each of the simple detector configurations into the model one, we invoke Equation 3-22 with regard to Equation 3-21:

$$\varepsilon^t ds5s = [(\frac{\varepsilon^t ds3s}{\varepsilon^t ps3s})^2 \varepsilon^2_{ps5s} + (\frac{\varepsilon^t ps5s \bullet \varepsilon^t ds3s}{(\varepsilon^t ps3s)^2})^2 \varepsilon^2_{ps3s} + (\frac{\varepsilon^t ps5s}{\varepsilon^t ps3s})^2 \varepsilon^2_{ds3s}]^{1/2} . \quad (3\text{-}32)$$

With these Equations 3-24 through 3-32, we apply them to Equations 3-7 through 3-10 for the Mo-99 decay scheme. Because the error analysis equations are quite lengthy, they are listed on pages 96 through 149 in Appendix C. Table 3.7 shows the results of the error analysis. For ease of reading, Table 3.7 shows the errors in percent, i.e., the error divided by the mean value.

Table 3.7 Error of Calculated Probabilities of Recording a Transition per Decay of Mo-99 using Detector #120

Energy Peak (keV)	% Error of Calculated Probability of Recording a Transition (at 10 cm)	% Error of Calculated Probability of Recording a Transition (at 0 cm)
778	4.621	7.303
740	2.316	5.540
411	1.105	1.930
366	49.29	38.92
181	2.207	4.848
142	10.17	11.32
140	1.778	5.295
40	5.880	8.024

It is apparent the probabilities for the 366 and 142 keV energy peaks suffer the most uncertainty. However, the errors for the 740, 411, 181, and 140 keV peaks seem to be quite reasonable. To be able to make a better judgment, we turn to the next chapter and compare the analytical results against the measured data.

4. AFTAC Experimental Data and Analysis

In this chapter, we compare the probabilities and face peak efficiencies from the analytical method with measurement data from AFTAC. Then we look at the values from the Canberra, Inc. coincidence correction program. Lastly, we the gamma-ray backscatter from the mounting materials of a planchet.

4.1 Comparison of Mo-99 and Cs-136 Data

To begin, AFTAC has provided measurement data as a benchmark for the probabilities of recording transitions during the decay of Mo-99 and Cs-136 with Detector #120. This data includes the probabilities of detecting nuclear transitions and the AFTAC adjust face peak efficiencies for Detector #120. However, AFTAC has removed data from its analysis on several Mo-99 and Cs-136 gamma-rays due to the difficulty in measuring their very low intensities. Nevertheless, Table 4.1 displays the analytical and measured results for the probabilities of Mo-99 nuclear transitions with the source on the face of the detector. The error in the experimental data is around ±2%.

Table 4.1 Probabilities of Detecting Nuclear Transitions of Mo-99 Source at 0 cm

Energy Peak (keV)	Analytical Method	AFTAC Measurement	% Relative Difference
778	2.467E-3	2.271E-3	8.62
740	5.210E-3	5.007E-3	4.06
366	1.334E-3	1.174E-3	13.6
181	9.989E-3	9.015E-3	10.8

Next, to see how the AFTAC adjusted face peak efficiencies compare, we use the ratios of the simplistic method to the analytical one in Tables 3.5 and 3.6 to scale the face peak efficiencies from the analytical method. Tables 4.2 and 4.3 show the significance of summing events for face measurements by altering the analytical efficiencies to nearly match several of the AFTAC adjusted efficiencies.

In reviewing the Cs-136 results, Table 4.3 shows the results from the analytical method. The peak efficiencies for 1048, 86, and 818 keV gamma-rays are under 2% relative difference to the experimental ones (AFTAC, 1997). The analytical peak efficiencies for the 273 and 1235 keV gamma-rays are moderately off by 6.6% and 8.3%. The remainder deviate by 13% to 50%. Yet, like the case with Mo-99, the errors associated with the other gamma-rays are suspected of compounding the error of these few energy peaks.

Table 4.2 Detector #120 Adjusted Face Peak Efficiencies with Mo-99 Source

Energy Peak (keV)	Adjusted Analytical Efficiency	Adjusted AFTAC Efficiency	% Relative Difference
778	0.05779	0.05356	7.90
740	0.04302	0.04172	3.12
366	0.1105	0.09876	11.9
181	0.1601	0.1493	7.23

Next, we compare results with the Canberra, Inc. coincidence correction program which is in development (Kolotov and others, 1997). Again, the software is proprietary, and the details of the code have not been released. Therefore, we can not determine how any differences in results happen. However, Canberra, Inc. has

Table 4.3 Detector #120 Adjusted Face Peak Efficiencies with Cs-136 Source

Energy Peak (keV)	Adjusted AFIT Face Peak Efficiency	Exp. Face Peak Efficiency	% Relative Difference
1235	0.02386	0.02203	8.307
1048	0.02629	0.02615	0.5354
818	0.03364	0.03318	1.386
340	0.06107	0.07467	-18.21
273	0.07226	0.07740	-6.641
176	0.09214	0.1878	-50.94
163	0.07729	0.1326	-41.71
153	0.1129	0.1424	-20.72
86	0.1102	0.1115	-1.166
66	0.06245	0.07185	-13.08

Table 4.4 Detector #120 Correction Factor with Mo-99 Source at 0 cm

Energy Peak (keV)	Analytical Method Correction Factor	Canberra, Inc. Correction Factor	% Relative Difference
778	0.999	1.000	0.100
740	0.712	0.042	-94.1
366	0.997	0.992	-0.502
181	0.803	0.739	-7.97

identified a problem in analyzing the 40 keV gamma-ray that is coincident with the 740 keV one for Mo-99. The 40 keV energy lies below the spectrum analysis cut-off of 60 keV which creates an error in a software module. Canberra, Inc. is addressing the issue.

In reviewing Table 4.4, the Canberra, Inc. correction factors for the 778 and 366 keV energy peaks match the values of the analytical method. However, for the 740 and 181 keV peaks, the Canberra factors differ significantly. Hence, there needs to be further investigation of the software to determine the cause of the discrepancy considering the results from analytical method closely approximate AFTAC's values for the 740 and 181 keV peaks.

5.2 Planchet Effect

The model of the source and detector has been a thin disk containing a uniformly distributed radioisotope

perfectly centered above and parallel to an ideal right-cylindrical detector. Due to the complication of modeling gamma-rays that backscatter into the detector, the copper disk and PVC cylinder have been removed from the scenario. See Figure 1.1. However, these materials are present during measurements. They can and do affect the results of the analytical method. The coincident gamma-rays that backscatter from the planchet and enter the detector cause a summing-out event. Other backscatter gamma-rays that enter the detector add to the absolute total efficiency. They do not add to the peak efficiency since they have lost some energy through scattering.

To determine the extent of not incorporating the full planchet, measurements were taken at AFIT of a source with and without the copper and PVC materials. The source was Cs-137 which emits a single gamma-ray of 662 keV. Table E.1 in Appendix E shows the experimental data. The experiment showed a minor but statistically significant 2 to 3% reduction in the peak-to-total efficiency ratio.

This reduction would directly apply in determining the peak and total efficiencies in the present analytical method. Due to the scope of this thesis, modeling and incorporating scattering effects are left for a follow-on effort. Such an effort directly applies to modeling a radioisotope suspended in solution in a vial. References in the bibliography

(Singh, 1983) and (Kolotov and others, 1997) provide the starting point for this investigation.

5. Conclusions

In this thesis, we addressed AFTAC's problem of showing that coincidence summing is the cause of the discrepancies in the initial activities when sources are on the face of the detector. We developed an analytical method to account for the summing events and obtain the true initial activity. Also, in the process, we showed that angular correlation was a minor effect for a Mo-99 source in a face geometry. Lastly, we looked at the Canberra, Inc. program to correct for summing events with mixed results, however.

In particular for AFTAC, the analytical method showed that it can duplicate with reasonable accuracy the adjusted peak efficiencies for the energy peaks of Mo-99 and Cs-136 compared to experimental values. For Mo-99, the 740 keV analytical (adjusted) face peak efficiency is only 4% off from the experimental value while two other analytical peak efficiencies (the 181 and 778 keV ones) are 7% to 8% off. For Cs-136, several analytical (adjusted) peak efficiencies (at 1048, 818, and 86 keV) are within 1.5% of the experimental values.

The accuracy in the analytical results are quite sensitive to the errors of the associated gamma-rays. Large errors in the coincident gamma-ray intensities and internal

conversion coefficients can compound significantly as in the case of the 366 keV peak of Mo-99.

As for the analytical code in the appendix, it can be readily modified to produce count distributions or adjusted peak efficiencies for other radioisotopes and detector geometries. The dimensions of the detector crystal can quickly be substituted as well as the factors in the empirical formula describing the peak efficiency energy curve. Also, the source-to-detector distances along the major axis can be modified. As for the gamma-rays and energy levels, they would need to be changed to model the new isotope. The section on determining angular correlation may be deleted if the effect is presumed to be minor.

As for restrictions in using the code, the source must be a thin disk with a radius smaller than that of the detector face. The source must be parallel to and centered along the major axis of the detector. The code can account for attenuation if there are absorbers between the source and detector. However, the code does not model the scattered radiation that adds to the total efficiency.

Unfortunately, performing the error analysis will take a fair degree of effort for moderately to highly complex decay schemes. The code will have to be written to account for all the errors of the transitions that cause summing-in and -out effects for each energy peak. In addition, since

many errors are usually given for an overall gamma-ray intensity, the errors for the decay mode fraction, β, and branching ratio, χ, will have to be derived. When accomplishing this effort for a long chain of cascading radiation, one will see how the errors build.

In summary, the analytical method provides a tool to the user to discern how much coincidence summing is affecting the recorded counts and calculated activity in a measurement. An experimenter may place a source as close to the detector as possible (keeping dead time and good counting statistics in mind) and determine the true activity in one trial.

Appendix A: Beta Particle Range

The analytical method presented in the text requires that beta particles, emitted in coincidence with the cascading gamma-rays, not to enter the detector and cause summing events. The method would need modification to account for these extra summing events. The method does not account for neutron emitting sources as well.

In order to use the method, an analysis must be done to verify that beta particles and their bremsstrahlung radiation will not significantly deposit their energy in the detector along with coincident gamma-rays. Since Mo-99 and Cs-136 are the model radioisotopes, an analysis is performed on both below:

The range of a β^- in low Z materials can be found by using Equation A-1 (Turner, 1995). The maximum energy of the β^- emitted by Mo-99 is 444.6 keV and by Cs-136 is 218.7 keV (ICRP, 1983):

$$R(\frac{g}{cm^2}) = 0.412T^{(1.27-0.945\ln T)} \quad 0.01 \text{ MeV} < T(\text{MeV}) < 2.5 \text{ MeV}; \quad \text{(A-1)}$$

$$R_{Mo-99}^{max\beta}(\frac{g}{cm^2}) = 0.412(0.4426)^{(1.27-0.945\ln(0.4426))} = 0.07810\frac{g}{cm^2}; \quad \text{(A-2)}$$

$$R^{max\beta}_{Cs-136}(\frac{g}{cm^2}) = 0.412(0.2187)^{(1.27-0.945\ln(0.2187))} = 0.006733\frac{g}{cm^2}. \quad (A-3)$$

The ranges are multiplied by the density of the absorbing material, aluminum, 2.70 g/cm^2 (Turner, 1995):

$$R^{max\beta}_{Mo-99}(cm) = \frac{R^{max\beta}_{Mo-99}(\frac{g}{cm^2})}{\rho_{Al}} = \frac{0.07810\frac{g}{cm^2}}{2.70\frac{g}{cm^3}} = 0.02893cm, \text{ and} \quad (A-4)$$

$$R^{max\beta}_{Cs-136}(cm) = \frac{R^{max\beta}_{Cs-136}(\frac{g}{cm^2})}{\rho_{Al}} = \frac{0.006733\frac{g}{cm^2}}{2.70\frac{g}{cm^3}} = 0.002494cm. \quad (A-5)$$

With the aluminum end cap of Detector #120 being 0.16 cm thick, neither β^- will penetrate and enter the detector.

The next task is to determine if the bremsstrahlung radiation created by the β^- has enough energy to cause a summing event with cascading gamma-rays. Equation A-6 is an empirical formula to calculate the fraction of the β^- energy that is converted to bremsstrahlung radiation. Z is the number of protons in the nucleus of the absorbing material atom, and T is the kinetic energy of the β^- in MeV:

$$Y = \frac{6\times10^{-4}ZT}{1+6\times10^{-4}ZT}\text{; thus we obtain} \qquad \text{(A-6)}$$

$$Y^{Al}_{Mo-99} = \frac{6\times10^{-4}(13)(0.4426)}{1+6\times10^{-4}(13)(0.4426)} = 0.003440\,, \qquad \text{(A-7)}$$

$$Y^{Al}_{Cs-136} = \frac{6\times10^{-4}(13)(0.2187)}{1+6\times10^{-4}(13)(0.2187)} = 0.001703\,, \qquad \text{(A-8)}$$

$$E^{brem}_{Mo-99} = Y^{Al}_{Mo-99}T = (0.003440)(442.6keV) = 1.52keV\,, \text{ and} \qquad \text{(A-9)}$$

$$E^{brem}_{Cs-136} = Y^{Al}_{Cs-136}T = (0.001703)(218.7keV) = 0.372keV\,. \qquad \text{(A-10)}$$

The bremsstrahlung x-rays of 1.52 and 0.372 keV will not create separate sum peaks due to the 1 to 2 keV resolution of the detector. These x-rays are likely to broaden or distort the existing full energy peaks. Thus, the analytical method is applicable for these radioisotopes and the given detector.

Appendix B: Angular Correlation Formula

In Chapter 2.2, we claim the first-principles expression, Equation 2-2, to calculate the normalized angular correlation factor, $\overline{W}$, is equivalent to Camp and Van Lehn's formula, Equations 2-8 through 2-11. In this appendix, we show some of the key steps in converting Equation 2-2 to the form of Equations 2-8 through 2-11.

First, we present Equation 2-2 noting the definition of the angles in Figure 2.3.:

$$\overline{W} = \frac{\iint \varepsilon(\Omega_a)\varepsilon(\Omega_b)W(\Omega_a,\Omega_b)\frac{d\Omega_a}{4\pi}\frac{d\Omega_b}{4\pi}}{\iint \varepsilon(\Omega_a)\varepsilon(\Omega_b)\frac{d\Omega_a}{4\pi}\frac{d\Omega_b}{4\pi}}. \qquad \text{(B-1)}$$

Then we substitute the coordinate components of Ω_a and Ω_b, i.e., α and ω. We will only consider the probability of interaction of the gamma-rays with the germanium crystal ignoring the aluminum end cap and lithium contact:

$$\overline{W} = \frac{\iiint \{1-\mathrm{Exp}[f_a]\}\{1-\mathrm{Exp}[f_b]\}W(\cos\theta)\frac{d\Delta\omega}{2\pi}\sin\alpha_b d\alpha_b \sin\alpha_a d\alpha_a}{\iint \{1-\mathrm{Exp}[f_a]\}\{1-\mathrm{Exp}[f_b]\}\sin\alpha_b d\alpha_b \sin\alpha_a d\alpha_a} \qquad \text{(B-1)}$$

where

$$f_\gamma = -x(\cos\alpha_\gamma)\Sigma(E_\gamma) \quad \text{and} \tag{B-3}$$

$$W(\cos\theta) = 1 + A_2P_2(\cos\theta) + A_4P_4(\cos\theta) \quad \text{where} \tag{B-4}$$

$$\cos\theta = \cos\alpha_a \cos\alpha_b + \sin\alpha_a \sin\alpha_b \cos\Delta\omega\,, \tag{B-5}$$

$$P_2(\cos\theta) = \frac{1}{2}(3\cos^2\theta - 1)\,, \quad \text{and} \tag{B-6}$$

$$P_4(\cos\theta) = \frac{1}{8}(35\cos^4\theta - 30\cos^2\theta + 3). \tag{B-7}$$

To begin the conversion, the integrals in Equation B-1 are separated into three parts with each containing one of the terms of Equation B-4, the correlation function. Also, for efficiency, we use the $\xi_\gamma = \cos\alpha_\gamma$ transformation:

$$\begin{aligned}\overline{W} = &\frac{\iiint \{1-\mathrm{Exp}[f_a]\}\{1-\mathrm{Exp}[f_b]\}(1)\frac{d\Delta\omega}{2\pi}d\xi_b d\xi_a}{\iint \{1-\mathrm{Exp}[f_a]\}\{1-\mathrm{Exp}[f_b]\}d\xi_b d\xi_a} + \\ &\frac{\iiint \{1-\mathrm{Exp}[f_a]\}\{1-\mathrm{Exp}[f_b]\}(A_2P_2(\xi_a,\xi_b,\Delta\omega))\frac{d\Delta\omega}{2\pi}d\xi_b d\xi_a}{\iint \{1-\mathrm{Exp}[f_a]\}\{1-\mathrm{Exp}[f_b]\}d\xi_b d\xi_a} + \\ &\frac{\iiint \{1-\mathrm{Exp}[f_a]\}\{1-\mathrm{Exp}[f_b]\}(A_4P_4(\xi_a,\xi_b,\Delta\omega))\frac{d\Delta\omega}{2\pi}d\xi_b d\xi_a}{\iint \{1-\mathrm{Exp}[f_a]\}\{1-\mathrm{Exp}[f_b]\}d\xi_b d\xi_a}.\end{aligned} \tag{B-8}$$

Then we continue with expanding the terms in the correlation function:

$$\overline{W} = \frac{(2\pi - 0)\frac{1}{2\pi}\iint \{1 - \mathrm{Exp}[f_a]\}\{1 - \mathrm{Exp}[f_b]\} d\xi_b d\xi_a}{\iint \{1 - \mathrm{Exp}[f_a]\}\{1 - \mathrm{Exp}[f_b]\} d\xi_b d\xi_a} +$$

$$A_2 \frac{\iiint \{1 - \mathrm{Exp}[f_a]\}\{1 - \mathrm{Exp}[f_b]\}(P_2(\xi_a, \xi_b, \Delta\omega))\frac{d\Delta\omega}{2\pi} d\xi_b d\xi_a}{\iint \{1 - \mathrm{Exp}[f_a]\}\{1 - \mathrm{Exp}[f_b]\} d\xi_b d\xi_a} + \qquad \text{(B-9)}$$

$$A_4 \frac{\iiint \{1 - \mathrm{Exp}[f_a]\}\{1 - \mathrm{Exp}[f_b]\}(P_4(\xi_a, \xi_b, \Delta\omega))\frac{d\Delta\omega}{2\pi} d\xi_b d\xi_a}{\iint \{1 - \mathrm{Exp}[f_a]\}\{1 - \mathrm{Exp}[f_b]\} d\xi_b d\xi_a},$$

and Equation B-10

$$\overline{W} = 1 +$$

$$A_2 \frac{\iiint \{1-\mathrm{Exp}[f_a]\}\{1-\mathrm{Exp}[f_b]\}\{\frac{3}{2}\xi_a^2\xi_b^2\}\frac{d\Delta\omega}{2\pi}d\xi_b d\xi_a}{\iint \{1-\mathrm{Exp}[f_a]\{1-\mathrm{Exp}[f_b]\}d\xi_b d\xi_a} +$$

$$A_2 \frac{\iiint \{1-\mathrm{Exp}[f_a]\{1-\mathrm{Exp}[f_b]\}\{\frac{3}{2}\xi_a^2\xi_b^2\cos^2\Delta\omega(1-\xi_a^2)(1-\xi_b^2)\}\frac{d\Delta\omega}{2\pi}d\xi_b d\xi_a}{\iint \{1-\mathrm{Exp}[f_a]\{1-\mathrm{Exp}[f_b]\}d\xi_b d\xi_a} +$$

$$A_2 \frac{\iiint \{1-\mathrm{Exp}[f_a]\{1-\mathrm{Exp}[f_b]\}\{3\xi_a\xi_b\cos\Delta\omega\sqrt{(1-\xi_a^2)(1-\xi_b^2)}-\frac{1}{2}\}\frac{d\Delta\omega}{2\pi}d\xi_b d\xi_a}{\iint \{1-\mathrm{Exp}[f_a]\{1-\mathrm{Exp}[f_b]\}d\xi_b d\xi_a} +$$

$$A_4 \frac{\iiint \{1-\mathrm{Exp}[f_a]\{1-\mathrm{Exp}[f_b]\}\{\frac{35}{8}\xi_a^4\xi_b^4+\frac{3}{8}\}\frac{d\Delta\omega}{2\pi}d\xi_b d\xi_a}{\iint \{1-\mathrm{Exp}[f_a]\{1-\mathrm{Exp}[f_b]\}d\xi_b d\xi_a} +$$

$$A_4 \frac{\iiint \{1-\mathrm{Exp}[f_a]\{1-\mathrm{Exp}[f_b]\}\{\frac{35}{8}\cos^4\Delta\omega(1-\xi_a^2)^2(1-\xi_b^2)^2\}\frac{d\Delta\omega}{2\pi}d\xi_b d\xi_a}{\iint \{1-\mathrm{Exp}[f_a]\{1-\mathrm{Exp}[f_b]\}d\xi_b d\xi_a} +$$

$$A_4 \frac{\iiint \{1-\mathrm{Exp}[f_a]\{1-\mathrm{Exp}[f_b]\}\{\frac{140}{8}\xi_a^3\xi_b^3\cos\Delta\omega\sqrt{(1-\xi_a^2)(1-\xi_b^2)}\}\frac{d\Delta\omega}{2\pi}d\xi_b d\xi_a}{\iint \{1-\mathrm{Exp}[f_a]\{1-\mathrm{Exp}[f_b]\}d\xi_b d\xi_a} +$$

$$A_4 \frac{\iiint \{1-\mathrm{Exp}[f_a]\{1-\mathrm{Exp}[f_b]\}\{\frac{210}{8}\xi_a^2\xi_b^2\cos^2\Delta\omega(1-\xi_a^2)(1-\xi_b^2)\}\frac{d\Delta\omega}{2\pi}d\xi_b d\xi_a}{\iint \{1-\mathrm{Exp}[f_a]\{1-\mathrm{Exp}[f_b]\}d\xi_b d\xi_a} +$$

$$A_4 \frac{\iiint \{1-\mathrm{Exp}[f_a]\{1-\mathrm{Exp}[f_b]\}\{\frac{140}{8}\xi_a\xi_b\cos^3\Delta\omega(1-\xi_a^2)^{\frac{3}{2}}(1-\xi_b^2)^{\frac{3}{2}}\}\frac{d\Delta\omega}{2\pi}d\xi_b d\xi_a}{\iint \{1-\mathrm{Exp}[f_a]\{1-\mathrm{Exp}[f_b]\}d\xi_b d\xi_a} -$$

$$A_4 \frac{\iiint \{1-\mathrm{Exp}[f_a]\{1-\mathrm{Exp}[f_b]\}\{\frac{30}{8}\xi_a^2\xi_b^2\}\frac{d\Delta\omega}{2\pi}d\xi_b d\xi_a}{\iint \{1-\mathrm{Exp}[f_a]\{1-\mathrm{Exp}[f_b]\}d\xi_b d\xi_a} -$$

$$A_4 \frac{\iiint \{1-\mathrm{Exp}[f_a]\{1-\mathrm{Exp}[f_b]\}\{\frac{30}{8}\cos^2\Delta\omega(1-\xi_a^2)(1-\xi_b^2)\}\frac{d\Delta\omega}{2\pi}d\xi_b d\xi_a}{\iint \{1-\mathrm{Exp}[f_a]\{1-\mathrm{Exp}[f_b]\}d\xi_b d\xi_a} -$$

$$A_4 \frac{\iiint \{1-\mathrm{Exp}[f_a]\{1-\mathrm{Exp}[f_b]\}\{\frac{60}{8}\xi_a\xi_b\cos\Delta\omega\sqrt{(1-\xi_a^2)(1-\xi_b^2)}\}\frac{d\Delta\omega}{2\pi}d\xi_b d\xi_a}{\iint \{1-\mathrm{Exp}[f_a]\{1-\mathrm{Exp}[f_b]\}d\xi_b d\xi_a}.$$

Now, we enter the integrals below into Equation B-10:

$$\int_0^{2\pi} \cos\Delta\omega \frac{d\Delta\omega}{2\pi} = 0,$$

$$\int_0^{2\pi} \cos^2\Delta\omega \frac{d\Delta\omega}{2\pi} = \frac{1}{2},$$

$$\int_0^{2\pi} \cos^3\Delta\omega \frac{d\Delta\omega}{2\pi} = 0, \text{and} \qquad \text{(B-11)}$$

$$\int_0^{2\pi} \cos^4\Delta\omega \frac{d\Delta\omega}{2\pi} = \frac{3}{8}.$$

The result is Equation B-12:

$$\overline{W} = 1 +$$

$$A_2 \frac{\iiint \{1-\mathrm{Exp}[f_a]\{1-\mathrm{Exp}[f_b]\}\frac{3}{2}\{\frac{3}{2}\xi_a^2\xi_b^2 - \frac{1}{2}\xi_a^2 - \frac{1}{2}\xi_b^2 + \frac{1}{6}\}\frac{d\Delta\omega}{2\pi}d\xi_b d\xi_a}{\iint \{1-\mathrm{Exp}[f_a]\{1-\mathrm{Exp}[f_b]\}d\xi_b d\xi_a} +$$

$$A_4 \frac{\iiint \{1-\mathrm{Exp}[f_a]\{1-\mathrm{Exp}[f_b]\}\frac{35}{8}\{\xi_a^4\xi_b^4 + \frac{3}{8}(1-2\xi_b^2+\xi_b^4-2\xi_a^2)\}\frac{d\Delta\omega}{2\pi}d\xi_b d\xi_a}{\iint \{1-\mathrm{Exp}[f_a]\{1-\mathrm{Exp}[f_b]\}d\xi_b d\xi_a} +$$

$$A_4 \frac{\iiint \{1-\mathrm{Exp}[f_a]\{1-\mathrm{Exp}[f_b]\}\frac{35}{8}\{\frac{3}{8}(4\xi_a^2\xi_b^2 - 2\xi_a^2\xi_b^4 + \xi_a^4)\}\frac{d\Delta\omega}{2\pi}d\xi_b d\xi_a}{\iint \{1-\mathrm{Exp}[f_a]\{1-\mathrm{Exp}[f_b]\}d\xi_b d\xi_a} +$$

$$A_4 \frac{\iiint \{1-\mathrm{Exp}[f_a]\{1-\mathrm{Exp}[f_b]\}\frac{35}{8}\{\frac{3}{8}(-2\xi_a^4\xi_b^2 + \xi_a^4\xi_b^4)\}\frac{d\Delta\omega}{2\pi}d\xi_b d\xi_a}{\iint \{1-\mathrm{Exp}[f_a]\{1-\mathrm{Exp}[f_b]\}d\xi_b d\xi_a} +$$

$$A_4 \frac{\iiint \{1-\mathrm{Exp}[f_a]\{1-\mathrm{Exp}[f_b]\}\frac{35}{8}\{3(\xi_a^2\xi_b^2 - \xi_a^4\xi_b^2 - \xi_a^2\xi_b^4 + \xi_a^4\xi_b^4)\}\frac{d\Delta\omega}{2\pi}d\xi_b d\xi_a}{\iint \{1-\mathrm{Exp}[f_a]\{1-\mathrm{Exp}[f_b]\}d\xi_b d\xi_a} -$$

$$A_4 \frac{\iiint \{1-\mathrm{Exp}[f_a]\{1-\mathrm{Exp}[f_b]\}\frac{30}{8}\{\xi_a^2\xi_b^2 + \frac{1}{2}(1-\xi_a^2-\xi_b^2+\xi_a^2\xi_b^2)\}\frac{d\Delta\omega}{2\pi}d\xi_b d\xi_a}{\iint \{1-\mathrm{Exp}[f_a]\{1-\mathrm{Exp}[f_b]\}d\xi_b d\xi_a} +$$

$$A_4 \frac{\iiint \{1-\mathrm{Exp}[f_a]\{1-\mathrm{Exp}[f_b]\}\{\frac{3}{8}\}\frac{d\Delta\omega}{2\pi}d\xi_b d\xi_a}{\iint \{1-\mathrm{Exp}[f_a]\{1-\mathrm{Exp}[f_b]\}d\xi_b d\xi_a}.$$

Next, the integrals are separated and solved for ξ_a and ξ_b assuming ξ_a and ξ_b are independent:

$$\overline{W} = 1 + A_2 \frac{\int \{\frac{1}{2}(3\xi_a^2 - 1)\}\{1 - \mathrm{Exp}[f_a]\}d\xi_a \int \{\frac{1}{2}(3\xi_b^2 - 1)\}\{1 - \mathrm{Exp}[f_b]\}d\xi_b}{\int \{1 - \mathrm{Exp}[f_a]\}d\xi_a \int \{1 - \mathrm{Exp}[f_b]\}d\xi_b} + A_4 \frac{\int \{(\frac{35}{8}\xi_a^4 - \frac{30}{8}\xi_a^2 + \frac{3}{8})\}\{1 - \mathrm{Exp}[f_a]\}d\xi_a \int \{(\frac{35}{8}\xi_b^4 - \frac{30}{8}\xi_b^2 + \frac{3}{8})\}\{1 - \mathrm{Exp}[f_b]\}d\xi_b}{\int \{1 - \mathrm{Exp}[f_a]\}d\xi_a \int \{1 - \mathrm{Exp}[f_b]\}d\xi_b}.$$

(B-13)

We recognize the form of the ξ_a and ξ_b functions as Legendre polynomials of orders 2 and 4:

$$\overline{W} = 1 + A_2 \frac{\int \{P_2(\xi_a)\}\{1 - \mathrm{Exp}[f_a]\}d\xi_a \int \{P_2(\xi_b)\}\{1 - \mathrm{Exp}[f_b]\}d\xi_b}{\int \{1 - \mathrm{Exp}[f_a]\}d\xi_a \int \{1 - \mathrm{Exp}[f_b]\}d\xi_b} + A_4 \frac{\int \{P_4(\xi_a)\}\{1 - \mathrm{Exp}[f_a]\}d\xi_a \int \{P_4(\xi_b)\}\{1 - \mathrm{Exp}[f_b]\}d\xi_b}{\int \{1 - \mathrm{Exp}[f_a]\}d\xi_a \int \{1 - \mathrm{Exp}[f_b]\}d\xi_b}. \quad \text{(B-14)}$$

Finally, we see that the integrals are functions of the Legendre polynomial and the probability of interaction for one gamma-ray which matches the J function of Camp and Van Lehn (1969), Equation 2-11:

$$\overline{W} = 1 + A_2 \frac{J_2(\gamma_a)J_2(\gamma_b)}{J_0(\gamma_a)J_0(\gamma_b)} + A_4 \frac{J_4(\gamma_a)J_4(\gamma_b)}{J_0(\gamma_a)J_0(\gamma_b)} \qquad \text{(B-15)}$$

Then, using the nomenclature of their formula, Equations 2-8 through 2-10, we obtain the desired form:

$$\overline{W} = 1 + A_2 Q_2 + A_4 Q_4 \quad \text{and} \qquad \text{(B-16)}$$

$$\overline{W} = 1 + A_2^{exp} + A_4^{exp} \, . \qquad \text{(B-17)}$$

Appendix C: Analytical Method Code for Mo-99

```
Off[General::spell1]
```

AFTAC Canberra Detector 120 peak efficiency was characterized using a NIST source 10 cm above the detector. This distance is large enough to ensure that the solid angle subtended makes the contribution from correlated cascading gammas negligible by a factor of Ω shown below.

The following are the dimensions for a Mo-99 disk source and Det#120 to calculate the solid angle subtended. The reference is Equation 8.10, pg. 254, in **(Tsoulfanidis, 1983)**.

Mo-99 disk source radius in cm. The precipitate area on the planchet is as follows:
1.667 cm^2 for Y, Ce, Nd, Sm, Eu, Tb
3.125 cm^2 for Sr, Zr, Mo, Ag, Cd, Cs, Ba
2.381 cm^2 for U, Np

```
Rsource = Sqrt[3.125 / π];
```

Det#120 crystal radius minus the Li contact in cm:

```
Lidepth = 0.05;

Rcrystal = 6.0 / 2 - Lidepth;
```

The thickness of the Al end cap in cm:

```
Aldepth = 0.16;
```

The spacing between the end cap and lithium contact in cm:

```
gap = 0.5;
```

Source to detector distance in cm:

```
sourceheight = 9.7;

z = (sourceheight + Aldepth + gap + Lidepth) / Rsource;

s = Rcrystal / Rsource;
```

```
Ωfar =
 s * NIntegrate[Exp[-ρ * z] * BesselJ[1, (ρ * s)] * BesselJ[1, ρ] / ρ, {ρ, 0, 10}]
```

```
0.0188295
```

Thus, summing contributions are about two percent of the total counts of the correlated energy peaks.

The following are the efficiency function coefficients for Detector 120 with the disk source at 10cm. The efficiency is calibrated only between 0.059 and 1.836 MeV. Thus, the peak efficiency for the 0.0405845 MeV gamma is suspect to large error. The error in the peak efficiencies for the calibrated range is no larger than 1.5% as Capt Weimer, AFTAC/TOD, stated on 25 Jul 97.

```
c1 = -5.927;

c2 = -0.8438;

c3 = -0.02031;

c4 = -.00007080;

c5 = .02496;

c6 = .01560;
```

The following is the peak efficiency function with the disk source at 10 cm.

```
εpds5sfar[e_] = Exp[c1 + c2 * Log[e] + c3 * (Log[e]) ^ 2 + c4 * (Log[e]) ^ 3 +
   c5 * (Log[e]) ^ 4 + c6 * (Log[e]) ^ 5];
```

```
Plot[εpds5sfar[e], {e, .02, 2.},
 PlotRange -> All, Frame -> True, GridLines -> Automatic, PlotLabel ->
  "Det#120 Absolute Peak Efficiency with Disk Source 10cm Above",
 FrameLabel -> {"Energy (MeV)", "ε peak"}]
```

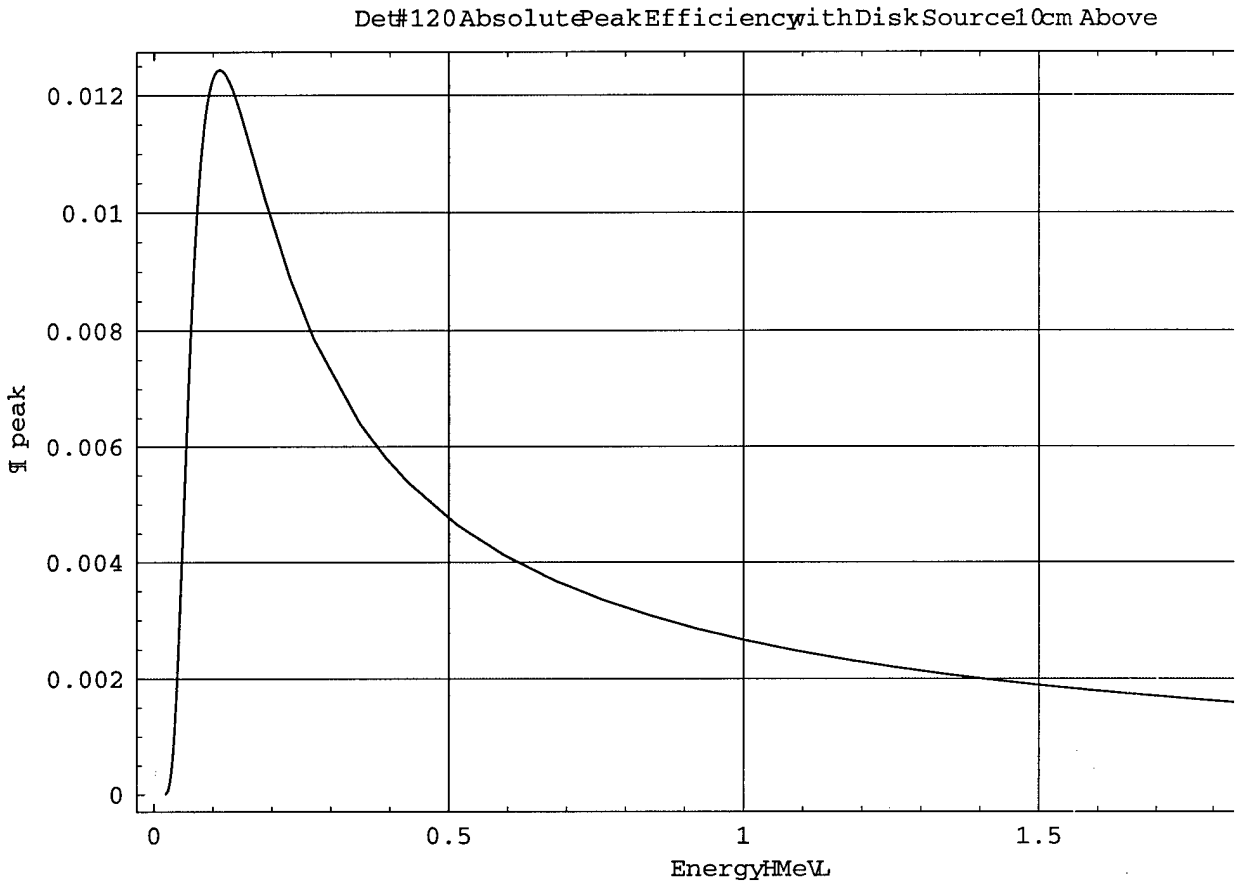

- Graphics -

The following are the Mo-99 gamma energies of interest with their corresponding peak efficiencies.

```
Mo99gammas = {.777921, .739500, .411491, .366421, .181068,
  .142675, .140511, .0405845};

εpds5sfarlist = Table[εpds5sfar[Mo99gammas[[i]]], {i, 1, 8}];
```

The row and column numbers of the matrix element represent the transition from level *i* to *k*.

```
εpfar = {{0, 0, 0, 0, 0, 0},
  {εpds5sfarlist[[7]], 0, 0, 0, 0, 0}, {εpds5sfarlist[[6]], 0, 0, 0, 0, 0},
  {εpds5sfarlist[[5]], εpds5sfarlist[[8]], 0, 0, 0, 0},
  {0, 0, εpds5sfarlist[[4]], 0, 0, 0},
  {0, 0, εpds5sfarlist[[1]], εpds5sfarlist[[2]], εpds5sfarlist[[3]], 0}};
```

The density (g/cm^3) at 300K is assumed to be similar to actual conditions of 77K for Ge and Li. The reference is **(Turner, 1995)**.

```
Gedensity = 5.32;
```

```
Aldensity = 2.70;
```

```
Lidensity = 0.53;
```

The atomic weight is in atoms per gram. The reference is **(Turner, 1995)**.

$$\text{Geatomicweight} = \frac{6.022 * 10^{23}}{72.59};$$

```
Geatomden = Gedensity * Geatomicweight;
```

$$\text{Alatomicweight} = \frac{6.022 * 10^{23}}{26.98154};$$

```
Alatomden = Aldensity * Alatomicweight;
```

$$\text{Liatomicweight} = \frac{6.022 * 10^{23}}{6.941};$$

```
Liatomden = Lidensity * Liatomicweight;
```

The following is a table of the compton scattering, photoelectric, and pair production cross sections in Ge, Al, and Li which will be turned into an interpolation function for use in computing total efficiencies. The reference is the Brookhaven National Laboratory website at TELNET bnlnd2.dne.bnl.gov, 23 Jul 1997. The gamma energies are in MeV and the cross sections in cm^2.

```
Gedata = Table[{{.02, (12.38 + 4996.) * 10^-24 * Geatomden},
   {.03, (14.00 + 1610.) * 10^-24 * Geatomden},
   {.04, (14.75 + 704.5) * 10^-24 * Geatomden},
   {.05, (15.05 + 367.0) * 10^-24 * Geatomden},
   {.06, (15.12 + 214.0) * 10^-24 * Geatomden},
   {.08, (14.94 + 90.61) * 10^-24 * Geatomden},
   {.10, (14.59 + 46.24) * 10^-24 * Geatomden},
   {.15, (13.57 + 13.56) * 10^-24 * Geatomden},
   {.20, (12.63 + 5.706) * 10^-24 * Geatomden},
   {.30, (11.13 + 1.733) * 10^-24 * Geatomden},
   {.40, (10.03 + .7731) * 10^-24 * Geatomden},
   {.50, (9.188 + .4270) * 10^-24 * Geatomden},
   {.60, (8.516 + .2699) * 10^-24 * Geatomden},
   {.80, (7.497 + .1379) * 10^-24 * Geatomden},
   {1.0, (6.747 + .08585) * 10^-24 * Geatomden},
   {1.022, (6.676 + .08158) * 10^-24 * Geatomden},
   {1.25, (6.038 + .05512 + .01073) * 10^-24 * Geatomden},
   {1.5, (5.490 + .03968 + .05320) * 10^-24 * Geatomden},
   {2.0, (4.687 + .02437 + .1971) * 10^-24 * Geatomden},
   {2.044, (4.629 + .02353 + .2116) * 10^-24 * Geatomden},
   {3.0, (3.689 + .01314 + .5378) * 10^-24 * Geatomden}}];

ΣGe = Interpolation[Gedata];
```

The macroscopic cross sections (in 1/cm) of Ge for the Mo-99 gamma energies are below:

```
ΣGelist = Table[ΣGe[Mo99gammas[[i]]], {i, 1, 8}];

ΣGem = {{0, 0, 0, 0, 0, 0},
  {ΣGelist[[7]], 0, 0, 0, 0, 0}, {ΣGelist[[6]], 0, 0, 0, 0, 0},
  {ΣGelist[[5]], ΣGelist[[8]], 0, 0, 0, 0}, {0, 0, ΣGelist[[4]], 0, 0, 0},
  {0, 0, ΣGelist[[1]], ΣGelist[[2]], ΣGelist[[3]], 0}};
```

```
Aldata = Table[{{.02, (6.142 + 138.9) * 10^-24 * Alatomden},
   {.03, (6.561 + 39.08) * 10^-24 * Alatomden},
   {.04, (6.695 + 15.70) * 10^-24 * Alatomden},
   {.05, (6.702 + 7.696) * 10^-24 * Alatomden},
   {.06, (6.645 + 4.285) * 10^-24 * Alatomden},
   {.08, (6.447 + 1.695) * 10^-24 * Alatomden},
   {.10, (6.218 + .8254) * 10^-24 * Alatomden},
   {.15, (5.678 + .2237) * 10^-24 * Alatomden},
   {.20, (5.233 + .08970) * 10^-24 * Alatomden},
   {.30, (4.573 + .02573) * 10^-24 * Alatomden},
   {.40, (4.105 + .01111) * 10^-24 * Alatomden},
   {.50, (3.752 + .006021) * 10^-24 * Alatomden},
   {.60, (3.474 + .003764) * 10^-24 * Alatomden},
   {.80, (3.053 + .001905) * 10^-24 * Alatomden},
   {1.0, (2.746 + .001184) * 10^-24 * Alatomden},
   {1.022, (2.717 + .001115) * 10^-24 * Alatomden},
   {1.25, (2.456 + .0007562 + .001404) * 10^-24 * Alatomden},
   {1.5, (2.232 + .0005476 + .007652) * 10^-24 * Alatomden},
   {2.0, (1.905 + .0003420 + .03023) * 10^-24 * Alatomden},
   {2.044, (1.882 + .0003307 + .03258) * 10^-24 * Alatomden},
   {3.0, (1.499 + .00031892 + .08595) * 10^-24 * Alatomden}}];

ΣAl = Interpolation[Aldata];
```

The macroscopic cross sections (in 1/cm) of Al for the Mo-99 gamma energies are below:

```
ΣAllist = Table[ΣAl[Mo99gammas[[i]]], {i, 1, 8}];

ΣAlm = {{0, 0, 0, 0, 0, 0},
  {ΣAllist[[7]], 0, 0, 0, 0, 0}, {ΣAllist[[6]], 0, 0, 0, 0, 0},
  {ΣAllist[[5]], ΣAllist[[8]], 0, 0, 0, 0}, {0, 0, ΣAllist[[4]], 0, 0, 0},
  {0, 0, ΣAllist[[1]], ΣAllist[[2]], ΣAllist[[3]], 0}};
```

```
Lidata = Table[{{.02, (1.702 + .1516) * 10^-24 * Liatomden},
   {.03, (1.718 + .03841) * 10^-24 * Liatomden},
   {.04, (1.692 + .01445) * 10^-24 * Liatomden},
   {.05, (1.656 + .006770) * 10^-24 * Liatomden},
   {.06, (1.617 + .003645) * 10^-24 * Liatomden},
   {.08, (1.540 + .001373) * 10^-24 * Liatomden},
   {.10, (1.471 + .0006464) * 10^-24 * Liatomden},
   {.15, (1.328 + .0001666) * 10^-24 * Liatomden},
   {.20, (1.218 + .00006481) * 10^-24 * Liatomden},
   {.30, (1.060 + .00001796) * 10^-24 * Liatomden},
   {.40, (.9499 + 7.615 * 10^-6) * 10^-24 * Liatomden},
   {.50, (.8676 + 4.081 * 10^-6) * 10^-24 * Liatomden},
   {.60, (.8027 + 2.533 * 10^-6) * 10^-24 * Liatomden},
   {.80, (.7053 + 1.276 * 10^-6) * 10^-24 * Liatomden},
   {1.0, (.6341 + 7.939 * 10^-7) * 10^-24 * Liatomden},
   {1.022, (.6274 + 7.038 * 10^-7) * 10^-24 * Liatomden},
   {1.25, (.5670 + 4.788 * 10^-7 + 7.052 * 10^-5) * 10^-24 * Liatomden},
   {1.5, (.5154 + 3.486 * 10^-7 + .0003953) * 10^-24 * Liatomden},
   {2.0, (.4398 + 2.212 * 10^-7 + .001583) * 10^-24 * Liatomden},
   {2.044, (.4344 + 2.141 * 10^-7 + .001707) * 10^-24 * Liatomden},
   {3.0, (.3460 + 1.250 * 10^-7 + .004545) * 10^-24 * Liatomden}}];

ΣLi = Interpolation[Lidata];
```

The macroscopic cross sections (in 1/cm) of Li for the Mo-99 gamma energies are below:

```
ΣLilist = Table[ΣLi[Mo99gammas[[i]]], {i, 1, 8}];

ΣLim = {{0, 0, 0, 0, 0, 0},
  {ΣLilist[[7]], 0, 0, 0, 0, 0}, {ΣLilist[[6]], 0, 0, 0, 0, 0},
  {ΣLilist[[5]], ΣLilist[[8]], 0, 0, 0, 0}, {0, 0, ΣLilist[[4]], 0, 0, 0},
  {0, 0, ΣLilist[[1]], ΣLilist[[2]], ΣLilist[[3]], 0}};
```

To review and compare the macroscopic cross sections of the elements involved:

```
TableForm[Table[{Mo99gammas[[i]], ΣGelist[[i]],
   ΣAllist[[i]], ΣLilist[[i]]}, {i, 1, 8}], TableHeadings ->
  {None, {"Mev", "ΣGe (1/cm)", "ΣAl (1/cm)", "ΣLi (1/cm)"}},
 TableAlignments -> Center]
```

Mev	ΣGe (1/cm)	ΣAl (1/cm)	ΣLi (1/cm)
0.777921	0.342247	0.186625	0.03287
0.7395	0.351296	0.19112	0.0336536
0.411491	0.469232	0.245234	0.0431885
0.366421	0.497454	0.256621	0.0451909
0.181068	1.13086	0.338259	0.0577854
0.142675	1.83996	0.378773	0.0619439
0.140511	1.97079	0.383828	0.0622062
0.0405845	30.3487	1.30237	0.078344

To better simulate the response of the detector, the Al end cap and Li contact will be included to account for their attenuation.

The path length of a gamma through the end cap and contact in cm. Since the end cap and contact extend beyond the crystal, there are no vertical edges affecting the path length for this simplified approach.

```
xAl[ξ_] = Aldepth / ξ;
```

```
xLi[ξ_] = Lidepth / ξ;
```

The following is the equation to compute the total efficiency of the five-sided detector crystal with a point source. The references are **(Camp and Van Lehn, 1969)**, pg. 237-238, **(McCallum and Coote, 1975)**, pg. 192, and **(Heath, 1964)**, pg. 21.

The radial depth of the five-sided crystal in cm:

```
Rdd = (6.0 - 0.8 - 2 * Lidepth) / 2;
```

The axial depth of the five sided crystal in cm:

```
Add = 5.1 - 3.65 - Lidepth;
```

The crystal length in cm:

```
Lcrystal = 5.1 - Lidepth;
```

The limits of integration for the five-sided cylinder:

```
Array[Aps5sfar, 4];
```

```
Array[Bps5sfar, 4];
```

```
Array[xps5sfar, 4];

Bps5sfar[4] = Cos[0];

Aps5sfar[4] = Cos[ArcTan[
    (Rcrystal - Rdd) / (sourceheight + Aldepth + gap + Lidepth + Lcrystal)]];

xps5sfar[4][ξ_] = Add / ξ;

Bps5sfar[3] = Aps5sfar[4];

Aps5sfar[3] = Cos[
  ArcTan[(Rcrystal - Rdd) / (sourceheight + Aldepth + gap + Lidepth + Add)]];

xps5sfar[3][ξ_] =
 (sourceheight + Aldepth + gap + Lidepth + Lcrystal + Add) / ξ -
  (Rcrystal - Rdd) / Sqrt[1 - ξ^2];

Bps5sfar[2] = Aps5sfar[3];

Aps5sfar[2] =
 Cos[ArcTan[Rcrystal / (sourceheight + Aldepth + gap + Lidepth + Lcrystal)]];

xps5sfar[2][ξ_] = Lcrystal / ξ;

Bps5sfar[1] = Aps5sfar[2];

Aps5sfar[1] =
 Cos[ArcTan[Rcrystal / (sourceheight + Aldepth + gap + Lidepth)]];

xps5sfar[1][ξ_] =
 Rcrystal / Sqrt[1 - ξ^2] - (sourceheight + Aldepth + gap + Lidepth) / ξ;

εtps5sfar[e_] := 1/2 * Sum[NIntegrate[(1 - Exp[-ΣGe[e] * xps5sfar[i][ξ]]) *
     Exp[-ΣAl[e] * xAl[ξ] - ΣLi[e] * xLi[ξ]],
    {ξ, Aps5sfar[i], Bps5sfar[i]}], {i, 1, 4}]
```

The total efficiency for the five-sided cylinder with a point source 10 cm above for the Mo-99 gamma energies:

```
εtps5sfarlist = Table[εtps5sfar[Mo99gammas[[n]]], {n, 1, 8}];

εtps5sfarm = {{0, 0, 0, 0, 0, 0},
  {εtps5sfarlist[[7]], 0, 0, 0, 0, 0}, {εtps5sfarlist[[6]], 0, 0, 0, 0, 0},
  {εtps5sfarlist[[5]], εtps5sfarlist[[8]], 0, 0, 0, 0},
  {0, 0, εtps5sfarlist[[4]], 0, 0, 0},
  {0, 0, εtps5sfarlist[[1]], εtps5sfarlist[[2]], εtps5sfarlist[[3]], 0}};
```

The following is the equation to compute the total efficiency of the solid cylindrical detector crystal with a point source 10cm above. The references is **(Heath, 1964)**, pg. 21.

The limits of integration for the solid cylinder with a point source:

```
Array[Aps3sfar, 2];

Array[Bps3sfar, 2];

Array[xps3sfar, 2];

Bps3sfar[2] = 1;

Aps3sfar[2] =
 Cos[ArcTan[Rcrystal / (sourceheight + Aldepth + gap + Lidepth + Lcrystal)]];

xps3sfar[2][ξ_] = Lcrystal / ξ;

Bps3sfar[1] = Aps3sfar[2];

Aps3sfar[1] =
 Cos[ArcTan[Rcrystal / (sourceheight + Aldepth + gap + Lidepth)]];

xps3sfar[1][ξ_] =
 Rcrystal / Sqrt[1 - ξ^2] - (sourceheight + Aldepth + gap + Lidepth) / ξ;

εtps3sfar[e_] := 1/2 * Sum[NIntegrate[(1 - Exp[-ΣGe[e] * xps3sfar[i][ξ]]) *
     Exp[-ΣAl[e] * xAl[ξ] - ΣLi[e] * xLi[ξ]],
    {ξ, Aps3sfar[i], Bps3sfar[i]}], {i, 1, 2}];

εtps3sfarlist = Table[εtps3sfar[Mo99gammas[[n]]], {n, 1, 8}];

εtps3sfarm = {{0, 0, 0, 0, 0, 0},
  {εtps3sfarlist[[7]], 0, 0, 0, 0, 0}, {εtps3sfarlist[[6]], 0, 0, 0, 0, 0},
  {εtps3sfarlist[[5]], εtps3sfarlist[[8]], 0, 0, 0, 0},
  {0, 0, εtps3sfarlist[[4]], 0, 0, 0},
  {0, 0, εtps3sfarlist[[1]], εtps3sfarlist[[2]], εtps3sfarlist[[3]], 0}};
```

To perform a quick check on the total efficiencies of the five sided cylinder, the efficiency contribution from the core will be subtracted from the efficiency of the solid three-sided cylinder computed above.

The limits of integration for the core cylinder with a point source:

```
Rcore = .8 / 2;

sourcecore = sourceheight + Aldepth + gap + Lidepth + Add;
```

```
coredepth = 3.65;

Array[Aps3score, 2];

Array[Bps3score, 2];

Array[xps3score, 2];

Bps3score[2] = 1;

Aps3score[2] = Cos[ArcTan[Rcore / (sourcecore + coredepth)]];

xps3score[2][ξ_] = coredepth / ξ;

Bps3score[1] = Aps3score[2];

Aps3score[1] = Cos[ArcTan[Rcore / sourcecore]];

xps3score[1][ξ_] = (Rcore / √(1 - ξ^2)) - (sourcecore / ξ);

εtps3scorefar[e_] :=
 1/2 * Σ_{i=1}^{2} NIntegrate[(1 - Exp[-ΣGe[e] * xps3score[i][ξ]]) *
     Exp[-ΣAl[e] * xAl[ξ] - ΣLi[e] * xLi[ξ] - (ΣGe[e] * Add / ξ)],
    {ξ, Aps3score[i], Bps3score[i]}];

εtps3scorefarlist = Table[εtps3scorefar[Mo99gammas[[n]]], {n, 1, 8}];
```

Now, we compare the total efficiency between the five-sided cyclinder and the reduced efficiency of the three-sided cylinder. The table shows the contribution of Zone 2 of the five-sided crystal letting gamma rays re-enter whereas the three-sided crystal removing all gamma rays that enter the core.

```
TableForm[Table[{Mo99gammas[[i]], εtps5sfarlist[[i]],
   (εtps3sfarlist[[i]] - εtps3scorefarlist[[i]])}, {i, 1, 8}],
 TableHeadings ->
  {None, {"Mev", "5s Total Eff.", "Delta 3s Total Eff."}},
 TableAlignments -> Center]
```

Mev	5s Total Eff.	Delta 3s Total Eff.
0.777921	0.0114423	0.0114321
0.7395	0.0115715	0.011561
0.411491	0.0128898	0.0128767
0.366421	0.0131267	0.0131132
0.181068	0.0155308	0.0155185
0.142675	0.0162487	0.0162428
0.140511	0.016326	0.016321
0.0405845	0.0151698	0.0151698

```
TableForm[Table[{Mo99gammas[[i]], εtps3sfarlist[[i]],
   εtps3scorefarlist[[i]]}, {i, 1, 8}], TableHeadings ->
  {None, {"Mev", "3s Total Eff.", "3s Core Total Eff."}},
 TableAlignments -> Center]
```

Mev	3s Total Eff.	3s Core Total Eff.
0.777921	0.011531	0.0000989049
0.7395	0.01166	0.0000989923
0.411491	0.0129726	0.0000959297
0.366421	0.0132075	0.0000943819
0.181068	0.0155667	0.0000482212
0.142675	0.0162615	0.0000187687
0.140511	0.0163367	0.0000156997
0.0405845	0.0151698	8.03424×10^{-23}

The following is the equation to compute the total efficiency of the solid cylindrical detector crystal with a disk source 10 cm above. The references is Scintillation Spectrometry 2nd Ed., Heath, R., 1964, pg. 21.

The limits of integration for the solid cylinder with a disk source:

```
A1ds3sfar = Cos[0];

B1ds3sfar[ϕ_, ρ_] =
 Cos[ArcTan[(-ρ * Sin[ϕ] + √(ρ^2 * (Sin[ϕ])^2 - (ρ^2 - Rcrystal^2))) /
    (sourceheight + Aldepth + gap + Lidepth + Lcrystal)]];

x1ds3sfar[ξ_] = Lcrystal / ξ;

A2ds3sfar[ϕ_, ρ_] =
 Cos[ArcTan[(-ρ * Sin[ϕ] + √(ρ^2 * (Sin[ϕ])^2 - (ρ^2 - Rcrystal^2))) /
    (sourceheight + Aldepth + gap + Lidepth + Lcrystal)]];

B2ds3sfar[ϕ_, ρ_] =
 Cos[ArcTan[(-ρ * Sin[ϕ] + √(ρ^2 * (Sin[ϕ])^2 - (ρ^2 - Rcrystal^2))) /
    (sourceheight + Aldepth + gap + Lidepth)]];

x2ds3sfar[ξ_, ϕ_, ρ_] =
 1/√(1 - ξ^2) (-ρ * Sin[ϕ] + √(ρ^2 * (Sin[ϕ])^2 - (ρ^2 - Rcrystal^2))) -
  (sourceheight + Aldepth + gap + Lidepth)/ξ;
```

```
εtds3sfar1[e_] := 1/(π (Rsource)^2) (NIntegrate[
    NIntegrate[
      NIntegrate[
         (1 - Exp[-ΣGe[e] * x1ds3sfar[ξ]]) *
        Exp[-ΣAl[e] * xAl[ξ] - ΣLi[e] * xLi[ξ]],
       {ξ, B1ds3sfar[ϕ, ρ], A1ds3sfar}] , {ϕ, -π/2, π/2}] * ρ,
    {ρ, 0, Rsource}])

εtds3sfar1list = Table[εtds3sfar1[Mo99gammas[[n]]], {n, 1, 8}];

εtds3sfar2[e_] := 1/(π (Rsource)^2) (NIntegrate[
    NIntegrate[
      NIntegrate[
         (1 - Exp[-ΣGe[e] * x2ds3sfar[ξ, ϕ, ρ]]) *
        Exp[-ΣAl[e] * xAl[ξ] - ΣLi[e] * xLi[ξ]],
       {ξ, B2ds3sfar[ϕ, ρ], A2ds3sfar[ϕ, ρ]}] , {ϕ, -π/2, π/2}] * ρ,
    {ρ, 0, Rsource}])

εtds3sfar2list = Table[εtds3sfar2[Mo99gammas[[n]]], {n, 1, 8}];

εtds3sfarlist = εtds3sfar1list + εtds3sfar2list;

εtds3sfarm = {{0, 0, 0, 0, 0, 0},
  {εtds3sfarlist[[7]], 0, 0, 0, 0, 0}, {εtds3sfarlist[[6]], 0, 0, 0, 0, 0},
  {εtds3sfarlist[[5]], εtds3sfarlist[[8]], 0, 0, 0, 0},
  {0, 0, εtds3sfarlist[[4]], 0, 0, 0},
  {0, 0, εtds3sfarlist[[1]], εtds3sfarlist[[2]], εtds3sfarlist[[3]], 0}};
```

The following table shows the contribution of each zone to the total efficiency of the three-sided cylinder with a disk source.

```
TableForm[Table[{εtds3sfar1list[[i]],
   εtds3sfar2list[[i]], εtds3sfarlist[[i]]}, {i, 1, 8}],
 TableHeadings -> {None, {"Inner Cone Total Eff.",
    "Outer Wedge Total Eff.", "Sum Total Eff."}},
 TableAlignments -> Center];
```

The following is the equation to compute the total efficiency of the five-sided cylindrical detector crystal with a disk source 10 cm above. It is assumed the ratio of the five-sided to three-sided crystal total efficiencies using a point source at a given distance is the same for using a disk source at the same distance.

```
εtds5sfarlist = (εtps5sfarlist / εtps3sfarlist) * εtds3sfarlist;

εtfar = {{0, 0, 0, 0, 0, 0},
  {εtds5sfarlist[[7]], 0, 0, 0, 0, 0}, {εtds5sfarlist[[6]], 0, 0, 0, 0, 0},
  {εtds5sfarlist[[5]], εtds5sfarlist[[8]], 0, 0, 0, 0},
  {0, 0, εtds5sfarlist[[4]], 0, 0, 0},
  {0, 0, εtds5sfarlist[[1]], εtds5sfarlist[[2]], εtds5sfarlist[[3]], 0}};
```

The following is the peak to total efficiency ratio which is presumed to be independent of distance. This ratio will allow finding the peak efficiency from the calculated total efficiency with a disk source on the face of the detector. The reference is Equation 11 and text, **(McCallum and Coote, 1975)**, pg. 192.

```
PKtoTTLds5slist = εpds5sfarlist / εtds5sfarlist;

TableForm[Table[{Mo99gammas[[i]], εtds5sfarlist[[i]],
   εpds5sfarlist[[i]], PKtoTTLds5slist[[i]]}, {i, 1, 8}],
 TableHeadings -> {None, {"Mev", "εtds5s", "εpds5s", "P/T"}},
 TableAlignments -> Center]
```

Mev	εtds5s	εpds5s	P/T
0.777921	0.0113962	0.00329189	0.288859
0.7395	0.0115246	0.00343397	0.29797
0.411491	0.0128343	0.00558991	0.435546
0.366421	0.0130694	0.00615309	0.4708
0.181068	0.0154519	0.0104779	0.678097
0.142675	0.0161608	0.0118159	0.731147
0.140511	0.0162371	0.0118833	0.73186
0.0405845	0.0150736	0.00231552	0.153614

```
TableForm[Table[{Mo99gammas[[i]], εtds3sfarlist[[i]],
   εtps5sfarlist[[i]], εtps3sfarlist[[i]]}, {i, 1, 8}],
 TableHeadings -> {None, {"Mev", "εtds3s", "εtps5s", "εtps3s"}},
 TableAlignments -> Center]
```

Mev	εtds3s	εtps5s	εtps3s
0.777921	0.0114845	0.0114423	0.011531
0.7395	0.0116127	0.0115715	0.01166
0.411491	0.0129168	0.0128898	0.0129726
0.366421	0.01315	0.0131267	0.0132075
0.181068	0.0154876	0.0155308	0.0155667
0.142675	0.0161736	0.0162487	0.0162615
0.140511	0.0162477	0.016326	0.0163367
0.0405845	0.0150736	0.0151698	0.0151698

Next, the total efficiency of the three-sided crystal with the disk source on the detector face is shown below. (The procedure of using the ratios of the efficiencies is repeated to find the total efficiency for the five-sided crystal.) The distance in cm between the detector's face and crystal includes the thickness of the Al can, the axial space (vacuum), and the Li contact.

```
sourceheight = 0;
```

The limits of integration for the five-sided cylinder:

```
Array[Aps5sface, 4];

Array[Bps5sface, 4];

Array[xps5sface, 4];

Bps5sface[4] = Cos[0];

Aps5sface[4] = Cos[ArcTan[
    (Rcrystal - Rdd) / (sourceheight + Aldepth + gap + Lidepth + Lcrystal)]];

xps5sface[4][ξ_] = Add / ξ;

Bps5sface[3] = Aps5sface[4];

Aps5sface[3] = Cos[
  ArcTan[(Rcrystal - Rdd) / (sourceheight + Aldepth + gap + Lidepth + Add)]];

xps5sface[3][ξ_] =
 (sourceheight + Aldepth + gap + Lidepth + Lcrystal + Add) / ξ -
  (Rcrystal - Rdd) / √(1 - ξ²);

Bps5sface[2] = Aps5sface[3];

Aps5sface[2] =
 Cos[ArcTan[Rcrystal / (sourceheight + Aldepth + gap + Lidepth + Lcrystal)]];

xps5sface[2][ξ_] = Lcrystal / ξ;

Bps5sface[1] = Aps5sface[2];

Aps5sface[1] =
 Cos[ArcTan[Rcrystal / (sourceheight + Aldepth + gap + Lidepth)]];

xps5sface[1][ξ_] =
 Rcrystal / √(1 - ξ²) - (sourceheight + Aldepth + gap + Lidepth) / ξ;
```

```
εtps5sface[e_] := 1/2 * Sum[NIntegrate[(1 - Exp[-ΣGe[e] * xps5sface[i][ξ]]) *
      Exp[-ΣAl[e] * xAl[ξ] - ΣLi[e] * xLi[ξ]],
     {ξ, Aps5sface[i], Bps5sface[i]}], {i, 1, 4}];

εtps5sfacelist = Table[εtps5sface[Mo99gammas[[n]]], {n, 1, 8}];
```

The limits of integration for the solid cylinder with a point source:

```
Array[Aps3sface, 2];

Array[Bps3sface, 2];

Array[xps3sface, 2];

Bps3sface[2] = Cos[0];

Aps3sface[2] =
 Cos[ArcTan[Rcrystal / (sourceheight + Aldepth + gap + Lidepth + Lcrystal)]];

xps3sface[2][ξ_] = Lcrystal / ξ;

Bps3sface[1] = Aps3sface[2];

Aps3sface[1] =
 Cos[ArcTan[Rcrystal / (sourceheight + Aldepth + gap + Lidepth)]];

xps3sface[1][ξ_] =
 Rcrystal / Sqrt[1 - ξ^2] - (sourceheight + Aldepth + gap + Lidepth) / ξ;

εtps3sface[e_] := 1/2 * Sum[NIntegrate[(1 - Exp[-ΣGe[e] * xps3sface[i][ξ]]) *
      Exp[-ΣAl[e] * xAl[ξ] - ΣLi[e] * xLi[ξ]],
     {ξ, Aps3sface[i], Bps3sface[i]}], {i, 1, 2}];

εtps3sfacelist = Table[εtps3sface[Mo99gammas[[n]]], {n, 1, 8}];
```

The limits of integration for the solid cylinder with a disk source:

```
A1ds3sface = Cos[0];

B1ds3sface[ϕ_, ρ_] =
 Cos[ArcTan[(-ρ * Sin[ϕ] + Sqrt[ρ^2 * (Sin[ϕ])^2 - (ρ^2 - Rcrystal^2)]) /
    (sourceheight + Aldepth + gap + Lidepth + Lcrystal)]];

x1ds3sface[ξ_] = Lcrystal / ξ;
```

```
A2ds3sface[ϕ_, ρ_] =
 Cos[ArcTan[(-ρ * Sin[ϕ] + √(ρ^2 * (Sin[ϕ])^2 - (ρ^2 - Rcrystal^2))) /
    (sourceheight + Aldepth + gap + Lidepth + Lcrystal)]];

B2ds3sface[ϕ_, ρ_] =
 Cos[ArcTan[(-ρ * Sin[ϕ] + √(ρ^2 * (Sin[ϕ])^2 - (ρ^2 - Rcrystal^2))) /
    (sourceheight + Aldepth + gap + Lidepth)]];

x2ds3sface[ξ_, ϕ_, ρ_] =
 1/√(1 - ξ^2) (-ρ * Sin[ϕ] + √(ρ^2 * (Sin[ϕ])^2 - (ρ^2 - Rcrystal^2))) -
  (sourceheight + Aldepth + gap + Lidepth)/ξ;

εtds3sface1[e_] := 1/(π (Rsource)^2) (NIntegrate[
    NIntegrate[
      NIntegrate[
         (1 - Exp[-ΣGe[e] * x1ds3sface[ξ]]) *
        Exp[-ΣAl[e] * xAl[ξ] - ΣLi[e] * xLi[ξ]],
       {ξ, B1ds3sface[ϕ, ρ], A1ds3sface}], {ϕ, -π/2, π/2}] * ρ,
    {ρ, 0, Rsource}])

εtds3sface1list = Table[εtds3sface1[Mo99gammas[[n]]], {n, 1, 8}];

εtds3sface2[e_] := 1/(π (Rsource)^2) (NIntegrate[
    NIntegrate[
      NIntegrate[
         (1 - Exp[-ΣGe[e] * x2ds3sface[ξ, ϕ, ρ]]) *
        Exp[-ΣAl[e] * xAl[ξ] - ΣLi[e] * xLi[ξ]],
       {ξ, B2ds3sface[ϕ, ρ], A2ds3sface[ϕ, ρ]}], {ϕ, -π/2, π/2}] * ρ,
    {ρ, 0, Rsource}])

εtds3sface2list = Table[εtds3sface2[Mo99gammas[[n]]], {n, 1, 8}];

εtds3sfacelist = εtds3sface1list + εtds3sface2list;
```

The following table shows the contribution of each zone to the total efficiency of the three-sided cylinder with a disk source.

```
TableForm[Table[{εtds3sface1list[[i]],
   εtds3sface2list[[i]], εtds3sfacelist[[i]]}, {i, 1, 8}],
 TableHeadings -> {None, {"Inner Cone Total Eff.",
    "Outer Wedge Total Eff.", "Sum Total Eff."}},
 TableAlignments -> Center];
```

The following is the equation to compute the total efficiency of the five-sided cylindrical detector crystal with a disk source at the face. It is assumed the ratio of the five-sided to three-sided crystal total efficiencies using a point source is the same for using a disk source at the same distance.

$$\varepsilon tds5sfacelist = \frac{\varepsilon tps5sfacelist}{\varepsilon tps3sfacelist} * \varepsilon tds3sfacelist;$$

Using the peak-to-total efficiency ratio calculated above, the peak efficiency of the five-sided crystal with a disk source at the face is shown below:

```
εpds5sfacelist = εtds5sfacelist * PKtoTTLds5slist;
```

To summarize the results up to present, a table is provided below.

```
TableForm[Table[{Mo99gammas[[i]], εtds5sfacelist[[i]],
   εpds5sfacelist[[i]]}, {i, 1, 8}], TableHeadings -> {None,
   {"Gamma (Mev)", "Total Face Efficiency", "Peak Face Efficiency"}},
 TableAlignments -> Center]
```

Gamma (Mev)	Total Face Efficiency	Peak Face Efficiency
0.777921	0.200224	0.0578365
0.7395	0.202814	0.0604324
0.411491	0.230221	0.100272
0.366421	0.235375	0.110815
0.181068	0.29407	0.199408
0.142675	0.311384	0.227668
0.140511	0.312996	0.22907
0.0405845	0.25664	0.0394235

```
TableForm[Table[{Mo99gammas[[i]], εtds3sfacelist[[i]],
   εtps5sfacelist[[i]], εtps3sfacelist[[i]]}, {i, 1, 8}],
 TableHeadings -> {None, {"Mev", "εtds3s", "εtps5s", "εtps3s"}},
 TableAlignments -> Center]
```

Mev	εtds3s	εtps5s	εtps3s
0.777921	0.20133	0.205031	0.206163
0.7395	0.203913	0.207689	0.208815
0.411491	0.231198	0.235803	0.236804
0.366421	0.236318	0.241084	0.242049
0.181068	0.294406	0.300605	0.300948
0.142675	0.31149	0.317405	0.317513
0.140511	0.313083	0.318911	0.319
0.0405845	0.25664	0.259284	0.259284

The next step is to place the various coefficients for the summing correction equations in matrix form. The reference is **(Andreev and others, 1972)**, pg. 1358-1360.

The internal conversion coefficients for Mo-99 are shown below. The reference is **(Peker, 1994)**, pg. 40-41. Due to *Mathematica*'s indexing, the ground state is level 1.

```
a = {{0, 0, 0, 0, 0, 0}, {0.119, 0, 0, 0, 0, 0},
   {29., 0, 0, 0, 0, 0}, {0.126, 3.2, 0, 0, 0, 0}, {0, 0, 0.0076, 0, 0, 0},
   {0, 0, 0.00059, 0.0016, 0.003, 0}};

MatrixForm[a];
```

The following are branch ratios for cascading Mo-99 gammas in Chain 1 (740-181&40-141), Chain 2 (777&411-366), and the Tc-99m Chain (142&2-140). The reference is **(Peker, 1994)**, pg. 40-41. Due to Mathematica's indexing, the ground state is level 1.

```
xMo1 = {{0, 0, 0, 0, 0, 0}, {1, 0, 0, 0, 0, 0}, {0, 0, 0, 0, 0, 0},
   {0.579, 0.421, 0, 0, 0, 0}, {0, 0, 0, 0, 0, 0}, {0, 0, 0, 0.739, 0, 0}};

MatrixForm[xMo1];

xMo2 = {{0, 0, 0, 0, 0, 0}, {0, 0, 0, 0, 0, 0}, {0, 0, 0, 0, 0, 0},
   {0, 0, 0, 0, 0, 0}, {0, 0, 1, 0, 0, 0}, {0, 0, 0.260, 0, 0.001, 0}};

MatrixForm[xMo2];

xTc1 = {{0, 0, 0, 0, 0, 0}, {1, 0, 0, 0, 0, 0}, {0.01, 0.99, 0, 0, 0, 0},
   {0, 0, 0, 0, 0, 0}, {0, 0, 0, 0, 0, 0}, {0, 0, 0, 0, 0, 0}};

MatrixForm[xTc1];
```

The peak face efficiencies are placed in a matrix according to their level transitions.

```
εpface = {{0, 0, 0, 0, 0, 0}, {εpds5sfacelist[[7]], 0, 0, 0, 0, 0},
  {εpds5sfacelist[[6]], 0, 0, 0, 0, 0},
  {εpds5sfacelist[[5]], εpds5sfacelist[[8]], 0, 0, 0, 0},
  {0, 0, εpds5sfacelist[[4]], 0, 0, 0}, {0, 0, εpds5sfacelist[[1]],
   εpds5sfacelist[[2]], εpds5sfacelist[[3]], 0}};

MatrixForm[εpface];

MatrixForm[εpfar];
```

The total face efficiencies are placed in a matrix according to their level transitions.

```
εtface = {{0, 0, 0, 0, 0, 0}, {εtds5sfacelist[[7]], 0, 0, 0, 0, 0},
  {εtds5sfacelist[[6]], 0, 0, 0, 0, 0},
  {εtds5sfacelist[[5]], εtds5sfacelist[[8]], 0, 0, 0, 0},
  {0, 0, εtds5sfacelist[[4]], 0, 0, 0}, {0, 0, εtds5sfacelist[[1]],
   εtds5sfacelist[[2]], εtds5sfacelist[[3]], 0}};

MatrixForm[εtface];

MatrixForm[εtfar];
```

The Mo-99 β- decay branch ratios are listed below in the array. The reference is **(Peker, 1994)**, pg. 42.

```
β = {0, 0, 0.824, 0, 0.012, 0.164};

MatrixForm[β];
```

The following method adjusts the theoretical or normalized angular correlation coefficients for the geometric relation between source and detector. The equation's form is $\bar{W} = 1 + A_{2\,exp} P_2(\cos\theta) + A_{4\,exp} P_4(\cos\theta)$ with $A_{kexp} = A_k Q_k(\gamma_1, \gamma_2)$, A_k being the theoretical coefficient, P_k being the Legendre polynomial of order k, θ being the angle between γ_1 and γ_2, $Q_k = \frac{J_k(\gamma_1)\, J_k(\gamma_2)}{J_0(\gamma_1)\, J_0(\gamma_2)}$ where $J_k(\gamma) = \sum_{i=1}^{Nzones} \int_{A(\alpha)\,i}^{B(\alpha)\,i} P_k(\cos\alpha)\,[1 - \mathrm{Exp}(-\tau(E_\gamma)\, x(\alpha)\, i)]\, \sin\alpha\, d\alpha$. The reference is **(Camp and Van Lehn, 1969)**, pg. 192-240. To calculate the J_k terms will involve repeating the above method of finding ratios of point source/disk source geometries.

The following determines J_2 and J_4 for the three-sided cylinder with the disk source at the face of the detector.

```
J2ds3sface[e_] := 1/(π (Rsource)^2) NIntegrate[
    NIntegrate[
      NIntegrate[
(3/2 * (ξ)^2 - 1/2) * (1 - Exp[-ΣGe[e] * x1ds3sface[ξ]]) *
        Exp[-ΣAl[e] * xAl[ξ] - ΣLi[e] * xLi[ξ]],
       {ξ, B1ds3sface[ϕ, ρ], A1ds3sface}] + NIntegrate[
         (3/2 * (ξ)^2 - 1/2) * (1 - Exp[-ΣGe[e] * x2ds3sface[ξ, ϕ, ρ]]) *
        Exp[-ΣAl[e] * xAl[ξ] - ΣLi[e] * xLi[ξ]],
       {ξ, B2ds3sface[ϕ, ρ], A2ds3sface[ϕ, ρ]}] ,
     {ϕ, -π/2, π/2}] * ρ,
   {ρ, 0, Rsource}]

J2ds3sfar[e_] := 1/(π (Rsource)^2) NIntegrate[
    NIntegrate[
      NIntegrate[
(3/2 * (ξ)^2 - 1/2) * (1 - Exp[-ΣGe[e] * x1ds3sfar[ξ]]) *
        Exp[-ΣAl[e] * xAl[ξ] - ΣLi[e] * xLi[ξ]],
       {ξ, B1ds3sfar[ϕ, ρ], A1ds3sfar}] + NIntegrate[
         (3/2 * (ξ)^2 - 1/2) * (1 - Exp[-ΣGe[e] * x2ds3sfar[ξ, ϕ, ρ]]) *
        Exp[-ΣAl[e] * xAl[ξ] - ΣLi[e] * xLi[ξ]],
       {ξ, B2ds3sfar[ϕ, ρ], A2ds3sfar[ϕ, ρ]}] ,
     {ϕ, -π/2, π/2}] * ρ,
   {ρ, 0, Rsource}]

J2ds3sfacelist = Table[J2ds3sface[Mo99gammas[[i]]], {i, 1, 8}];

J2ds3sfarlist = Table[J2ds3sfar[Mo99gammas[[i]]], {i, 1, 8}];
```

```
J4ds3sface[e_] := 1/(π (Rsource)^2) NIntegrate[
    NIntegrate[
      NIntegrate[
(35/8 * (ξ)^4 - 30/8 * (ξ)^2 + 3/8) * (1 - Exp[-ΣGe[e] * x1ds3sface[ξ]]) *
        Exp[-ΣAl[e] * xAl[ξ] - ΣLi[e] * xLi[ξ]],
       {ξ, B1ds3sface[ϕ, ρ], A1ds3sface}] + NIntegrate[
         (35/8 * (ξ)^4 - 30/8 * (ξ)^2 + 3/8) *
         (1 - Exp[-ΣGe[e] * x2ds3sface[ξ, ϕ, ρ]]) *
         Exp[-ΣAl[e] * xAl[ξ] - ΣLi[e] * xLi[ξ]],
        {ξ, B2ds3sface[ϕ, ρ], A2ds3sface[ϕ, ρ]}] ,
     {ϕ, -π/2, π/2}] * ρ,
   {ρ, 0, Rsource}]

J4ds3sfar[e_] := 1/(π (Rsource)^2) NIntegrate[
    NIntegrate[
      NIntegrate[
(35/8 * (ξ)^4 - 30/8 * (ξ)^2 + 3/8) * (1 - Exp[-ΣGe[e] * x1ds3sfar[ξ]]) *
        Exp[-ΣAl[e] * xAl[ξ] - ΣLi[e] * xLi[ξ]],
       {ξ, B1ds3sfar[ϕ, ρ], A1ds3sfar}] + NIntegrate[
         (35/8 * (ξ)^4 - 30/8 * (ξ)^2 + 3/8) *
         (1 - Exp[-ΣGe[e] * x2ds3sfar[ξ, ϕ, ρ]]) *
         Exp[-ΣAl[e] * xAl[ξ] - ΣLi[e] * xLi[ξ]],
        {ξ, B2ds3sfar[ϕ, ρ], A2ds3sfar[ϕ, ρ]}] ,
     {ϕ, -π/2, π/2}] * ρ,
   {ρ, 0, Rsource}]

J4ds3sfacelist = Table[J4ds3sface[Mo99gammas[[i]]], {i, 1, 8}];

J4ds3sfarlist = Table[J4ds3sfar[Mo99gammas[[i]]], {i, 1, 8}];

Q2ds3sface = Table[1, {i, 1, 6}, {k, 1, 6}, {l, 1, 6}, {m, 1, 6}];

Q2ds3sfar = Table[1, {i, 1, 6}, {k, 1, 6}, {l, 1, 6}, {m, 1, 6}];

Q4ds3sface = Table[1, {i, 1, 6}, {k, 1, 6}, {l, 1, 6}, {m, 1, 6}];

Q4ds3sfar = Table[1, {i, 1, 6}, {k, 1, 6}, {l, 1, 6}, {m, 1, 6}];
```

$$\text{Q2ds3sface[[6, 4, 4, 1]]} = \frac{\text{J2ds3sfacelist[[2]]} * \text{J2ds3sfacelist[[5]]}}{\text{εtds3sfacelist[[2]]} * \text{εtds3sfacelist[[5]]}};$$

$$\text{Q2ds3sfar[[6, 4, 4, 1]]} = \frac{\text{J2ds3sfarlist[[2]]} * \text{J2ds3sfarlist[[5]]}}{\text{εtds3sfarlist[[2]]} * \text{εtds3sfarlist[[5]]}};$$

$$\text{Q4ds3sface[[6, 4, 4, 1]]} = \frac{\text{J4ds3sfacelist[[2]]} * \text{J4ds3sfacelist[[5]]}}{\text{εtds3sfacelist[[2]]} * \text{εtds3sfacelist[[5]]}};$$

$$\text{Q4ds3sfar[[6, 4, 4, 1]]} = \frac{\text{J4ds3sfarlist[[2]]} * \text{J4ds3sfarlist[[5]]}}{\text{εtds3sfarlist[[2]]} * \text{εtds3sfarlist[[5]]}};$$

$$\text{Q2ds3sface[[6, 4, 4, 2]]} = \frac{\text{J2ds3sfacelist[[2]]} * \text{J2ds3sfacelist[[8]]}}{\text{εtds3sfacelist[[2]]} * \text{εtds3sfacelist[[8]]}};$$

$$\text{Q2ds3sfar[[6, 4, 4, 2]]} = \frac{\text{J2ds3sfarlist[[2]]} * \text{J2ds3sfarlist[[8]]}}{\text{εtds3sfarlist[[2]]} * \text{εtds3sfarlist[[8]]}};$$

$$\text{Q4ds3sface[[6, 4, 4, 2]]} = \frac{\text{J4ds3sfacelist[[2]]} * \text{J4ds3sfacelist[[8]]}}{\text{εtds3sfacelist[[2]]} * \text{εtds3sfacelist[[8]]}};$$

$$\text{Q4ds3sfar[[6, 4, 4, 2]]} = \frac{\text{J4ds3sfarlist[[2]]} * \text{J4ds3sfarlist[[8]]}}{\text{εtds3sfarlist[[2]]} * \text{εtds3sfarlist[[8]]}};$$

$$\text{Q2ds3sface[[6, 4, 2, 1]]} = \frac{\text{J2ds3sfacelist[[2]]} * \text{J2ds3sfacelist[[7]]}}{\text{εtds3sfacelist[[2]]} * \text{εtds3sfacelist[[7]]}};$$

$$\text{Q2ds3sfar[[6, 4, 2, 1]]} = \frac{\text{J2ds3sfarlist[[2]]} * \text{J2ds3sfarlist[[7]]}}{\text{εtds3sfarlist[[2]]} * \text{εtds3sfarlist[[7]]}};$$

$$\text{Q4ds3sface[[6, 4, 2, 1]]} = \frac{\text{J4ds3sfacelist[[2]]} * \text{J4ds3sfacelist[[7]]}}{\text{εtds3sfacelist[[2]]} * \text{εtds3sfacelist[[7]]}};$$

$$\text{Q4ds3sfar[[6, 4, 2, 1]]} = \frac{\text{J4ds3sfarlist[[2]]} * \text{J4ds3sfarlist[[7]]}}{\text{εtds3sfarlist[[2]]} * \text{εtds3sfarlist[[7]]}};$$

$$\text{Q2ds3sface[[4, 2, 2, 1]]} = \frac{\text{J2ds3sfacelist[[8]]} * \text{J2ds3sfacelist[[7]]}}{\text{εtds3sfacelist[[8]]} * \text{εtds3sfacelist[[7]]}};$$

$$\text{Q2ds3sfar[[4, 2, 2, 1]]} = \frac{\text{J2ds3sfarlist[[8]]} * \text{J2ds3sfarlist[[7]]}}{\text{εtds3sfarlist[[8]]} * \text{εtds3sfarlist[[7]]}};$$

$$\text{Q4ds3sface[[4, 2, 2, 1]]} = \frac{\text{J4ds3sfacelist[[8]]} * \text{J4ds3sfacelist[[7]]}}{\text{εtds3sfacelist[[8]]} * \text{εtds3sfacelist[[7]]}};$$

$$\text{Q4ds3sfar[[4, 2, 2, 1]]} = \frac{\text{J4ds3sfarlist[[8]]} * \text{J4ds3sfarlist[[7]]}}{\text{εtds3sfarlist[[8]]} * \text{εtds3sfarlist[[7]]}};$$

The following determines J_2 and J_4 for the five-sided cylinder with the point source at the face of the detector.

```
J2ps5sface[e_] :=
 1/2 * Sum[NIntegrate[ (3/2 * (ξ)^2 - 1/2) * (1 - Exp[-ΣGe[e] * xps5sface[i][ξ]]) *
     Exp[-ΣAl[e] * xAl[ξ] - ΣLi[e] * xLi[ξ]],
    {ξ, Aps5sface[i], Bps5sface[i]}], {i, 1, 4}];

J2ps5sfar[e_] :=
 1/2 * Sum[NIntegrate[ (3/2 * (ξ)^2 - 1/2) * (1 - Exp[-ΣGe[e] * xps5sfar[i][ξ]]) *
     Exp[-ΣAl[e] * xAl[ξ] - ΣLi[e] * xLi[ξ]],
    {ξ, Aps5sfar[i], Bps5sfar[i]}], {i, 1, 4}];

J2ps5sfacelist = Table[J2ps5sface[Mo99gammas[[i]]], {i, 1, 8}];

J2ps5sfarlist = Table[J2ps5sfar[Mo99gammas[[i]]], {i, 1, 8}];

J4ps5sface[e_] := 1/2 * Sum[NIntegrate[
     (35/8 * (ξ)^4 - 30/8 * (ξ)^2 + 3/8) * (1 - Exp[-ΣGe[e] * xps5sface[i][ξ]]) *
     Exp[-ΣAl[e] * xAl[ξ] - ΣLi[e] * xLi[ξ]],
    {ξ, Aps5sface[i], Bps5sface[i]}], {i, 1, 4}];

J4ps5sfar[e_] := 1/2 * Sum[NIntegrate[
     (35/8 * (ξ)^4 - 30/8 * (ξ)^2 + 3/8) * (1 - Exp[-ΣGe[e] * xps5sfar[i][ξ]]) *
     Exp[-ΣAl[e] * xAl[ξ] - ΣLi[e] * xLi[ξ]],
    {ξ, Aps5sfar[i], Bps5sfar[i]}], {i, 1, 4}];

J4ps5sfacelist = Table[J4ps5sface[Mo99gammas[[i]]], {i, 1, 8}];

J4ps5sfarlist = Table[J4ps5sfar[Mo99gammas[[i]]], {i, 1, 8}];

Q2ps5sface = Table[1, {i, 1, 6}, {k, 1, 6}, {l, 1, 6}, {m, 1, 6}];

Q2ps5sfar = Table[1, {i, 1, 6}, {k, 1, 6}, {l, 1, 6}, {m, 1, 6}];

Q4ps5sface = Table[1, {i, 1, 6}, {k, 1, 6}, {l, 1, 6}, {m, 1, 6}];

Q4ps5sfar = Table[1, {i, 1, 6}, {k, 1, 6}, {l, 1, 6}, {m, 1, 6}];

Q2ps5sface[[6, 4, 4, 1]] = J2ps5sfacelist[[2]] * J2ps5sfacelist[[5]] /
                           εtps5sfacelist[[2]] * εtps5sfacelist[[5]];
```

$$Q2ps5sfar[[6,4,4,1]] = \frac{J2ps5sfarlist[[2]] * J2ps5sfarlist[[5]]}{\varepsilon tps5sfarlist[[2]] * \varepsilon tps5sfarlist[[5]]};$$

$$Q4ps5sface[[6,4,4,1]] = \frac{J4ps5sfacelist[[2]] * J4ps5sfacelist[[5]]}{\varepsilon tps5sfacelist[[2]] * \varepsilon tps5sfacelist[[5]]};$$

$$Q4ps5sfar[[6,4,4,1]] = \frac{J4ps5sfarlist[[2]] * J4ps5sfarlist[[5]]}{\varepsilon tps5sfarlist[[2]] * \varepsilon tps5sfarlist[[5]]};$$

$$Q2ps5sface[[6,4,4,2]] = \frac{J2ps5sfacelist[[2]] * J2ps5sfacelist[[8]]}{\varepsilon tps5sfacelist[[2]] * \varepsilon tps5sfacelist[[8]]};$$

$$Q2ps5sfar[[6,4,4,2]] = \frac{J2ps5sfarlist[[2]] * J2ps5sfarlist[[8]]}{\varepsilon tps5sfarlist[[2]] * \varepsilon tps5sfarlist[[8]]};$$

$$Q4ps5sface[[6,4,4,2]] = \frac{J4ps5sfacelist[[2]] * J4ps5sfacelist[[8]]}{\varepsilon tps5sfacelist[[2]] * \varepsilon tps5sfacelist[[8]]};$$

$$Q4ps5sfar[[6,4,4,2]] = \frac{J4ps5sfarlist[[2]] * J4ps5sfarlist[[8]]}{\varepsilon tps5sfarlist[[2]] * \varepsilon tps5sfarlist[[8]]};$$

$$Q2ps5sface[[6,4,2,1]] = \frac{J2ps5sfacelist[[2]] * J2ps5sfacelist[[7]]}{\varepsilon tps5sfacelist[[2]] * \varepsilon tps5sfacelist[[7]]};$$

$$Q2ps5sfar[[6,4,2,1]] = \frac{J2ps5sfarlist[[2]] * J2ps5sfarlist[[7]]}{\varepsilon tps5sfarlist[[2]] * \varepsilon tps5sfarlist[[7]]};$$

$$Q4ps5sface[[6,4,2,1]] = \frac{J4ps5sfacelist[[2]] * J4ps5sfacelist[[7]]}{\varepsilon tps5sfacelist[[2]] * \varepsilon tps5sfacelist[[7]]};$$

$$Q4ps5sfar[[6,4,2,1]] = \frac{J4ps5sfarlist[[2]] * J4ps5sfarlist[[7]]}{\varepsilon tps5sfarlist[[2]] * \varepsilon tps5sfarlist[[7]]};$$

$$Q2ps5sface[[4,2,2,1]] = \frac{J2ps5sfacelist[[8]] * J2ps5sfacelist[[7]]}{\varepsilon tps5sfacelist[[8]] * \varepsilon tps5sfacelist[[7]]};$$

$$Q2ps5sfar[[4,2,2,1]] = \frac{J2ps5sfarlist[[8]] * J2ps5sfarlist[[7]]}{\varepsilon tps5sfarlist[[8]] * \varepsilon tps5sfarlist[[7]]};$$

$$Q4ps5sface[[4,2,2,1]] = \frac{J4ps5sfacelist[[8]] * J4ps5sfacelist[[7]]}{\varepsilon tps5sfacelist[[8]] * \varepsilon tps5sfacelist[[7]]};$$

$$Q4ps5sfar[[4,2,2,1]] = \frac{J4ps5sfarlist[[8]] * J4ps5sfarlist[[7]]}{\varepsilon tps5sfarlist[[8]] * \varepsilon tps5sfarlist[[7]]};$$

The following determines J_2 and J_4 for the three-sided cylinder with the point source at the face of the detector.

```
J2ps3sface[e_] :=
 1/2 * Sum[NIntegrate[(3/2 * (ξ)^2 - 1/2) * (1 - Exp[-ΣGe[e] * κps3sface[i][ξ]]) *
     Exp[-ΣAl[e] * κAl[ξ] - ΣLi[e] * κLi[ξ]],
    {ξ, Aps3sface[i], Bps3sface[i]}], {i, 1, 2}];

J2ps3sfar[e_] :=
 1/2 * Sum[NIntegrate[(3/2 * (ξ)^2 - 1/2) * (1 - Exp[-ΣGe[e] * κps3sfar[i][ξ]]) *
     Exp[-ΣAl[e] * κAl[ξ] - ΣLi[e] * κLi[ξ]],
    {ξ, Aps3sfar[i], Bps3sfar[i]}], {i, 1, 2}];

J2ps3sfacelist = Table[J2ps3sface[Mo99gammas[[i]]], {i, 1, 8}];

J2ps3sfarlist = Table[J2ps3sfar[Mo99gammas[[i]]], {i, 1, 8}];

J4ps3sface[e_] := 1/2 * Sum[NIntegrate[
    (35/8 * (ξ)^4 - 30/8 * (ξ)^2 + 3/8) * (1 - Exp[-ΣGe[e] * κps3sface[i][ξ]]) *
     Exp[-ΣAl[e] * κAl[ξ] - ΣLi[e] * κLi[ξ]],
    {ξ, Aps3sface[i], Bps3sface[i]}], {i, 1, 2}];

J4ps3sfar[e_] := 1/2 * Sum[NIntegrate[
    (35/8 * (ξ)^4 - 30/8 * (ξ)^2 + 3/8) * (1 - Exp[-ΣGe[e] * κps3sfar[i][ξ]]) *
     Exp[-ΣAl[e] * κAl[ξ] - ΣLi[e] * κLi[ξ]],
    {ξ, Aps3sfar[i], Bps3sfar[i]}], {i, 1, 2}];

J4ps3sfacelist = Table[J4ps3sface[Mo99gammas[[i]]], {i, 1, 8}];

J4ps3sfarlist = Table[J4ps3sfar[Mo99gammas[[i]]], {i, 1, 8}];

Q2ps3sface = Table[1, {i, 1, 6}, {k, 1, 6}, {l, 1, 6}, {m, 1, 6}];

Q2ps3sfar = Table[1, {i, 1, 6}, {k, 1, 6}, {l, 1, 6}, {m, 1, 6}];

Q4ps3sface = Table[1, {i, 1, 6}, {k, 1, 6}, {l, 1, 6}, {m, 1, 6}];

Q4ps3sfar = Table[1, {i, 1, 6}, {k, 1, 6}, {l, 1, 6}, {m, 1, 6}];

Q2ps3sface[[6, 4, 4, 1]] = J2ps3sfacelist[[2]] * J2ps3sfacelist[[5]] /
    εtps3sfacelist[[2]] * εtps3sfacelist[[5]];
```

$$Q2ps3sfar[[6,4,4,1]] = \frac{J2ps3sfarlist[[2]] * J2ps3sfarlist[[5]]}{\varepsilon tps3sfarlist[[2]] * \varepsilon tps3sfarlist[[5]]};$$

$$Q4ps3sface[[6,4,4,1]] = \frac{J4ps3sfacelist[[2]] * J4ps3sfacelist[[5]]}{\varepsilon tps3sfacelist[[2]] * \varepsilon tps3sfacelist[[5]]};$$

$$Q4ps3sfar[[6,4,4,1]] = \frac{J4ps3sfarlist[[2]] * J4ps3sfarlist[[5]]}{\varepsilon tps3sfarlist[[2]] * \varepsilon tps3sfarlist[[5]]};$$

$$Q2ps3sface[[6,4,4,2]] = \frac{J2ps3sfacelist[[2]] * J2ps3sfacelist[[8]]}{\varepsilon tps3sfacelist[[2]] * \varepsilon tps3sfacelist[[8]]};$$

$$Q2ps3sfar[[6,4,4,2]] = \frac{J2ps3sfarlist[[2]] * J2ps3sfarlist[[8]]}{\varepsilon tps3sfarlist[[2]] * \varepsilon tps3sfarlist[[8]]};$$

$$Q4ps3sface[[6,4,4,2]] = \frac{J4ps3sfacelist[[2]] * J4ps3sfacelist[[8]]}{\varepsilon tps3sfacelist[[2]] * \varepsilon tps3sfacelist[[8]]};$$

$$Q4ps3sfar[[6,4,4,2]] = \frac{J4ps3sfarlist[[2]] * J4ps3sfarlist[[8]]}{\varepsilon tps3sfarlist[[2]] * \varepsilon tps3sfarlist[[8]]};$$

$$Q2ps3sface[[6,4,2,1]] = \frac{J2ps3sfacelist[[2]] * J2ps3sfacelist[[7]]}{\varepsilon tps3sfacelist[[2]] * \varepsilon tps3sfacelist[[7]]};$$

$$Q2ps3sfar[[6,4,2,1]] = \frac{J2ps3sfarlist[[2]] * J2ps3sfarlist[[7]]}{\varepsilon tps3sfarlist[[2]] * \varepsilon tps3sfarlist[[7]]};$$

$$Q4ps3sface[[6,4,2,1]] = \frac{J4ps3sfacelist[[2]] * J4ps3sfacelist[[7]]}{\varepsilon tps3sfacelist[[2]] * \varepsilon tps3sfacelist[[7]]};$$

$$Q4ps3sfar[[6,4,2,1]] = \frac{J4ps3sfarlist[[2]] * J4ps3sfarlist[[7]]}{\varepsilon tps3sfarlist[[2]] * \varepsilon tps3sfarlist[[7]]};$$

$$Q2ps3sface[[4,2,2,1]] = \frac{J2ps3sfacelist[[8]] * J2ps3sfacelist[[7]]}{\varepsilon tps3sfacelist[[8]] * \varepsilon tps3sfacelist[[7]]};$$

$$Q2ps3sfar[[4,2,2,1]] = \frac{J2ps3sfarlist[[8]] * J2ps3sfarlist[[7]]}{\varepsilon tps3sfarlist[[8]] * \varepsilon tps3sfarlist[[7]]};$$

$$Q4ps3sface[[4,2,2,1]] = \frac{J4ps3sfacelist[[8]] * J4ps3sfacelist[[7]]}{\varepsilon tps3sfacelist[[8]] * \varepsilon tps3sfacelist[[7]]};$$

$$Q4ps3sfar[[4,2,2,1]] = \frac{J4ps3sfarlist[[8]] * J4ps3sfarlist[[7]]}{\varepsilon tps3sfarlist[[8]] * \varepsilon tps3sfarlist[[7]]};$$

The following is the equation to compute the J_k of the five-sided cylindrical detector crystal with a disk source at the face. It is assumed the ratio of the five-sided to three-sided crystal J_k's using a point source is the same for using a disk source at the same distance.

$$J2ds5sfacelist = \frac{J2ps5sfacelist}{J2ps3sfacelist} * J2ds3sfacelist;$$

$$J2ds5sfarlist = \frac{J2ps5sfarlist}{J2ps3sfarlist} * J2ds3sfarlist;$$

$$J4ds5sfacelist = \frac{J4ps5sfacelist}{J4ps3sfacelist} * J4ds3sfacelist;$$

$$J4ds5sfarlist = \frac{J4ps5sfarlist}{J4ps3sfarlist} * J4ds3sfarlist;$$

```
Q2ds5sface = Table[1, {i, 1, 6}, {k, 1, 6}, {l, 1, 6}, {m, 1, 6}];

Q2ds5sfar = Table[1, {i, 1, 6}, {k, 1, 6}, {l, 1, 6}, {m, 1, 6}];

Q4ds5sface = Table[1, {i, 1, 6}, {k, 1, 6}, {l, 1, 6}, {m, 1, 6}];

Q4ds5sfar = Table[1, {i, 1, 6}, {k, 1, 6}, {l, 1, 6}, {m, 1, 6}];
```

$$Q2ds5sface[[6, 4, 4, 1]] = \frac{J2ds5sfacelist[[2]] * J2ds5sfacelist[[5]]}{\varepsilon tds5sfacelist[[2]] * \varepsilon tds5sfacelist[[5]]};$$

$$Q2ds5sfar[[6, 4, 4, 1]] = \frac{J2ds5sfarlist[[2]] * J2ds5sfarlist[[5]]}{\varepsilon tds5sfarlist[[2]] * \varepsilon tds5sfarlist[[5]]};$$

$$Q4ds5sface[[6, 4, 4, 1]] = \frac{J4ds5sfacelist[[2]] * J4ds5sfacelist[[5]]}{\varepsilon tds5sfacelist[[2]] * \varepsilon tds5sfacelist[[5]]};$$

$$Q4ds5sfar[[6, 4, 4, 1]] = \frac{J4ds5sfarlist[[2]] * J4ds5sfarlist[[5]]}{\varepsilon tds5sfarlist[[2]] * \varepsilon tds5sfarlist[[5]]};$$

$$Q2ds5sface[[6, 4, 4, 2]] = \frac{J2ds5sfacelist[[2]] * J2ds5sfacelist[[8]]}{\varepsilon tds5sfacelist[[2]] * \varepsilon tds5sfacelist[[8]]};$$

$$Q2ds5sfar[[6, 4, 4, 2]] = \frac{J2ds5sfarlist[[2]] * J2ds5sfarlist[[8]]}{\varepsilon tds5sfarlist[[2]] * \varepsilon tds5sfarlist[[8]]};$$

$$Q4ds5sface[[6, 4, 4, 2]] = \frac{J4ds5sfacelist[[2]] * J4ds5sfacelist[[8]]}{\varepsilon tds5sfacelist[[2]] * \varepsilon tds5sfacelist[[8]]};$$

$$Q4ds5sfar[[6, 4, 4, 2]] = \frac{J4ds5sfarlist[[2]] * J4ds5sfarlist[[8]]}{\varepsilon tds5sfarlist[[2]] * \varepsilon tds5sfarlist[[8]]};$$

$$Q2ds5sface[[6, 4, 2, 1]] = \frac{J2ds5sfacelist[[2]] * J2ds5sfacelist[[7]]}{\varepsilon tds5sfacelist[[2]] * \varepsilon tds5sfacelist[[7]]};$$

$$Q2ds5sfar[[6, 4, 2, 1]] = \frac{J2ds5sfarlist[[2]] * J2ds5sfarlist[[7]]}{\varepsilon tds5sfarlist[[2]] * \varepsilon tds5sfarlist[[7]]};$$

$$Q4ds5sface[[6, 4, 2, 1]] = \frac{J4ds5sfacelist[[2]] * J4ds5sfacelist[[7]]}{\varepsilon tds5sfacelist[[2]] * \varepsilon tds5sfacelist[[7]]};$$

$$Q4ds5sfar[[6,4,2,1]] = \frac{J4ds5sfarlist[[2]] * J4ds5sfarlist[[7]]}{\varepsilon tds5sfarlist[[2]] * \varepsilon tds5sfarlist[[7]]};$$

$$Q2ds5sface[[4,2,2,1]] = \frac{J2ds5sfacelist[[8]] * J2ds5sfacelist[[7]]}{\varepsilon tds5sfacelist[[8]] * \varepsilon tds5sfacelist[[7]]};$$

$$Q2ds5sfar[[4,2,2,1]] = \frac{J2ds5sfarlist[[8]] * J2ds5sfarlist[[7]]}{\varepsilon tds5sfarlist[[8]] * \varepsilon tds5sfarlist[[7]]};$$

$$Q4ds5sface[[4,2,2,1]] = \frac{J4ds5sfacelist[[8]] * J4ds5sfacelist[[7]]}{\varepsilon tds5sfacelist[[8]] * \varepsilon tds5sfacelist[[7]]};$$

$$Q4ds5sfar[[4,2,2,1]] = \frac{J4ds5sfarlist[[8]] * J4ds5sfarlist[[7]]}{\varepsilon tds5sfarlist[[8]] * \varepsilon tds5sfarlist[[7]]};$$

The following creates and initializes the matrix of angular correlation coefficients between cascading Mo-99 gammas. The reference is **(Gardulski and Wiedenbeck, 1974)**, pg. 262-265.

```
Wps5sface = Table[1, {i, 1, 6}, {k, 1, 6}, {l, 1, 6}, {m, 1, 6}];

Wps5sfar = Table[1, {i, 1, 6}, {k, 1, 6}, {l, 1, 6}, {m, 1, 6}];

Wps5sface[[6, 4, 4, 1]] =
 1 + .061 * Q2ps5sface[[6, 4, 4, 1]] - .004 * Q4ps5sface[[6, 4, 4, 1]];

Wps5sfar[[6, 4, 4, 1]] =
 1 + .061 * Q2ps5sfar[[6, 4, 4, 1]] - .004 * Q4ps5sfar[[6, 4, 4, 1]];

Wps5sface[[6, 4, 4, 2]] =
 1 - .089 * Q2ps5sface[[6, 4, 4, 2]] - .002 * Q4ps5sface[[6, 4, 4, 2]];

Wps5sfar[[6, 4, 4, 2]] =
 1 - .089 * Q2ps5sfar[[6, 4, 4, 2]] - .002 * Q4ps5sfar[[6, 4, 4, 2]];

Wps5sface[[6, 4, 2, 1]] =
 1 - .083 * Q2ps5sface[[6, 4, 2, 1]] + .007 * Q4ps5sface[[6, 4, 2, 1]];

Wps5sfar[[6, 4, 2, 1]] =
 1 - .083 * Q2ps5sfar[[6, 4, 2, 1]] + .007 * Q4ps5sfar[[6, 4, 2, 1]];

Wps5sface[[4, 2, 2, 1]] =
 1 + .113 * Q2ps5sface[[4, 2, 2, 1]] + .004 * Q4ps5sface[[4, 2, 2, 1]];

Wps5sfar[[4, 2, 2, 1]] =
 1 + .113 * Q2ps5sfar[[4, 2, 2, 1]] + .004 * Q4ps5sfar[[4, 2, 2, 1]];

Wps3sface = Table[1, {i, 1, 6}, {k, 1, 6}, {l, 1, 6}, {m, 1, 6}];

Wps3sfar = Table[1, {i, 1, 6}, {k, 1, 6}, {l, 1, 6}, {m, 1, 6}];
```

```
Wps3sface[[6, 4, 4, 1]] =
 1 + .061 * Q2ps3sface[[6, 4, 4, 1]] - .004 * Q4ps3sface[[6, 4, 4, 1]];

Wps3sfar[[6, 4, 4, 1]] =
 1 + .061 * Q2ps3sfar[[6, 4, 4, 1]] - .004 * Q4ps3sfar[[6, 4, 4, 1]];

Wps3sface[[6, 4, 4, 2]] =
 1 - .089 * Q2ps3sface[[6, 4, 4, 2]] - .002 * Q4ps3sface[[6, 4, 4, 2]];

Wps3sfar[[6, 4, 4, 2]] =
 1 - .089 * Q2ps3sfar[[6, 4, 4, 2]] - .002 * Q4ps3sfar[[6, 4, 4, 2]];

Wps3sface[[6, 4, 2, 1]] =
 1 - .083 * Q2ps3sface[[6, 4, 2, 1]] + .007 * Q4ps3sface[[6, 4, 2, 1]];

Wps3sfar[[6, 4, 2, 1]] =
 1 - .083 * Q2ps3sfar[[6, 4, 2, 1]] + .007 * Q4ps3sfar[[6, 4, 2, 1]];

Wps3sface[[4, 2, 2, 1]] =
 1 + .113 * Q2ps3sface[[4, 2, 2, 1]] + .004 * Q4ps3sface[[4, 2, 2, 1]];

Wps3sfar[[4, 2, 2, 1]] =
 1 + .113 * Q2ps3sfar[[4, 2, 2, 1]] + .004 * Q4ps3sfar[[4, 2, 2, 1]];

Wds3sface = Table[1, {i, 1, 6}, {k, 1, 6}, {l, 1, 6}, {m, 1, 6}];

Wds3sfar = Table[1, {i, 1, 6}, {k, 1, 6}, {l, 1, 6}, {m, 1, 6}];

Wds3sface[[6, 4, 4, 1]] =
 1 + .061 * Q2ds3sface[[6, 4, 4, 1]] - .004 * Q4ds3sface[[6, 4, 4, 1]];

Wds3sfar[[6, 4, 4, 1]] =
 1 + .061 * Q2ds3sfar[[6, 4, 4, 1]] - .004 * Q4ds3sfar[[6, 4, 4, 1]];

Wds3sface[[6, 4, 4, 2]] =
 1 - .089 * Q2ds3sface[[6, 4, 4, 2]] - .002 * Q4ds3sface[[6, 4, 4, 2]];

Wds3sfar[[6, 4, 4, 2]] =
 1 - .089 * Q2ds3sfar[[6, 4, 4, 2]] - .002 * Q4ds3sfar[[6, 4, 4, 2]];

Wds3sface[[6, 4, 2, 1]] =
 1 - .083 * Q2ds3sface[[6, 4, 2, 1]] + .007 * Q4ds3sface[[6, 4, 2, 1]];

Wds3sfar[[6, 4, 2, 1]] =
 1 - .083 * Q2ds3sfar[[6, 4, 2, 1]] + .007 * Q4ds3sfar[[6, 4, 2, 1]];

Wds3sface[[4, 2, 2, 1]] =
 1 + .113 * Q2ds3sface[[4, 2, 2, 1]] + .004 * Q4ds3sface[[4, 2, 2, 1]];
```

```
Wds3sfar[[4, 2, 2, 1]] =
 1 + .113 * Q2ds3sfar[[4, 2, 2, 1]] + .004 * Q4ds3sfar[[4, 2, 2, 1]];
```

Now, the correlation factors are combined to make the one for the five-sided detector with a disk source.

```
Wds5sface = Table[1, {i, 1, 6}, {k, 1, 6}, {l, 1, 6}, {m, 1, 6}];

Wds5sfar = Table[1, {i, 1, 6}, {k, 1, 6}, {l, 1, 6}, {m, 1, 6}];

Wds5sface[[6, 4, 4, 1]] =
 1 + .061 * Q2ds5sface[[6, 4, 4, 1]] - .004 * Q4ds5sface[[6, 4, 4, 1]];

Wds5sfar[[6, 4, 4, 1]] =
 1 + .061 * Q2ds5sfar[[6, 4, 4, 1]] - .004 * Q4ds5sfar[[6, 4, 4, 1]];

Wds5sface[[6, 4, 4, 2]] =
 1 - .089 * Q2ds5sface[[6, 4, 4, 2]] - .002 * Q4ds5sface[[6, 4, 4, 2]];

Wds5sfar[[6, 4, 4, 2]] =
 1 - .089 * Q2ds5sfar[[6, 4, 4, 2]] - .002 * Q4ds5sfar[[6, 4, 4, 2]];

Wds5sface[[6, 4, 2, 1]] =
 1 - .083 * Q2ds5sface[[6, 4, 2, 1]] + .007 * Q4ds5sface[[6, 4, 2, 1]];

Wds5sfar[[6, 4, 2, 1]] =
 1 - .083 * Q2ds5sfar[[6, 4, 2, 1]] + .007 * Q4ds5sfar[[6, 4, 2, 1]];

Wds5sface[[4, 2, 2, 1]] =
 1 + .113 * Q2ds5sface[[4, 2, 2, 1]] + .004 * Q4ds5sface[[4, 2, 2, 1]];

Wds5sfar[[4, 2, 2, 1]] =
 1 + .113 * Q2ds5sfar[[4, 2, 2, 1]] + .004 * Q4ds5sfar[[4, 2, 2, 1]];

wlist = {"W[6,4,4,1]", "W[6,4,4,2]", "W[6,4,2,1]", "W[4,2,2,1]"};
```

The tables below compare the correlation factors for the various geometries.

```
TableForm[{{wlist[[1]], Wps3sfar[[6, 4, 4, 1]],
   Wps5sfar[[6, 4, 4, 1]], Wds3sfar[[6, 4, 4, 1]], Wds5sfar[[6, 4, 4, 1]]},
  {wlist[[2]], Wps3sfar[[6, 4, 4, 2]],
   Wps5sfar[[6, 4, 4, 2]], Wds3sfar[[6, 4, 4, 2]], Wds5sfar[[6, 4, 4, 2]]},
  {wlist[[3]], Wps3sfar[[6, 4, 2, 1]],
   Wps5sfar[[6, 4, 2, 1]], Wds3sfar[[6, 4, 2, 1]], Wds5sfar[[6, 4, 2, 1]]},
  {wlist[[4]], Wps3sfar[[4, 2, 2, 1]], Wps5sfar[[4, 2, 2, 1]],
   Wds3sfar[[4, 2, 2, 1]], Wds5sfar[[4, 2, 2, 1]]}}, TableHeadings ->
  {None, {"Cascade", "Wps3sfar", "Wps5sfar", "Wds3sfar", "Wds5sfar"}},
 TableAlignments -> Center]
```

Cascade	Wps3sfar	Wps5sfar	Wds3sfar	Wds5sfar
W[6,4,4,1]	1.0525	1.05248	1.05206	1.05204
W[6,4,4,2]	0.918297	0.918327	0.919145	0.919175
W[6,4,2,1]	0.929824	0.929846	0.930396	0.930418
W[4,2,2,1]	1.1039	1.10389	1.10273	1.10272

```
TableForm[{{wlist[[1]], Wps3sface[[6, 4, 4, 1]], Wps5sface[[6, 4, 4, 1]],
   Wds3sface[[6, 4, 4, 1]], Wds5sface[[6, 4, 4, 1]]},
  {wlist[[2]], Wps3sface[[6, 4, 4, 2]], Wps5sface[[6, 4, 4, 2]],
   Wds3sface[[6, 4, 4, 2]], Wds5sface[[6, 4, 4, 2]]},
  {wlist[[3]], Wps3sface[[6, 4, 2, 1]], Wps5sface[[6, 4, 2, 1]],
   Wds3sface[[6, 4, 2, 1]], Wds5sface[[6, 4, 2, 1]]},
  {wlist[[4]], Wps3sface[[4, 2, 2, 1]], Wps5sface[[4, 2, 2, 1]],
   Wds3sface[[4, 2, 2, 1]], Wds5sface[[4, 2, 2, 1]]}},
 TableHeadings -> {None,
   {"Cascade", "Wps3sface", "Wps5sface", "Wds3sface", "Wds5sface"}},
 TableAlignments -> Center]
```

Cascade	Wps3sface	Wps5sface	Wds3sface	Wds5sface
W[6,4,4,1]	1.00405	1.00398	1.00423	1.00415
W[6,4,4,2]	0.994496	0.994563	0.994286	0.994356
W[6,4,2,1]	0.995169	0.99524	0.99492	0.994993
W[4,2,2,1]	1.00459	1.00458	1.0049	1.0049

The following method determines the fraction of counts underneath an observed energy peak. The peak represents the sum of direct and true coincidence gamma rays depositing the given energy. The true activity has been normalized to one. This method does not include the angular correlation coefficient W. The reference is **(Andreev and others, 1972)**, pg. 1359.

The number of energy levels in Mo-99 in the simplified decay scheme is six (five plus ground state). However due to Mathematica's automatic indexing at one, m = 6. The terms are decoupled along the decay chains in order to calculate their contributions. They will be summed at the end.

```
m = 6;

aMo1far = Table[xMo1[[i, k]] * εpfar[[i, k]] / (1 + a[[i, k]]), {i, 1, m}, {k, 1, m}];

aMo1face = Table[xMo1[[i, k]] * εpface[[i, k]] / (1 + a[[i, k]]), {i, 1, m}, {k, 1, m}];

MatrixForm[aMo1face];

MatrixForm[aMo1far];

bMo1face = Table[xMo1[[i, k]] * (1 - εtface[[i, k]] / (1 + a[[i, k]])), {i, 1, m}, {k, 1, m}];

bMo1far = Table[xMo1[[i, k]] * (1 - εtfar[[i, k]] / (1 + a[[i, k]])), {i, 1, m}, {k, 1, m}];

MatrixForm[bMo1face];

MatrixForm[bMo1far];

ℬMo1face = {0, 0, 0, 0, 0, 0};

ℬMo1far = {0, 0, 0, 0, 0, 0};

Do[ℬMo1face[[i]] = β[[i]] + Sum[ℬMo1face[[n]] * bMo1face[[n, i]], {n, i+1, m}],
 {i, m, 1, -1}]

Do[ℬMo1far[[i]] = β[[i]] + Sum[ℬMo1far[[n]] * bMo1far[[n, i]], {n, i+1, m}], {i, m, 1, -1}]

MatrixForm[ℬMo1face];

MatrixForm[ℬMo1far];

𝒩Mo1face = {1, 1, 1, 1, 1, 0};

𝒩Mo1far = {1, 1, 1, 1, 1, 0};

mm = m - 1;

Do[𝒩Mo1face[[k]] = Sum[bMo1face[[k, j]] * 𝒩Mo1face[[j]], {j, 1, k-1}], {k, 2, mm}]

Do[𝒩Mo1far[[k]] = Sum[bMo1far[[k, j]] * 𝒩Mo1far[[j]], {j, 1, k-1}], {k, 2, mm}]

MatrixForm[𝒩Mo1face];
```

```
MatrixForm[𝒩Mo1far];

𝒜Mo1face = Table[0, {i, 1, m}, {j, 1, m}];

𝒜Mo1far = Table[0, {i, 1, m}, {j, 1, m}];

Do[Do[𝒜Mo1face[[i, k]] =
    aMo1face[[i, k]] + Sum[aMo1face[[i, j]] * 𝒜Mo1face[[j, k]], {j, k+1, i-1}], {k, 1, i}],
 {i, 2, m}]

Do[Do[𝒜Mo1far[[i, k]] =
    aMo1far[[i, k]] + Sum[aMo1far[[i, j]] * 𝒜Mo1far[[j, k]], {j, k+1, i-1}], {k, 1, i}],
 {i, 2, m}]

MatrixForm[𝒜Mo1face];

MatrixForm[𝒜Mo1far];

𝒮Mo1face = Table[ℬMo1face[[i]] * 𝒜Mo1face[[i, k]] * 𝒩Mo1face[[k]],
  {i, 1, m}, {k, 1, m}];

𝒮Mo1far =
 Table[ℬMo1far[[i]] * 𝒜Mo1far[[i, k]] * 𝒩Mo1far[[k]], {i, 1, m}, {k, 1, m}];

MatrixForm[𝒮Mo1face];

MatrixForm[𝒮Mo1far];
```

The following is the contribution from the second, decoupled Mo-99 decay chain.

```
ℬMo2face = {0, 0, 0, 0, 0, 0};

ℬMo2far = {0, 0, 0, 0, 0, 0};

𝒜Mo2face = Table[0, {i, 1, m}, {j, 1, m}];

𝒜Mo2far = Table[0, {i, 1, m}, {j, 1, m}];

𝒩Mo2face = {0, 0, 0, 0, 0, 0};

𝒩Mo2far = {0, 0, 0, 0, 0, 0};

𝒮Mo2face = Table[0, {i, 1, m}, {k, 1, m}];

𝒮Mo2far = Table[0, {i, 1, m}, {k, 1, m}];
```

$$\mathcal{B}\text{Mo2face}[[5]] = \left(\beta[[5]] + \beta[[6]] * x\text{Mo2}[[6, 5]] * \left(1 - \frac{\varepsilon\text{tface}[[6, 5]]}{1 + a[[6, 5]]}\right)\right);$$

$$\mathcal{A}\text{Mo2face}[[5, 3]] = \left(\frac{x\text{Mo2}[[5, 3]] * \varepsilon\text{pface}[[5, 3]]}{1 + a[[5, 3]]}\right);$$

$$\mathcal{M}\text{Mo2face}[[3]] = (1);$$

$$\mathcal{S}\text{Mo2face}[[5, 3]] = \left(\beta[[5]] + \beta[[6]] * x\text{Mo2}[[6, 5]] * \left(1 - \frac{\varepsilon\text{tface}[[6, 5]]}{1 + a[[6, 5]]}\right)\right) * \left(\frac{x\text{Mo2}[[5, 3]] * \varepsilon\text{pface}[[5, 3]]}{1 + a[[5, 3]]}\right) * (1);$$

$$\mathcal{B}\text{Mo2far}[[5]] = \left(\beta[[5]] + \beta[[6]] * x\text{Mo2}[[6, 5]] * \left(1 - \frac{\varepsilon\text{tfar}[[6, 5]]}{1 + a[[6, 5]]}\right)\right);$$

$$\mathcal{A}\text{Mo2far}[[5, 3]] = \left(\frac{x\text{Mo2}[[5, 3]] * \varepsilon\text{pfar}[[5, 3]]}{1 + a[[5, 3]]}\right);$$

$$\mathcal{M}\text{Mo2far}[[3]] = (1);$$

$$\mathcal{S}\text{Mo2far}[[5, 3]] = \left(\beta[[5]] + \beta[[6]] * x\text{Mo2}[[6, 5]] * \left(1 - \frac{\varepsilon\text{tfar}[[6, 5]]}{1 + a[[6, 5]]}\right)\right) * \left(\frac{x\text{Mo2}[[5, 3]] * \varepsilon\text{pfar}[[5, 3]]}{1 + a[[5, 3]]}\right) * (1);$$

$$\mathcal{B}\text{Mo2face}[[6]] = (\beta[[6]]);$$

$$\mathcal{A}\text{Mo2face}[[6, 3]] = \left(\frac{x\text{Mo2}[[6, 3]] * \varepsilon\text{pface}[[6, 3]]}{1 + a[[6, 3]]} + \frac{x\text{Mo2}[[5, 3]] * \varepsilon\text{pface}[[5, 3]]}{1 + a[[5, 3]]} * \frac{x\text{Mo2}[[6, 5]] * \varepsilon\text{pface}[[6, 5]]}{1 + a[[6, 5]]}\right);$$

$$\mathcal{M}\text{Mo2face}[[3]] = (1);$$

$$\mathcal{S}\text{Mo2face}[[6, 3]] = (\beta[[6]]) * \left(\frac{x\text{Mo2}[[6, 3]] * \varepsilon\text{pface}[[6, 3]]}{1 + a[[6, 3]]} + \frac{x\text{Mo2}[[5, 3]] * \varepsilon\text{pface}[[5, 3]]}{1 + a[[5, 3]]} * \frac{x\text{Mo2}[[6, 5]] * \varepsilon\text{pface}[[6, 5]]}{1 + a[[6, 5]]}\right) * (1);$$

$$\mathcal{B}\text{Mo2far}[[6]] = (\beta[[6]]);$$

$$\mathcal{A}\text{Mo2far}[[6, 3]] = \left(\frac{x\text{Mo2}[[6, 3]] * \varepsilon\text{pfar}[[6, 3]]}{1 + a[[6, 3]]} + \frac{x\text{Mo2}[[5, 3]] * \varepsilon\text{pfar}[[5, 3]]}{1 + a[[5, 3]]} * \frac{x\text{Mo2}[[6, 5]] * \varepsilon\text{pfar}[[6, 5]]}{1 + a[[6, 5]]}\right);$$

$$\mathcal{M}\text{Mo2far}[[3]] = (1);$$

$$\mathcal{S}\text{Mo2far}[[6,3]] = (\beta[[6]]) * \left(\frac{x\text{Mo2}[[6,3]] * \varepsilon\text{pfar}[[6,3]]}{1+a[[6,3]]} + \frac{x\text{Mo2}[[5,3]] * \varepsilon\text{pfar}[[5,3]]}{1+a[[5,3]]} * \frac{x\text{Mo2}[[6,5]] * \varepsilon\text{pfar}[[6,5]]}{1+a[[6,5]]}\right) * (1);$$

$$\mathcal{A}\text{Mo2face}[[6,5]] = \left(\frac{x\text{Mo2}[[6,5]] * \varepsilon\text{pface}[[6,5]]}{1+a[[6,5]]}\right);$$

$$\mathcal{M}\text{Mo2face}[[5]] = x\text{Mo2}[[5,3]] * \left(1 - \frac{\varepsilon\text{tface}[[5,3]]}{1+a[[5,3]]}\right);$$

$$\mathcal{S}\text{Mo2face}[[6,5]] = (\beta[[6]]) * \left(\frac{x\text{Mo2}[[6,5]] * \varepsilon\text{pface}[[6,5]]}{1+a[[6,5]]}\right) * \left(x\text{Mo2}[[5,3]] * \left(1 - \frac{\varepsilon\text{tface}[[5,3]]}{1+a[[5,3]]}\right)\right);$$

$$\mathcal{A}\text{Mo2far}[[6,5]] = \left(\frac{x\text{Mo2}[[6,5]] * \varepsilon\text{pfar}[[6,5]]}{1+a[[6,5]]}\right);$$

$$\mathcal{M}\text{Mo2far}[[5]] = x\text{Mo2}[[5,3]] * \left(1 - \frac{\varepsilon\text{tfar}[[5,3]]}{1+a[[5,3]]}\right);$$

$$\mathcal{S}\text{Mo2far}[[6,5]] = (\beta[[6]]) * \left(\frac{x\text{Mo2}[[6,5]] * \varepsilon\text{pfar}[[6,5]]}{1+a[[6,5]]}\right) * \left(x\text{Mo2}[[5,3]] * \left(1 - \frac{\varepsilon\text{tfar}[[5,3]]}{1+a[[5,3]]}\right)\right);$$

The following is the contribution from the third, decoupled Tc-99m decay chain. Due to the near zero detection efficiency of a 2.1726 keV gamma ray, the $\mathcal{S}$Tc1[[3,2]] contribution is negligible.

$$\beta\text{Tc1} = \frac{\beta[[6]] * x\text{Mo2}[[6,3]]}{1+a[[6,3]]} + \frac{\beta[[5]] * x\text{Mo2}[[5,3]]}{1+a[[5,3]]} * \left(1 + \frac{\beta[[6]] * x\text{Mo2}[[6,5]]}{1+a[[6,5]]}\right) + \beta[[3]];$$

```
ℬTc1face = {0, 0, 0, 0, 0, 0};

ℬTc1far = {0, 0, 0, 0, 0, 0};

𝒜Tc1face = Table[0, {i, 1, m}, {j, 1, m}];

𝒜Tc1far = Table[0, {i, 1, m}, {j, 1, m}];

ℳTc1face = {0, 0, 0, 0, 0, 0};

ℳTc1far = {0, 0, 0, 0, 0, 0};

𝒮Tc1face = Table[0, {i, 1, m}, {k, 1, m}];
```

```
STc1far = Table[0, {i, 1, m}, {k, 1, m}];

BTc1face[[2]] = (βTc1 * xTc1[[3, 2]]);

ATc1face[[2, 1]] = (xTc1[[2, 1]] * εpface[[2, 1]]) / (1 + a[[2, 1]]);

MTc1face[[1]] = (1);

STc1face[[2, 1]] =
 (βTc1 * xTc1[[3, 2]]) * (xTc1[[2, 1]] * εpface[[2, 1]]) / (1 + a[[2, 1]]) * (1);

BTc1far[[2]] = (βTc1 * xTc1[[3, 2]]);

ATc1far[[2, 1]] = (xTc1[[2, 1]] * εpfar[[2, 1]]) / (1 + a[[2, 1]]);

MTc1far[[1]] = (1);

STc1far[[2, 1]] = (βTc1 * xTc1[[3, 2]]) * (xTc1[[2, 1]] * εpfar[[2, 1]]) / (1 + a[[2, 1]]) * (1);

BTc1face[[3]] = (βTc1);

ATc1face[[3, 1]] = (xTc1[[3, 1]] * εpface[[3, 1]]) / (1 + a[[3, 1]]);

STc1face[[3, 1]] = (βTc1) * (xTc1[[3, 1]] * εpface[[3, 1]]) / (1 + a[[3, 1]]) * (1);

BTc1far[[3]] = (βTc1);

ATc1far[[3, 1]] = (xTc1[[3, 1]] * εpfar[[3, 1]]) / (1 + a[[3, 1]]);

STc1far[[3, 1]] = (βTc1) * (xTc1[[3, 1]] * εpfar[[3, 1]]) / (1 + a[[3, 1]]) * (1);
```

The following combines all the contributions from the decoupled decay chains. Note: It is assumed that Tc-99m is in secular equilibrium with Mo-99; i.e., their activities are equal.

```
Sfar = STc1far + SMo1far + SMo2far;
```

```
MatrixForm[Sfar]
```

$$\begin{pmatrix} 0 & 0 & 0 & 0 & 0 & 0 \\ 0.00976995 & 0 & 0 & 0 & 0 & 0 \\ 3.4602\times10^{-6} & 0 & 0 & 0 & 0 & 0 \\ 0.000645766 & 0.0000274028 & 0 & 0 & 0 & 0 \\ 0 & 0 & 0.0000742688 & 0 & 0 & 0 \\ 2.23977\times10^{-6} & 9.50439\times10^{-8} & 0.000140289 & 0.000409061 & 9.02149\times10^{-7} & 0 \end{pmatrix}$$

```
Sface = STc1face + SMo1face + SMo2face;
```

```
MatrixForm[Sface]
```

$$\begin{pmatrix} 0 & 0 & 0 & 0 & 0 & 0 \\ 0.185865 & 0 & 0 & 0 & 0 & 0 \\ 0.0000666706 & 0 & 0 & 0 & 0 & 0 \\ 0.00998895 & 0.000275118 & 0 & 0 & 0 & 0 \\ 0 & 0 & 0.00133364 & 0 & 0 & 0 \\ 0.000755717 & 0.0000208141 & 0.0024665 & 0.00521012 & 0.0000125654 & 0 \end{pmatrix}$$

The following is to show an estimate of the uncorrected values ignoring summing-in and -out effects.

```
Sunface = Table[0, {i, 1, m}, {k, 1, m}];
```

```
Sunfar = Table[0, {i, 1, m}, {k, 1, m}];
```

```
x = xMo1 + xMo2 + xTc1;
```

```
x[[2, 1]] = 1;
```

```
Do[
 Do[Sunface[[i, k]] = β[[i]] + Sum[Sunface[[n, i]] * x[[n, i]], {n, i+1, m}], {k, 1, mm}],
 {i, m, 1, -1}]
```

```
Do[Do[Sunfar[[i, k]] = β[[i]] + Sum[Sunfar[[n, i]] * x[[n, i]], {n, i+1, m}], {k, 1, mm}],
 {i, m, 1, -1}]
```

```
Aunface = Table[0, {i, 1, m}, {j, 1, m}];
```

```
Aunfar = Table[0, {i, 1, m}, {j, 1, m}];
```

```
Do[Do[Aunface[[i, k]] = x[[i, k]] * εpface[[i, k]] / (1 + a[[i, k]]), {k, 1, i}], {i, 2, m}]
```

```
Do[Do[Aunfar[[i, k]] = x[[i, k]] * εpfar[[i, k]] / (1 + a[[i, k]]), {k, 1, i}], {i, 2, m}]
```

```
Munface = Table[1, {i, 1, m}, {k, 1, m}];

Munfar = Table[1, {i, 1, m}, {k, 1, m}];

Sunface = Table[Bunface[[i, k]] * Aunface[[i, k]] * Munface[[i, k]],
  {i, 1, m}, {k, 1, m}];

Sunfacelist =
 {Sunface[[6, 3]], Sunface[[6, 4]], Sunface[[6, 5]], Sunface[[5, 3]],
  Sunface[[4, 1]], Sunface[[3, 1]], Sunface[[2, 1]], Sunface[[4, 2]]};

Sunfar = Table[Bunfar[[i, k]] * Afunfar[[i, k]] * Munfar[[i, k]],
  {i, 1, m}, {k, 1, m}];

Sunfarlist =
 {Sunfar[[6, 3]], Sunfar[[6, 4]], Sunfar[[6, 5]], Sunfar[[5, 3]],
  Sunfar[[4, 1]], Sunfar[[3, 1]], Sunfar[[2, 1]], Sunfar[[4, 2]]};

MatrixForm[Sunface]
```

$$\begin{pmatrix} 0 & 0 & 0 & 0 & 0 & 0 \\ 0.188545 & 0 & 0 & 0 & 0 & 0 \\ 0.0000666917 & 0 & 0 & 0 & 0 & 0 \\ 0.0124271 & 0.000478934 & 0 & 0 & 0 & 0 \\ 0 & 0 & 0.00133778 & 0 & 0 & 0 \\ 0 & 0 & 0.00246469 & 0.00731246 & 0.0000163954 & 0 \end{pmatrix}$$

```
MatrixForm[Sunfar]
```

$$\begin{pmatrix} 0 & 0 & 0 & 0 & 0 & 0 \\ 0.00978103 & 0 & 0 & 0 & 0 & 0 \\ 3.46129 \times 10^{-6} & 0 & 0 & 0 & 0 & 0 \\ 0.000652984 & 0.00002813 & 0 & 0 & 0 & 0 \\ 0 & 0 & 0.0000742816 & 0 & 0 & 0 \\ 0 & 0 & 0.000140284 & 0.000415519 & 9.14004 \times 10^{-7} & 0 \end{pmatrix}$$

```
MatrixForm[Evaluate[Sface / Sunface]];

Ratiofacelist =
 {Evaluate[Sface / Sunface][[6, 3]], Evaluate[Sface / Sunface][[6, 4]],
  Evaluate[Sface / Sunface][[6, 5]], Evaluate[Sface / Sunface][[5, 3]],
  Evaluate[Sface / Sunface][[4, 1]], Evaluate[Sface / Sunface][[3, 1]],
  Evaluate[Sface / Sunface][[2, 1]], Evaluate[Sface / Sunface][[4, 2]]};

MatrixForm[Evaluate[Sfar / Sunfar]];
```

```
Ratiofarlist =
 {Evaluate[Sfar / Sunfar][[6, 3]], Evaluate[Sfar / Sunfar][[6, 4]],
  Evaluate[Sfar / Sunfar][[6, 5]], Evaluate[Sfar / Sunfar][[5, 3]],
  Evaluate[Sfar / Sunfar][[4, 1]], Evaluate[Sfar / Sunfar][[3, 1]],
  Evaluate[Sfar / Sunfar][[2, 1]], Evaluate[Sfar / Sunfar][[4, 2]]};
```

$$\text{MatrixForm}\left[\text{Evaluate}\left[\frac{\text{Sface} - \text{Sunface}}{\text{Sface}}\right]\right];$$

$$\text{MatrixForm}\left[\text{Evaluate}\left[\frac{\text{Sfar} - \text{Sunfar}}{\text{Sfar}}\right]\right];$$

The tables below compare the corrected and uncorrected peak count fraction--the fraction of decays that result in gamma rays depositing their full energy in the detector crystal and causing a count in the full energy peak.

```
Sfacelist = {Sface[[6, 3]], Sface[[6, 4]], Sface[[6, 5]], Sface[[5, 3]],
  Sface[[4, 1]], Sface[[3, 1]], Sface[[2, 1]], Sface[[4, 2]]};

Sfarlist = {Sfar[[6, 3]], Sfar[[6, 4]], Sfar[[6, 5]], Sfar[[5, 3]],
  Sfar[[4, 1]], Sfar[[3, 1]], Sfar[[2, 1]], Sfar[[4, 2]]};

TableForm[Table[{Mo99gammas[[i]],
   Sunfarlist[[i]], Sfarlist[[i]], Ratiofarlist[[i]]}, {i, 1, 8}],
 TableHeadings -> {None, {"Gamma (Mev)",
    "Far, Uncrtd Peak Prob", "Far, Crtd Peak Prob", "Ratio"}},
 TableAlignments -> Center]
```

Gamma (Mev)	Far, Uncrtd Peak Prob	Far, Crtd Peak Prob	Ratio
0.777921	0.000140284	0.000140289	1.00004
0.7395	0.000415519	0.000409061	0.984457
0.411491	9.14004×10^{-7}	9.02149×10^{-7}	0.987029
0.366421	0.0000742816	0.0000742688	0.999827
0.181068	0.000652984	0.000645766	0.988946
0.142675	3.46129×10^{-6}	3.4602×10^{-6}	0.999684
0.140511	0.00978103	0.00976995	0.998868
0.0405845	0.00002813	0.0000274028	0.97415

```
TableForm[Table[{Mo99gammas[[i]],
   Sunfacelist[[i]], Sfacelist[[i]], Ratiofacelist[[i]]}, {i, 1, 8}],
 TableHeadings -> {None, {"Gamma (Mev)",
    "Face, Uncrtd Peak Prob", "Face, Crtd Peak Prob", "Ratio"}},
 TableAlignments -> Center]
```

Gamma (Mev)	Face, Uncrtd Peak Prob	Face, Crtd Peak Prob	Ratio
0.777921	0.00246469	0.0024665	1.00073
0.7395	0.00731246	0.00521012	0.712499
0.411491	0.0000163954	0.0000125654	0.7664
0.366421	0.00133778	0.00133364	0.996905
0.181068	0.0124271	0.00998895	0.803802
0.142675	0.0000666917	0.0000666706	0.999684
0.140511	0.188545	0.185865	0.985784
0.0405845	0.000478934	0.000275118	0.574438

```
AFTACεpds5sface =
 Table[εpds5sfacelist[[i]] * Ratiofacelist[[i]], {i, 1, 8}];
```

The table below shows the adjusted face peak efficiency that AFTAC could use in its ananlysis.

```
TableForm[Table[{Mo99gammas[[i]], εpds5sfacelist[[i]],
   Ratiofacelist[[i]], AFTACεpds5sface[[i]]}, {i, 1, 8}],
 TableHeadings -> {None, {"Gamma (Mev)",
    "Face Peak Eff.", "Ratio", "Adjusted Face Peak Eff."}},
 TableAlignments -> Center]
```

Gamma (Mev)	Face Peak Eff.	Ratio	Adjusted Face Peak Eff.
0.777921	0.0578365	1.00073	0.0578788
0.7395	0.0604324	0.712499	0.043058
0.411491	0.100272	0.7664	0.0768482
0.366421	0.110815	0.996905	0.110472
0.181068	0.199408	0.803802	0.160284
0.142675	0.227668	0.999684	0.227596
0.140511	0.22907	0.985784	0.225813
0.0405845	0.0394235	0.574438	0.0226463

The following section is the error propagation of the correction factors. Standard deviations come from **(Peker, 1994)**, pg. 40-41 unless otherwise noted.

```
σa = {{0, 0, 0, 0, 0, 0}, {0.003, 0, 0, 0, 0, 0},
  {3., 0, 0, 0, 0, 0}, {0.007, 0.2, 0, 0, 0, 0}, {0, 0, 0.0010, 0, 0, 0},
  {0, 0, 0.00008, 0.0004, 0.001, 0}};
```

$$\sigma i = \frac{\beta[[6]] * xMo1[[6,4]]}{1+a[[6,4]]} * \{\{0,0,0,0,0,0\},\{0.0019,0,0,0,0,0\},$$
$$\{0.00002,0,0,0,0,0\},\{0.006,0.0027,0,0,0,0\},$$
$$\{0,0,0.0011,0,0,0\},\{0,0,0.004,0.01,0.00005,0\}\};$$

$$\sigma\varepsilon pfar = \{\{0,0,0,0,0,0\},\{0.015*\varepsilon pds5sfarlist[[7]],0,0,0,0,0\},$$
$$\{0.015*\varepsilon pds5sfarlist[[6]],0,0,0,0,0\},$$
$$\{0.015*\varepsilon pds5sfarlist[[5]],0.015*\varepsilon pds5sfarlist[[8]],0,0,0,0\},$$
$$\{0,0,0.015*\varepsilon pds5sfarlist[[4]],0,0,0\},$$
$$\{0,0,0.015*\varepsilon pds5sfarlist[[1]],0.015*\varepsilon pds5sfarlist[[2]],$$
$$0.015*\varepsilon pds5sfarlist[[3]],0\}\};$$

The following tolerances in the branch ratios are derived standard deviations from the gamma ray intensity. The error from angular correlation is neglected due to its small effect on the resulting correction factors. The deviation of the total efficiency is not explicity known, but it is on the order of 1% to 2% higher than that of the peak efficiency. Thus a constant 3% is used.

$$\sigma\varepsilon tps5sfar = \{\{0,0,0,0,0,0\},\{0.03*\varepsilon tps5sfarlist[[7]],0,0,0,0,0\},$$
$$\{0.03*\varepsilon tps5sfarlist[[6]],0,0,0,0,0\},$$
$$\{0.03*\varepsilon tps5sfarlist[[5]],0.03*\varepsilon tps5sfarlist[[8]],0,0,0,0\},\{0,0,$$
$$0.03*\varepsilon tps5sfarlist[[4]],0,0,0\},\{0,0,0.03*\varepsilon tps5sfarlist[[1]],$$
$$0.03*\varepsilon tps5sfarlist[[2]],0.03*\varepsilon tps5sfarlist[[3]],0\}\};$$

$$\sigma\varepsilon tps3sfar = \{\{0,0,0,0,0,0\},\{0.03*\varepsilon tps3sfarlist[[7]],0,0,0,0,0\},$$
$$\{0.03*\varepsilon tps3sfarlist[[6]],0,0,0,0,0\},$$
$$\{0.03*\varepsilon tps3sfarlist[[5]],0.03*\varepsilon tps3sfarlist[[8]],0,0,0,0\},\{0,0,$$
$$0.03*\varepsilon tps3sfarlist[[4]],0,0,0\},\{0,0,0.03*\varepsilon tps3sfarlist[[1]],$$
$$0.03*\varepsilon tps3sfarlist[[2]],0.03*\varepsilon tps3sfarlist[[3]],0\}\};$$

$$\sigma\varepsilon tds3sfar = \{\{0,0,0,0,0,0\},\{0.03*\varepsilon tds3sfarlist[[7]],0,0,0,0,0\},$$
$$\{0.03*\varepsilon tds3sfarlist[[6]],0,0,0,0,0\},$$
$$\{0.03*\varepsilon tds3sfarlist[[5]],0.03*\varepsilon tds3sfarlist[[8]],0,0,0,0\},\{0,0,$$
$$0.03*\varepsilon tds3sfarlist[[4]],0,0,0\},\{0,0,0.03*\varepsilon tds3sfarlist[[1]],$$
$$0.03*\varepsilon tds3sfarlist[[2]],0.03*\varepsilon tds3sfarlist[[3]],0\}\};$$

$$\sigma\varepsilon tfar = Table[0,\{i,1,m\},\{k,1,m\}];$$

$$\sigma\varepsilon tfar[[2,1]] = \left(\left(\frac{\varepsilon tds3sfarlist[[7]]}{\varepsilon tps3sfarlist[[7]]}\right)^2 * \sigma\varepsilon tps5sfar[[2,1]]^2 + ((\varepsilon tps5sfarlist[[7]] * \varepsilon tds3sfarlist[[7]]) / \varepsilon tps3sfarlist[[7]]^2)\,\hat{}\,2 * \sigma\varepsilon tps3sfar[[2,1]]^2 + \left(\frac{\varepsilon tps5sfarlist[[7]]}{\varepsilon tps3sfarlist[[7]]}\right)^2 * \sigma\varepsilon tds3sfar[[2,1]]^2\right)\,\hat{}\,\frac{1}{2};$$

$$\sigma\varepsilon tfar[[3,1]] = \left(\left(\frac{\varepsilon tds3sfarlist[[6]]}{\varepsilon tps3sfarlist[[6]]}\right)^2 * \sigma\varepsilon tps5sfar[[3,1]]^2 + ((\varepsilon tps5sfarlist[[6]] * \varepsilon tds3sfarlist[[6]]) / \varepsilon tps3sfarlist[[6]]^2)\,\hat{}\,2 * \sigma\varepsilon tps3sfar[[3,1]]^2 + \left(\frac{\varepsilon tps5sfarlist[[6]]}{\varepsilon tps3sfarlist[[6]]}\right)^2 * \sigma\varepsilon tds3sfar[[3,1]]^2\right)\,\hat{}\,\frac{1}{2};$$

$$\sigma\varepsilon tfar[[4,1]] = \left(\left(\frac{\varepsilon tds3sfarlist[[5]]}{\varepsilon tps3sfarlist[[5]]}\right)^2 * \sigma\varepsilon tps5sfar[[4,1]]^2 + ((\varepsilon tps5sfarlist[[5]] * \varepsilon tds3sfarlist[[5]]) / \varepsilon tps3sfarlist[[5]]^2)\,\hat{}\,2 * \sigma\varepsilon tps3sfar[[4,1]]^2 + \left(\frac{\varepsilon tps5sfarlist[[5]]}{\varepsilon tps3sfarlist[[5]]}\right)^2 * \sigma\varepsilon tds3sfar[[4,1]]^2\right)\,\hat{}\,\frac{1}{2};$$

$$\sigma\varepsilon tfar[[4,2]] = \left(\left(\frac{\varepsilon tds3sfarlist[[8]]}{\varepsilon tps3sfarlist[[8]]}\right)^2 * \sigma\varepsilon tps5sfar[[4,2]]^2 + ((\varepsilon tps5sfarlist[[8]] * \varepsilon tds3sfarlist[[8]]) / \varepsilon tps3sfarlist[[8]]^2)\,\hat{}\,2 * \sigma\varepsilon tps3sfar[[4,2]]^2 + \left(\frac{\varepsilon tps5sfarlist[[8]]}{\varepsilon tps3sfarlist[[8]]}\right)^2 * \sigma\varepsilon tds3sfar[[4,2]]^2\right)\,\hat{}\,\frac{1}{2};$$

```
σεtfar[[5, 3]] = (((εtds3sfarlist[[4]]) / εtps3sfarlist[[4]])^2 * σεtps5sfar[[5, 3]]^2 +
    ((εtps5sfarlist[[4]] * εtds3sfarlist[[4]]) / εtps3sfarlist[[4]]^2)^2 *
     σεtps3sfar[[5, 3]]^2 +
    ((εtps5sfarlist[[4]]) / εtps3sfarlist[[4]])^2 * σεtds3sfar[[5, 3]]^2)^
  1/2;

σεtfar[[6, 3]] = (((εtds3sfarlist[[3]]) / εtps3sfarlist[[3]])^2 * σεtps5sfar[[6, 3]]^2 +
    ((εtps5sfarlist[[3]] * εtds3sfarlist[[3]]) / εtps3sfarlist[[3]]^2)^2 *
     σεtps3sfar[[6, 3]]^2 +
    ((εtps5sfarlist[[3]]) / εtps3sfarlist[[3]])^2 * σεtds3sfar[[6, 3]]^2)^
  1/2;

σεtfar[[6, 4]] = (((εtds3sfarlist[[2]]) / εtps3sfarlist[[2]])^2 * σεtps5sfar[[6, 4]]^2 +
    ((εtps5sfarlist[[2]] * εtds3sfarlist[[2]]) / εtps3sfarlist[[2]]^2)^2 *
     σεtps3sfar[[6, 4]]^2 +
    ((εtps5sfarlist[[2]]) / εtps3sfarlist[[2]])^2 * σεtds3sfar[[6, 4]]^2)^
  1/2;

σεtfar[[6, 5]] = (((εtds3sfarlist[[1]]) / εtps3sfarlist[[1]])^2 * σεtps5sfar[[6, 5]]^2 +
    ((εtps5sfarlist[[1]] * εtds3sfarlist[[1]]) / εtps3sfarlist[[1]]^2)^2 *
     σεtps3sfar[[6, 5]]^2 +
    ((εtps5sfarlist[[1]]) / εtps3sfarlist[[1]])^2 * σεtds3sfar[[6, 5]]^2)^
  1/2;

σx = Table[0, {i, 1, m}, {k, 1, m}];

σx[[2, 1]] = σi[[2, 1]] * xTc1[[2, 1]] *
  (1 + a[[2, 1]]) / (xTc1[[3, 2]] * xTc1[[2, 1]] * (β[[6]] * xMo2[[6, 3]] / (1 + a[[6, 3]]) +
      β[[5]] * xMo2[[5, 3]] / (1 + a[[5, 3]]) * (1 + β[[6]] * xMo2[[6, 5]] / (1 + a[[6, 5]])) + β[[3]]));
```

```
σx[[3, 1]] = σi[[3, 1]] * xTc1[[3, 1]] *
  (1 + a[[3, 1]]) / (xTc1[[3, 1]] * (β[[6]] * xMo2[[6, 3]] / (1 + a[[6, 3]]) +
      β[[5]] * xMo2[[5, 3]] / (1 + a[[5, 3]]) * (1 + β[[6]] * xMo2[[6, 5]] / (1 + a[[6, 5]])) + β[[3]]));

σx[[4, 2]] = σi[[4, 2]] * xMo1[[4, 2]] *
  (1 + a[[4, 2]]) / (xMo1[[4, 2]] * (β[[6]] * xMo1[[6, 4]] / (1 + a[[6, 4]])));

σx[[4, 1]] = σi[[4, 1]] * xMo1[[4, 1]] *
  (1 + a[[4, 1]]) / (xMo1[[4, 1]] * (β[[6]] * xMo1[[6, 4]] / (1 + a[[6, 4]])));

σx[[5, 3]] = σi[[5, 3]] * xMo2[[5, 3]] *
  (1 + a[[5, 3]]) / (xMo2[[5, 3]] * (β[[5]] + β[[6]] * xMo2[[6, 5]] / (1 + a[[6, 5]])));

σx[[6, 3]] =
 σi[[6, 3]] * xMo2[[6, 3]] / (xMo2[[6, 3]] * (β[[6]] * xMo2[[6, 3]] / (1 + a[[6, 3]])));

σx[[6, 4]] =
 σi[[6, 4]] * xMo1[[6, 4]] / (xMo1[[6, 4]] * (β[[6]] * xMo1[[6, 4]] / (1 + a[[6, 4]])));

σx[[6, 5]] =
 σi[[6, 5]] * xMo2[[6, 5]] / (xMo2[[6, 5]] * (β[[6]] * xMo2[[6, 5]] / (1 + a[[6, 5]])));

MatrixForm[σx];
```

The following section computes the error in the major terms $\mathcal{B}$, $\mathcal{A}$, and $\mathcal{M}$ of the formula for S.

```
σ2ℬMo1far = Table[0, {i, 1, m}, {k, 1, m}];

σ2ℬMo2far = Table[0, {i, 1, m}, {k, 1, m}];

σ2ℬTc1far = Table[0, {i, 1, m}, {k, 1, m}];

σ2ℬMo2far[[5, 3]] = σx[[6, 5]]^2 * (β[[6]] * (1 - εtfar[[6, 5]] / (1 + a[[6, 5]])))^2 +
  σa[[6, 5]]^2 * (β[[6]] * xMo2[[6, 5]] * (εtfar[[6, 5]] / (1 + a[[6, 5]])^2))^2 +
  σεtfar[[6, 5]]^2 * (β[[6]] * xMo2[[6, 5]])^2;
```

$$\sigma 2\mathcal{B}\text{Mo1far}[[4,2]] = \sigma x[[4,2]]^2 * \left(\beta[[6]] * \left(1 - \frac{\varepsilon\text{tfar}[[4,2]]}{1+a[[4,2]]}\right)\right)\text{^}2 +$$
$$\sigma a[[4,2]]^2 * \left(\beta[[6]] * x\text{Mo1}[[4,2]] * \left(\frac{\varepsilon\text{tfar}[[4,2]]}{(1+a[[4,2]])^2}\right)\right)\text{^}2 +$$
$$\sigma\varepsilon\text{tfar}[[4,2]]^2 * (\beta[[6]] * x\text{Mo1}[[4,2]])\text{^}2;$$

$$\sigma 2\mathcal{B}\text{Mo1far}[[4,1]] = \sigma x[[4,1]]^2 * \left(\beta[[6]] * \left(1 - \frac{\varepsilon\text{tfar}[[4,1]]}{1+a[[4,1]]}\right)\right)\text{^}2 +$$
$$\sigma a[[4,2]]^2 * \left(\beta[[6]] * x\text{Mo1}[[4,1]] * \left(\frac{\varepsilon\text{tfar}[[4,1]]}{(1+a[[4,1]])^2}\right)\right)\text{^}2 +$$
$$\sigma\varepsilon\text{tfar}[[4,1]]^2 * (\beta[[6]] * x\text{Mo1}[[4,1]])\text{^}2;$$

$$\sigma 2\mathcal{B}\text{Tc1far}[[3,1]] =$$
$$\sigma x[[5,3]]^2 * \left(\left(\beta[[5]] + \frac{\beta[[6]] * x\text{Mo2}[[6,5]]}{1+a[[6,5]]}\right) * \frac{1}{1+a[[5,3]]}\right)\text{^}2 +$$
$$\sigma a[[5,3]]^2 * \left(\left(\beta[[5]] + \frac{\beta[[6]] * x\text{Mo2}[[6,5]]}{1+a[[6,5]]}\right) * \frac{x\text{Mo2}[[5,3]]}{(1+a[[5,3]])^2}\right)\text{^}2 +$$
$$\sigma x[[6,5]]^2 * \left(\frac{\beta[[6]]}{1+a[[6,5]]} * \frac{x\text{Mo2}[[5,3]]}{1+a[[5,3]]}\right)\text{^}2 +$$
$$\sigma a[[6,5]]^2 * \left(\frac{\beta[[6]] * x\text{Mo2}[[6,5]]}{(1+a[[6,5]])^2} * \frac{x\text{Mo2}[[5,3]]}{1+a[[5,3]]}\right)\text{^}2 +$$
$$\sigma x[[6,3]]^2 * \left(\frac{\beta[[6]]}{1+a[[6,3]]}\right)\text{^}2 + \sigma a[[6,3]]^2 * \left(\frac{\beta[[6]] * x\text{Mo2}[[6,3]]}{(1+a[[6,3]])^2}\right)\text{^}2;$$

$$\sigma 2\beta Mo1far[[2,1]] = \sigma x[[4,2]]^2 *$$
$$\left(\beta[[6]] * xMo1[[6,4]] * \left(1 - \frac{\varepsilon tfar[[6,4]]}{1+a[[6,4]]}\right) * \left(1 - \frac{\varepsilon tfar[[4,2]]}{1+a[[4,2]]}\right)\right)\text{^}2 +$$
$$\sigma a[[4,2]]^2 * \left(\beta[[6]] * xMo1[[6,4]] *$$
$$\left(1 - \frac{\varepsilon tfar[[6,4]]}{1+a[[6,4]]}\right) * \left(\frac{xMo1[[4,2]] * \varepsilon tfar[[4,2]]}{(1+a[[4,2]])^2}\right)\right)\text{^}2 +$$
$$\sigma \varepsilon tfar[[4,2]]^2 *$$
$$\left(\beta[[6]] * xMo1[[6,4]] * \left(1 - \frac{\varepsilon tfar[[6,4]]}{1+a[[6,4]]}\right) * \left(\frac{xMo1[[4,2]]}{1+a[[4,2]]}\right)\right)\text{^}2 +$$
$$\sigma x[[6,4]]^2 *$$
$$\left(\beta[[6]] * \left(1 - \frac{\varepsilon tfar[[6,4]]}{1+a[[6,4]]}\right) * xMo1[[4,2]] * \left(1 - \frac{\varepsilon tfar[[4,2]]}{1+a[[4,2]]}\right)\right)\text{^}2 +$$
$$\sigma a[[6,4]]^2 * \left(\beta[[6]] * xMo1[[6,4]] *$$
$$\left(\frac{\varepsilon tfar[[6,4]]}{(1+a[[6,4]])^2}\right) * xMo1[[4,2]] * \left(1 - \frac{\varepsilon tfar[[4,2]]}{1+a[[4,2]]}\right)\right)\text{^}2 +$$
$$\sigma \varepsilon tfar[[6,4]]^2 *$$
$$\left(\beta[[6]] * xMo1[[6,4]] * xMo1[[4,2]] * \left(1 - \frac{\varepsilon tfar[[4,2]]}{1+a[[4,2]]}\right)\right)\text{^}2 ;$$

```
σ2ℬTc1far[[2, 1]] =
 σx[[3, 2]]^2 * (((β[[3]] + xMo2[[5, 3]]/(1 + a[[5, 3]]) * (β[[5]] + (β[[6]] * xMo2[[6, 5]])/(1 + a[[6, 5]])) +
        (β[[6]] * xMo2[[6, 3]])/(1 + a[[6, 3]])) * (1 - εtfar[[3, 2]]/(1 + a[[3, 2]])))^2 +
  σa[[3, 2]]^2 * (((β[[3]] + xMo2[[5, 3]]/(1 + a[[5, 3]]) *
        (β[[5]] + (β[[6]] * xMo2[[6, 5]])/(1 + a[[6, 5]])) + (β[[6]] * xMo2[[6, 3]])/(1 + a[[6, 3]])) *
      (xTc1[[3, 2]] * εtfar[[3, 2]]/(1 + a[[3, 2]])^2))^2 +
  σεtfar[[3, 2]]^2 *
   (((β[[3]] + xMo2[[5, 3]]/(1 + a[[5, 3]]) * (β[[5]] + (β[[6]] * xMo2[[6, 5]])/(1 + a[[6, 5]])) +
        (β[[6]] * xMo2[[6, 3]])/(1 + a[[6, 3]])) * (xTc1[[3, 2]]/(1 + a[[3, 2]])))^2 +
  σx[[6, 3]]^2 * (β[[6]]/(1 + a[[6, 3]]) * xTc1[[3, 2]] * (1 - εtfar[[3, 2]]/(1 + a[[3, 2]])))^2 +
  σa[[6, 3]]^2 * (β[[6]]/(1 + a[[6, 3]])^2 * xTc1[[3, 2]] * (1 - εtfar[[3, 2]]/(1 + a[[3, 2]])))^2 +
  σx[[5, 3]]^2 * (((1/(1 + a[[5, 3]]) * (β[[5]] + (β[[6]] * xMo2[[6, 5]])/(1 + a[[6, 5]])) +
        (β[[6]] * xMo2[[6, 3]])/(1 + a[[6, 3]])) * (1 - εtfar[[3, 2]]/(1 + a[[3, 2]])))^2 +
  σa[[5, 3]]^2 * (((xMo2[[5, 3]]/(1 + a[[5, 3]])^2 *
        (β[[5]] + (β[[6]] * xMo2[[6, 5]])/(1 + a[[6, 5]])) + (β[[6]] * xMo2[[6, 3]])/(1 + a[[6, 3]])) *
      xTc1[[3, 2]] * (1 - εtfar[[3, 2]]/(1 + a[[3, 2]])))^2 +
  σx[[6, 5]]^2 *
   (((xMo2[[5, 3]]/(1 + a[[5, 3]]) * β[[6]]/(1 + a[[6, 5]])) * xTc1[[3, 2]] * (1 - εtfar[[3, 2]]/(1 + a[[3, 2]])))^2 +
  σa[[6, 5]]^2 * (((xMo2[[5, 3]]/(1 + a[[5, 3]]) * (β[[6]] * xTc1[[6, 5]])/(1 + a[[6, 5]])^2) *
      xTc1[[3, 2]] * (1 - εtfar[[3, 2]]/(1 + a[[3, 2]])))^
    2;

σ2ℜMo1far = Table[0, {i, 1, m}, {k, 1, m}];
```

```
σ2ℜMo2far = Table[0, {i, 1, m}, {k, 1, m}];

σ2ℜTc1far = Table[0, {i, 1, m}, {k, 1, m}];

σ2ℜMo1far[[2, 1]] = σx[[2, 1]]^2 * (εpfar[[2, 1]] / (1 + a[[2, 1]]))^2 +
  σa[[2, 1]]^2 * (xMo1[[2, 1]] * εpfar[[2, 1]] / (1 + a[[2, 1]])^2)^2 +
  σεpfar[[2, 1]]^2 * (xMo1[[2, 1]] / (1 + a[[2, 1]]))^2;

σ2ℜTc1far[[2, 1]] = σx[[2, 1]]^2 * (εpfar[[2, 1]] / (1 + a[[2, 1]]))^2 +
  σa[[2, 1]]^2 * (xTc1[[2, 1]] * εpfar[[2, 1]] / (1 + a[[2, 1]])^2)^2 +
  σεpfar[[2, 1]]^2 * (xTc1[[2, 1]] / (1 + a[[2, 1]]))^2;

σ2ℜTc1far[[3, 1]] = σx[[3, 1]]^2 * (εpfar[[3, 1]] / (1 + a[[3, 1]]))^2 +
  σa[[3, 1]]^2 * (xTc1[[3, 1]] * εpfar[[3, 1]] / (1 + a[[3, 1]])^2)^2 +
  σεpfar[[3, 1]]^2 * (xTc1[[3, 1]] / (1 + a[[3, 1]]))^2 + σx[[3, 2]]^2 *
   (εpfar[[3, 2]] / (1 + a[[3, 2]]) * xTc1[[2, 1]] * εpfar[[2, 1]] / (1 + a[[2, 1]]))^2 + σa[[3, 2]]^2 *
   (xTc1[[3, 2]] * εpfar[[3, 2]] / (1 + a[[3, 2]])^2 * xTc1[[2, 1]] * εpfar[[2, 1]] / (1 + a[[2, 1]]))^2 +
  σεpfar[[3, 2]]^2 *
   (xTc1[[3, 2]] / (1 + a[[3, 2]]) * xTc1[[2, 1]] * εpfar[[2, 1]] / (1 + a[[2, 1]]))^2 + σx[[2, 1]]^2 *
   (xTc1[[3, 2]] * εpfar[[3, 2]] / (1 + a[[3, 2]]) * εpfar[[2, 1]] / (1 + a[[2, 1]]))^2 + σa[[2, 1]]^2 *
   (xTc1[[3, 2]] * εpfar[[3, 2]] / (1 + a[[3, 2]]) * xTc1[[2, 1]] * εpfar[[2, 1]] / (1 + a[[2, 1]])^2)^2 +
  σεpfar[[2, 1]]^2 * (xTc1[[3, 2]] * εpfar[[3, 2]] / (1 + a[[3, 2]]) * xTc1[[2, 1]] / (1 + a[[2, 1]]))^2;
```

$$\sigma 2\mathcal{R}\text{Mo1far}[[4,1]] = \sigma x[[4,1]]^2 * \left(\frac{\varepsilon\text{pfar}[[4,1]]}{1+a[[4,1]]}\right)\text{^}2 +$$
$$\sigma a[[4,1]]^2 * \left(\frac{x\text{Mo1}[[4,1]] * \varepsilon\text{pfar}[[4,1]]}{(1+a[[4,1]])^2}\right)\text{^}2 +$$
$$\sigma\varepsilon\text{pfar}[[4,1]]^2 * \left(\frac{x\text{Mo1}[[4,1]]}{1+a[[4,1]]}\right)\text{^}2 + \sigma x[[4,2]]^2 *$$
$$\left(\frac{\varepsilon\text{pfar}[[4,2]]}{1+a[[4,2]]} * \frac{x\text{Mo1}[[2,1]] * \varepsilon\text{pfar}[[2,1]]}{1+a[[2,1]]}\right)\text{^}2 + \sigma a[[4,2]]^2 *$$
$$\left(\frac{x\text{Mo1}[[4,2]] * \varepsilon\text{pfar}[[4,2]]}{(1+a[[4,2]])^2} * \frac{x\text{Mo1}[[2,1]] * \varepsilon\text{pfar}[[2,1]]}{1+a[[2,1]]}\right)\text{^}2 +$$
$$\sigma\varepsilon\text{pfar}[[4,2]]^2 *$$
$$\left(\frac{x\text{Mo1}[[4,2]]}{1+a[[4,2]]} * \frac{x\text{Mo1}[[2,1]] * \varepsilon\text{pfar}[[2,1]]}{1+a[[2,1]]}\right)\text{^}2 + \sigma x[[2,1]]^2 *$$
$$\left(\frac{x\text{Mo1}[[4,2]] * \varepsilon\text{pfar}[[4,2]]}{1+a[[4,2]]} * \frac{\varepsilon\text{pfar}[[2,1]]}{1+a[[2,1]]}\right)\text{^}2 + \sigma a[[2,1]]^2 *$$
$$\left(\frac{x\text{Mo1}[[4,2]] * \varepsilon\text{pfar}[[4,2]]}{1+a[[4,2]]} * \frac{x\text{Mo1}[[2,1]] * \varepsilon\text{pfar}[[2,1]]}{(1+a[[2,1]])^2}\right)\text{^}2 +$$
$$\sigma\varepsilon\text{pfar}[[2,1]]^2 * \left(\frac{x\text{Mo1}[[4,2]] * \varepsilon\text{pfar}[[4,2]]}{1+a[[4,2]]} * \frac{x\text{Mo1}[[2,1]]}{1+a[[2,1]]}\right)\text{^}2;$$

$$\sigma 2\mathcal{R}\text{Mo1far}[[4,2]] = \sigma x[[4,2]]^2 * \left(\frac{\varepsilon\text{pfar}[[4,2]]}{1+a[[4,2]]}\right)\text{^}2 +$$
$$\sigma a[[4,2]]^2 * \left(\frac{x\text{Mo1}[[4,2]] * \varepsilon\text{pfar}[[4,2]]}{(1+a[[4,2]])^2}\right)\text{^}2 +$$
$$\sigma\varepsilon\text{pfar}[[4,2]]^2 * \left(\frac{x\text{Mo1}[[4,2]]}{1+a[[4,2]]}\right)\text{^}2;$$

$$\sigma 2\mathcal{R}\text{Mo2far}[[5,3]] = \sigma x[[5,3]]^2 * \left(\frac{\varepsilon\text{pfar}[[5,3]]}{1+a[[5,3]]}\right)\text{^}2 +$$
$$\sigma a[[5,3]]^2 * \left(\frac{x\text{Mo2}[[5,3]] * \varepsilon\text{pfar}[[5,3]]}{(1+a[[5,3]])^2}\right)\text{^}2 +$$
$$\sigma\varepsilon\text{pfar}[[5,3]]^2 * \left(\frac{x\text{Mo2}[[5,3]]}{1+a[[5,3]]}\right)\text{^}2;$$

```
σ2ℜMo2far[[6, 3]] = σx[[6, 3]]^2 * (εpfar[[6, 3]] / (1 + a[[6, 3]])) ^2 +
  σa[[6, 3]]^2 * (xMo2[[6, 3]] * εpfar[[6, 3]] / (1 + a[[6, 3]])^2) ^2 +
  σεpfar[[6, 3]]^2 * (xMo2[[6, 3]] / (1 + a[[6, 3]])) ^2 + σx[[6, 5]]^2 *
   (εpfar[[6, 5]] / (1 + a[[6, 5]]) * xMo2[[5, 3]] * εpfar[[5, 3]] / (1 + a[[5, 3]])) ^2 + σa[[6, 5]]^2 *
   (xMo2[[6, 5]] * εpfar[[6, 5]] / (1 + a[[6, 5]])^2 * xMo2[[5, 3]] * εpfar[[5, 3]] / (1 + a[[5, 3]])) ^2 +
  σεpfar[[6, 5]]^2 *
   (xMo2[[6, 5]] / (1 + a[[6, 5]]) * xMo2[[5, 3]] * εpfar[[5, 3]] / (1 + a[[5, 3]])) ^2 + σx[[5, 3]]^2 *
   (xMo2[[6, 5]] * εpfar[[6, 5]] / (1 + a[[6, 5]]) * εpfar[[5, 3]] / (1 + a[[5, 3]])) ^2 + σa[[5, 3]]^2 *
   (xMo2[[6, 5]] * εpfar[[6, 5]] / (1 + a[[6, 5]]) * xMo2[[5, 3]] * εpfar[[5, 3]] / (1 + a[[5, 3]])^2) ^2 +
  σεpfar[[5, 3]]^2 * (xMo2[[6, 5]] * εpfar[[6, 5]] / (1 + a[[6, 5]]) * xMo2[[5, 3]] / (1 + a[[5, 3]])) ^2;

σ2ℜMo1far[[6, 4]] = σx[[6, 4]]^2 * (εpfar[[6, 4]] / (1 + a[[6, 4]])) ^2 +
  σa[[6, 4]]^2 * (xMo1[[6, 4]] * εpfar[[6, 4]] / (1 + a[[6, 4]])^2) ^2 +
  σεpfar[[6, 4]]^2 * (xMo1[[6, 4]] / (1 + a[[6, 4]])) ^2;

σ2ℜMo1far[[6, 5]] = σx[[6, 5]]^2 * (εpfar[[6, 5]] / (1 + a[[6, 5]])) ^2 +
  σa[[6, 5]]^2 * (xMo2[[6, 5]] * εpfar[[6, 5]] / (1 + a[[6, 5]])^2) ^2 +
  σεpfar[[6, 5]]^2 * (xMo2[[6, 5]] / (1 + a[[6, 5]])) ^2;

σ2ℳMo1far = Table[0, {i, 1, m}, {k, 1, m}];

σ2ℳMo2far = Table[0, {i, 1, m}, {k, 1, m}];

σ2ℳTc1far = Table[0, {i, 1, m}, {k, 1, m}];
```

$$\sigma 2\mathcal{M}\text{Mo1far}[[4,2]] = \sigma x[[2,1]]^2 * \left(1 - \frac{\varepsilon\text{tfar}[[2,1]]}{1+a[[2,1]]}\right)\text{^}2 +$$
$$\sigma a[[2,1]]^2 * \left(x\text{Mo1}[[2,1]] * \frac{\varepsilon\text{tfar}[[2,1]]}{(1+a[[1,2]])^2}\right)\text{^}2 +$$
$$\sigma\varepsilon\text{tfar}[[2,1]]^2 * (x\text{Mo1}[[2,1]])\text{^}2;$$

$$\sigma 2\mathcal{M}\text{Mo1far}[[6,4]] =$$
$$\sigma x[[2,1]]^2 * \left(\left(1 - \frac{\varepsilon\text{tfar}[[2,1]]}{1+a[[2,1]]}\right) * x\text{Mo1}[[4,2]] * \left(1 - \frac{\varepsilon\text{tfar}[[4,2]]}{1+a[[4,2]]}\right)\right)\text{^}2 +$$
$$\sigma a[[2,1]]^2 * \left(\left(x\text{Mo1}[[2,1]] * \frac{\varepsilon\text{tfar}[[2,1]]}{(1+a[[2,1]])^2}\right) *$$
$$x\text{Mo1}[[4,2]] * \left(1 - \frac{\varepsilon\text{tfar}[[4,2]]}{1+a[[4,2]]}\right)\right)\text{^}2 +$$
$$\sigma\varepsilon\text{tfar}[[2,1]]^2 * \left((x\text{Mo1}[[2,1]]) * x\text{Mo1}[[4,2]] * \left(1 - \frac{\varepsilon\text{tfar}[[4,2]]}{1+a[[4,2]]}\right)\right)\text{^}2 +$$
$$\sigma x[[4,2]]^2 * \left(x\text{Mo1}[[2,1]] * \left(1 - \frac{\varepsilon\text{tfar}[[2,1]]}{1+a[[2,1]]}\right) * \left(1 - \frac{\varepsilon\text{tfar}[[4,2]]}{1+a[[4,2]]}\right)\right)\text{^}2 +$$
$$\sigma a[[4,2]]^2 *$$
$$\left(x\text{Mo1}[[2,1]] * \left(1 - \frac{\varepsilon\text{tfar}[[2,1]]}{1+a[[1,2]]}\right) * x\text{Mo1}[[4,2]] * \frac{\varepsilon\text{tfar}[[4,2]]}{(1+a[[4,2]])^2}\right)\text{^}2 +$$
$$\sigma\varepsilon\text{tfar}[[4,2]]^2 *$$
$$\left(x\text{Mo1}[[2,1]] * \left(1 - \frac{\varepsilon\text{tfar}[[2,1]]}{1+a[[2,1]]}\right) * x\text{Mo1}[[4,2]] * \frac{1}{1+a[[4,2]]}\right)\text{^}2;$$

$$\sigma 2\mathcal{M}\text{Mo2far}[[6,5]] = \sigma x[[5,3]]^2 * \left(1 - \frac{\varepsilon\text{tfar}[[5,3]]}{1+a[[5,3]]}\right)\text{^}2 +$$
$$\sigma a[[5,3]]^2 * \left(x\text{Mo2}[[5,3]] * \frac{\varepsilon\text{tfar}[[5,3]]}{(1+a[[5,3]])^2}\right)\text{^}2 +$$
$$\sigma\varepsilon\text{tfar}[[5,3]]^2 * \left(x\text{Mo2}[[5,3]] * \frac{1}{1+a[[5,3]]}\right)\text{^}2;$$

The following combines the constituent errors from the major terms $\mathcal{B}$, $\mathcal{A}$, and $\mathcal{M}$ into a total error for S, the peak count fraction.

$$\sigma S\text{Mo1far} = (\text{Table}[\sigma 2\mathcal{B}\text{Mo1far}[[i,k]] * \mathcal{A}\text{Mo1far}[[i,k]]^2 * \mathcal{M}\text{Mo1far}[[k]]^2 +$$
$$\sigma 2\mathcal{A}\text{Mo1far}[[i,k]] * \mathcal{B}\text{Mo1far}[[i]]^2 * \mathcal{M}\text{Mo1far}[[k]]^2 +$$
$$\sigma 2\mathcal{M}\text{Mo1far}[[i,k]] * \mathcal{A}\text{Mo1far}[[i,k]]^2 * \mathcal{B}\text{Mo1far}[[i]]^2,$$
$$\{i,1,m\},\{k,1,m\}])\text{^}\frac{1}{2};$$

```
σSMo2far = (Table[σ2BMo2far[[i, k]] * AMo2far[[i, k]]^2 * MMo2far[[k]]^2 +
     σ2AMo2far[[i, k]] * BMo2far[[i]]^2 * MMo2far[[k]]^2 +
     σ2MMo2far[[i, k]] * AMo2far[[i, k]]^2 * BMo2far[[i]]^2,
    {i, 1, m}, {k, 1, m}]) ^
  1/2;

σSTc1far = (Table[σ2BTc1far[[i, k]] * ATc1far[[i, k]]^2 * MTc1far[[k]]^2 +
     σ2ATc1far[[i, k]] * BTc1far[[i]]^2 * MTc1far[[k]]^2 +
     σ2MTc1far[[i, k]] * ATc1far[[i, k]]^2 * BTc1far[[i]]^2,
    {i, 1, m}, {k, 1, m}]) ^
  1/2;

σSfar = σSMo1far + σSMo2far + σSTc1far;

MatrixForm[σSfar];

percentσSfarlist =
 100 * {σSfar[[6, 3]] / Sfar[[6, 3]], σSfar[[6, 4]] / Sfar[[6, 4]],
   σSfar[[6, 5]] / Sfar[[6, 5]], σSfar[[5, 3]] / Sfar[[5, 3]],
   σSfar[[4, 1]] / Sfar[[4, 1]], σSfar[[3, 1]] / Sfar[[3, 1]],
   σSfar[[2, 1]] / Sfar[[2, 1]], σSfar[[4, 2]] / Sfar[[4, 2]]};

TableForm[Table[
  {Mo99gammas[[i]], Sfarlist[[i]], percentσSfarlist[[i]]}, {i, 1, 8}],
 TableHeadings -> {None, {"Gamma (Mev)", "Peak Prob, 10cm", "% Dev"}},
 TableAlignments -> Center]
```

Gamma (Mev)	Peak Prob, 10cm	% Dev
0.777921	0.000140289	4.6209
0.7395	0.000409061	2.31596
0.411491	9.02149×10^{-7}	1.10471
0.366421	0.0000742688	49.2925
0.181068	0.000645766	2.2063
0.142675	3.4602×10^{-6}	10.1708
0.140511	0.00976995	1.77762
0.0405845	0.0000274028	5.88082

The procedure is repeated now for the face efficiency standard deviations.

```
σεtps5sface = {{0, 0, 0, 0, 0, 0}, {0.03 * εtps5sfacelist[[7]], 0, 0, 0, 0, 0},
  {0.03 * εtps5sfacelist[[6]], 0, 0, 0, 0, 0},
  {0.03 * εtps5sfacelist[[5]], 0.03 * εtps5sfacelist[[8]], 0, 0, 0, 0},
  {0, 0, 0.03 * εtps5sfacelist[[4]], 0, 0, 0},
  {0, 0, 0.03 * εtps5sfacelist[[1]], 0.03 * εtps5sfacelist[[2]],
   0.03 * εtps5sfacelist[[3]], 0}};
```

```
σεtps3sface = {{0, 0, 0, 0, 0, 0}, {0.03 * εtps3sfacelist[[7]], 0, 0, 0, 0, 0},
  {0.03 * εtps3sfacelist[[6]], 0, 0, 0, 0, 0},
  {0.03 * εtps3sfacelist[[5]], 0.03 * εtps3sfacelist[[8]], 0, 0, 0, 0},
  {0, 0, 0.03 * εtps3sfacelist[[4]], 0, 0, 0},
  {0, 0, 0.03 * εtps3sfacelist[[1]], 0.03 * εtps3sfacelist[[2]],
   0.03 * εtps3sfacelist[[3]], 0}};

σεtds3sface = {{0, 0, 0, 0, 0, 0}, {0.03 * εtds3sfacelist[[7]], 0, 0, 0, 0, 0},
  {0.03 * εtds3sfacelist[[6]], 0, 0, 0, 0, 0},
  {0.03 * εtds3sfacelist[[5]], 0.03 * εtds3sfacelist[[8]], 0, 0, 0, 0},
  {0, 0, 0.03 * εtds3sfacelist[[4]], 0, 0, 0},
  {0, 0, 0.03 * εtds3sfacelist[[1]], 0.03 * εtds3sfacelist[[2]],
   0.03 * εtds3sfacelist[[3]], 0}};

σεtface = Table[0, {i, 1, m}, {k, 1, m}];

σεtface[[2, 1]] = (εtds3sfacelist[[7]] / εtps3sfacelist[[7]])^2 * σεtps5sface[[2, 1]]^2 +
    ((εtps5sfacelist[[7]] * εtds3sfacelist[[7]]) /
       εtps3sfacelist[[7]]^2)^2 *
     σεtps3sface[[2, 1]]^2 +
    (εtps5sfacelist[[7]] / εtps3sfacelist[[7]])^2 * σεtds3sface[[2, 1]]^2)^
  1/2;

σεtface[[3, 1]] = (εtds3sfacelist[[6]] / εtps3sfacelist[[6]])^2 * σεtps5sface[[3, 1]]^2 +
    ((εtps5sfacelist[[6]] * εtds3sfacelist[[6]]) /
       εtps3sfacelist[[6]]^2)^2 *
     σεtps3sface[[3, 1]]^2 +
    (εtps5sfacelist[[6]] / εtps3sfacelist[[6]])^2 * σεtds3sface[[3, 1]]^2)^
  1/2;
```

$$\sigma\varepsilon\text{tface}[[4,1]] = \left(\left(\frac{\varepsilon\text{tds3sfacelist}[[5]]}{\varepsilon\text{tps3sfacelist}[[5]]}\right)^2 * \sigma\varepsilon\text{tps5sface}[[4,1]]^2 + ((\varepsilon\text{tps5sfacelist}[[5]] * \varepsilon\text{tds3sfacelist}[[5]]) / \varepsilon\text{tps3sfacelist}[[5]]^2)\,\hat{}\,2 * \sigma\varepsilon\text{tps3sface}[[4,1]]^2 + \left(\frac{\varepsilon\text{tps5sfacelist}[[5]]}{\varepsilon\text{tps3sfacelist}[[5]]}\right)^2 * \sigma\varepsilon\text{tds3sface}[[4,1]]^2\right)\,\hat{}\,\frac{1}{2};$$

$$\sigma\varepsilon\text{tface}[[4,2]] = \left(\left(\frac{\varepsilon\text{tds3sfacelist}[[8]]}{\varepsilon\text{tps3sfacelist}[[8]]}\right)^2 * \sigma\varepsilon\text{tps5sface}[[4,2]]^2 + ((\varepsilon\text{tps5sfacelist}[[8]] * \varepsilon\text{tds3sfacelist}[[8]]) / \varepsilon\text{tps3sfacelist}[[8]]^2)\,\hat{}\,2 * \sigma\varepsilon\text{tps3sface}[[4,2]]^2 + \left(\frac{\varepsilon\text{tps5sfacelist}[[8]]}{\varepsilon\text{tps3sfacelist}[[8]]}\right)^2 * \sigma\varepsilon\text{tds3sface}[[4,2]]^2\right)\,\hat{}\,\frac{1}{2};$$

$$\sigma\varepsilon\text{tface}[[5,3]] = \left(\left(\frac{\varepsilon\text{tds3sfacelist}[[4]]}{\varepsilon\text{tps3sfacelist}[[4]]}\right)^2 * \sigma\varepsilon\text{tps5sface}[[5,3]]^2 + ((\varepsilon\text{tps5sfacelist}[[4]] * \varepsilon\text{tds3sfacelist}[[4]]) / \varepsilon\text{tps3sfacelist}[[4]]^2)\,\hat{}\,2 * \sigma\varepsilon\text{tps3sface}[[5,3]]^2 + \left(\frac{\varepsilon\text{tps5sfacelist}[[4]]}{\varepsilon\text{tps3sfacelist}[[4]]}\right)^2 * \sigma\varepsilon\text{tds3sface}[[5,3]]^2\right)\,\hat{}\,\frac{1}{2};$$

$$\sigma\varepsilon\text{tface}[[6,3]] = \left(\left(\frac{\varepsilon\text{tds3sfacelist}[[1]]}{\varepsilon\text{tps3sfacelist}[[1]]}\right)^2 * \sigma\varepsilon\text{tps5sface}[[6,3]]^2 + ((\varepsilon\text{tps5sfacelist}[[1]] * \varepsilon\text{tds3sfacelist}[[1]]) / \varepsilon\text{tps3sfacelist}[[1]]^2)\,\hat{}\,2 * \sigma\varepsilon\text{tps3sface}[[6,3]]^2 + \left(\frac{\varepsilon\text{tps5sfacelist}[[1]]}{\varepsilon\text{tps3sfacelist}[[1]]}\right)^2 * \sigma\varepsilon\text{tds3sface}[[6,3]]^2\right)\,\hat{}\,\frac{1}{2};$$

```
σεtface[[6, 4]] = ((εtds3sfacelist[[2]] / εtps3sfacelist[[2]])^2 * σεtps5sface[[6, 4]]^2 +
    ((εtps5sfacelist[[2]] * εtds3sfacelist[[2]]) /
       εtps3sfacelist[[2]]^2)^2 *
     σεtps3sface[[6, 4]]^2 +
    (εtps5sfacelist[[2]] / εtps3sfacelist[[2]])^2 * σεtds3sface[[6, 4]]^2)^
  1/2;

σεtface[[6, 5]] = ((εtds3sfacelist[[3]] / εtps3sfacelist[[3]])^2 * σεtps5sface[[6, 5]]^2 +
    ((εtps5sfacelist[[3]] * εtds3sfacelist[[3]]) /
       εtps3sfacelist[[3]]^2)^2 *
     σεtps3sface[[6, 5]]^2 +
    (εtps5sfacelist[[3]] / εtps3sfacelist[[3]])^2 * σεtds3sface[[6, 5]]^2)^
  1/2;

σPKtoTTLds5s = Table[0, {i, 1, m}, {k, 1, m}];

σPKtoTTLds5s[[2, 1]] = (1 / εtds5sfarlist[[7]])^2 * σεpfar[[2, 1]]^2 +
  (εpds5sfarlist[[7]] / εtds5sfarlist[[7]]^2)^2 * σεtfar[[2, 1]]^2;

σPKtoTTLds5s[[3, 1]] = (1 / εtds5sfarlist[[6]])^2 * σεpfar[[3, 1]]^2 +
  (εpds5sfarlist[[6]] / εtds5sfarlist[[6]]^2)^2 * σεtfar[[3, 1]]^2;

σPKtoTTLds5s[[4, 1]] = (1 / εtds5sfarlist[[5]])^2 * σεpfar[[4, 1]]^2 +
  (εpds5sfarlist[[5]] / εtds5sfarlist[[5]]^2)^2 * σεtfar[[4, 1]]^2;

σPKtoTTLds5s[[4, 2]] = (1 / εtds5sfarlist[[8]])^2 * σεpfar[[4, 2]]^2 +
  (εpds5sfarlist[[8]] / εtds5sfarlist[[8]]^2)^2 * σεtfar[[4, 2]]^2;
```

$$\sigma PKtoTTLds5s[[5, 3]] = \left(\frac{1}{\varepsilon tds5sfarlist[[6]]}\right)^2 * \sigma\varepsilon pfar[[5, 3]]^2 + \left(\frac{\varepsilon pds5sfarlist[[6]]}{\varepsilon tds5sfarlist[[6]]^2}\right)^2 * \sigma\varepsilon tfar[[5, 3]]^2;$$

$$\sigma PKtoTTLds5s[[6, 3]] = \left(\frac{1}{\varepsilon tds5sfarlist[[1]]}\right)^2 * \sigma\varepsilon pfar[[6, 3]]^2 + \left(\frac{\varepsilon pds5sfarlist[[1]]}{\varepsilon tds5sfarlist[[1]]^2}\right)^2 * \sigma\varepsilon tfar[[6, 3]]^2;$$

$$\sigma PKtoTTLds5s[[6, 4]] = \left(\frac{1}{\varepsilon tds5sfarlist[[2]]}\right)^2 * \sigma\varepsilon pfar[[6, 4]]^2 + \left(\frac{\varepsilon pds5sfarlist[[2]]}{\varepsilon tds5sfarlist[[2]]^2}\right)^2 * \sigma\varepsilon tfar[[6, 4]]^2;$$

$$\sigma PKtoTTLds5s[[6, 5]] = \left(\frac{1}{\varepsilon tds5sfarlist[[3]]}\right)^2 * \sigma\varepsilon pfar[[6, 5]]^2 + \left(\frac{\varepsilon pds5sfarlist[[3]]}{\varepsilon tds5sfarlist[[3]]^2}\right)^2 * \sigma\varepsilon tfar[[6, 5]]^2;$$

```
σεpface = Table[0, {i, 1, m}, {k, 1, m}];

σεpface[[2, 1]] = ((PKtoTTLds5slist[[7]])^2 * σεtface[[2, 1]]^2 +
    (εtface[[2, 1]])^2 * σPKtoTTLds5s[[2, 1]]^2) ^
  1/2;

σεpface[[3, 1]] = ((PKtoTTLds5slist[[6]])^2 * σεtface[[3, 1]]^2 +
    (εtface[[3, 1]])^2 * σPKtoTTLds5s[[3, 1]]^2) ^
  1/2;

σεpface[[4, 1]] = ((PKtoTTLds5slist[[5]])^2 * σεtface[[4, 1]]^2 +
    (εtface[[4, 1]])^2 * σPKtoTTLds5s[[4, 1]]^2) ^
  1/2;

σεpface[[4, 2]] = ((PKtoTTLds5slist[[8]])^2 * σεtface[[4, 2]]^2 +
    (εtface[[4, 2]])^2 * σPKtoTTLds5s[[4, 2]]^2) ^
  1/2;
```

```
σεpface[[5, 3]] = ((PKtoTTLds5slist[[4]])^2 * σεtface[[5, 3]]^2 +
    (εtface[[5, 3]])^2 * σPKtoTTLds5s[[5, 3]]^2) ^
  1/2;

σεpface[[6, 3]] = ((PKtoTTLds5slist[[1]])^2 * σεtface[[6, 3]]^2 +
    (εtface[[6, 3]])^2 * σPKtoTTLds5s[[6, 3]]^2) ^
  1/2;

σεpface[[6, 4]] = ((PKtoTTLds5slist[[2]])^2 * σεtface[[6, 4]]^2 +
    (εtface[[6, 4]])^2 * σPKtoTTLds5s[[6, 4]]^2) ^
  1/2;

σεpface[[6, 5]] = ((PKtoTTLds5slist[[3]])^2 * σεtface[[6, 5]]^2 +
    (εtface[[6, 5]])^2 * σPKtoTTLds5s[[6, 5]]^2) ^
  1/2;

σ2ℬMo1face = Table[0, {i, 1, m}, {k, 1, m}];

σ2ℬMo2face = Table[0, {i, 1, m}, {k, 1, m}];

σ2ℬTc1face = Table[0, {i, 1, m}, {k, 1, m}];

σ2ℬMo2face[[5, 3]] = σx[[6, 5]]^2 * (β[[6]] * (1 - εtface[[6, 5]]/(1 + a[[6, 5]])))^2 +
  σa[[6, 5]]^2 * (β[[6]] * xMo2[[6, 5]] * (εtfar[[6, 5]]/(1 + a[[6, 5]])^2))^2 +
  σεtface[[6, 5]]^2 * (β[[6]] * xMo2[[6, 5]])^2;

σ2ℬMo1face[[4, 2]] = σx[[4, 2]]^2 * (β[[6]] * (1 - εtface[[4, 2]]/(1 + a[[4, 2]])))^2 +
  σa[[4, 2]]^2 * (β[[6]] * xMo1[[4, 2]] * (εtfar[[4, 2]]/(1 + a[[4, 2]])^2))^2 +
  σεtface[[4, 2]]^2 * (β[[6]] * xMo1[[4, 2]])^2;

σ2ℬMo1face[[4, 1]] = σx[[4, 1]]^2 * (β[[6]] * (1 - εtface[[4, 1]]/(1 + a[[4, 1]])))^2 +
  σa[[4, 2]]^2 * (β[[6]] * xMo1[[4, 1]] * (εtface[[4, 1]]/(1 + a[[4, 1]])^2))^2 +
  σεtface[[4, 1]]^2 * (β[[6]] * xMo1[[4, 1]])^2;
```

$$\sigma 2\mathcal{B}\text{Tc1face}[[3,1]] =$$

$$\sigma x[[5,3]]^2 * \left(\left(\beta[[5]] + \frac{\beta[[6]] * x\text{Mo2}[[6,5]]}{1+a[[6,5]]}\right) * \frac{1}{1+a[[5,3]]}\right)\text{^}2 +$$

$$\sigma a[[5,3]]^2 * \left(\left(\beta[[5]] + \frac{\beta[[6]] * x\text{Mo2}[[6,5]]}{1+a[[6,5]]}\right) * \frac{x\text{Mo2}[[5,3]]}{(1+a[[5,3]])^2}\right)\text{^}2 +$$

$$\sigma x[[6,5]]^2 * \left(\frac{\beta[[6]]}{1+a[[6,5]]} * \frac{x\text{Mo2}[[5,3]]}{1+a[[5,3]]}\right)\text{^}2 +$$

$$\sigma a[[6,5]]^2 * \left(\frac{\beta[[6]] * x\text{Mo2}[[6,5]]}{(1+a[[6,5]])^2} * \frac{x\text{Mo2}[[5,3]]}{1+a[[5,3]]}\right)\text{^}2 +$$

$$\sigma x[[6,3]]^2 * \left(\frac{\beta[[6]]}{1+a[[6,3]]}\right)\text{^}2 + \sigma a[[6,3]]^2 * \left(\frac{\beta[[6]] * x\text{Mo2}[[6,3]]}{(1+a[[6,3]])^2}\right)\text{^}2;$$

$$\sigma 2\mathcal{B}\text{Mo1face}[[2,1]] = \sigma x[[4,2]]^2 *$$

$$\left(\beta[[6]] * x\text{Mo1}[[6,4]] * \left(1 - \frac{\varepsilon\text{tface}[[6,4]]}{1+a[[6,4]]}\right) * \left(1 - \frac{\varepsilon\text{tface}[[4,2]]}{1+a[[4,2]]}\right)\right)\text{^}2 +$$

$$\sigma a[[4,2]]^2 * \left(\beta[[6]] * x\text{Mo1}[[6,4]] *$$

$$\left(1 - \frac{\varepsilon\text{tface}[[6,4]]}{1+a[[6,4]]}\right) * \left(\frac{x\text{Mo1}[[4,2]] * \varepsilon\text{tfar}[[4,2]]}{(1+a[[4,2]])^2}\right)\right)\text{^}2 +$$

$$\sigma\varepsilon\text{tface}[[4,2]]^2 *$$

$$\left(\beta[[6]] * x\text{Mo1}[[6,4]] * \left(1 - \frac{\varepsilon\text{tface}[[6,4]]}{1+a[[6,4]]}\right) * \left(\frac{x\text{Mo1}[[4,2]]}{1+a[[4,2]]}\right)\right)\text{^}2 +$$

$$\sigma x[[6,4]]^2 *$$

$$\left(\beta[[6]] * \left(1 - \frac{\varepsilon\text{tface}[[6,4]]}{1+a[[6,4]]}\right) * x\text{Mo1}[[4,2]] * \left(1 - \frac{\varepsilon\text{tface}[[4,2]]}{1+a[[4,2]]}\right)\right)\text{^}2 +$$

$$\sigma a[[6,4]]^2 * \left(\beta[[6]] * x\text{Mo1}[[6,4]] *$$

$$\left(\frac{\varepsilon\text{tface}[[6,4]]}{(1+a[[6,4]])^2}\right) * x\text{Mo1}[[4,2]] * \left(1 - \frac{\varepsilon\text{tface}[[4,2]]}{1+a[[4,2]]}\right)\right)\text{^}2 +$$

$$\sigma\varepsilon\text{tface}[[6,4]]^2 *$$

$$\left(\beta[[6]] * x\text{Mo1}[[6,4]] * x\text{Mo1}[[4,2]] * \left(1 - \frac{\varepsilon\text{tface}[[4,2]]}{1+a[[4,2]]}\right)\right)\text{^}2;$$

```
σ2ℬTc1face[[2, 1]] =
 σx[[3, 2]]^2 * (((β[[3]] + xMo2[[5, 3]]/(1 + a[[5, 3]]) * (β[[5]] + (β[[6]] * xMo2[[6, 5]])/(1 + a[[6, 5]])) +
        (β[[6]] * xMo2[[6, 3]])/(1 + a[[6, 3]])) * (1 - εtface[[3, 2]]/(1 + a[[3, 2]])))^2 +
  σa[[3, 2]]^2 * (((β[[3]] + xMo2[[5, 3]]/(1 + a[[5, 3]]) *
        (β[[5]] + (β[[6]] * xMo2[[6, 5]])/(1 + a[[6, 5]])) + (β[[6]] * xMo2[[6, 3]])/(1 + a[[6, 3]])) *
     (xTc1[[3, 2]] * εtface[[3, 2]])/(1 + a[[3, 2]])^2))^2 +
  σεtface[[3, 2]]^2 *
   (((β[[3]] + xMo2[[5, 3]]/(1 + a[[5, 3]]) * (β[[5]] + (β[[6]] * xMo2[[6, 5]])/(1 + a[[6, 5]])) +
        (β[[6]] * xMo2[[6, 3]])/(1 + a[[6, 3]])) * (xTc1[[3, 2]]/(1 + a[[3, 2]])))^2 +
  σx[[6, 3]]^2 * (β[[6]]/(1 + a[[6, 3]]) * xTc1[[3, 2]] * (1 - εtface[[3, 2]]/(1 + a[[3, 2]])))^2 +
  σa[[6, 3]]^2 * (β[[6]]/(1 + a[[6, 3]])^2 * xTc1[[3, 2]] * (1 - εtface[[3, 2]]/(1 + a[[3, 2]])))^2 +
  σx[[5, 3]]^2 * (((1/(1 + a[[5, 3]]) *
        (β[[5]] + (β[[6]] * xMo2[[6, 5]])/(1 + a[[6, 5]])) + (β[[6]] * xMo2[[6, 3]])/(1 + a[[6, 3]])) *
     (1 - εtface[[3, 2]]/(1 + a[[3, 2]])))^2 +
  σa[[5, 3]]^2 * (((xMo2[[5, 3]]/(1 + a[[5, 3]])^2 *
        (β[[5]] + (β[[6]] * xMo2[[6, 5]])/(1 + a[[6, 5]])) + (β[[6]] * xMo2[[6, 3]])/(1 + a[[6, 3]])) *
     xTc1[[3, 2]] * (1 - εtface[[3, 2]]/(1 + a[[3, 2]])))^2 +
  σx[[6, 5]]^2 *
   (((xMo2[[5, 3]]/(1 + a[[5, 3]]) * β[[6]]/(1 + a[[6, 5]])) * xTc1[[3, 2]] * (1 - εtface[[3, 2]]/(1 + a[[3, 2]])))^2 +
  σa[[6, 5]]^2 * (((xMo2[[5, 3]]/(1 + a[[5, 3]]) * (β[[6]] * xTc1[[6, 5]])/(1 + a[[6, 5]])^2) *
     xTc1[[3, 2]] * (1 - εtface[[3, 2]]/(1 + a[[3, 2]])))^
   2;
```

```
σ2ℜMo1face = Table[0, {i, 1, m}, {k, 1, m}];

σ2ℜMo2face = Table[0, {i, 1, m}, {k, 1, m}];

σ2ℜTc1face = Table[0, {i, 1, m}, {k, 1, m}];

σ2ℜMo1face[[2, 1]] = σx[[2, 1]]^2 * (εpface[[2, 1]] / (1 + a[[2, 1]]))^2 +
  σa[[2, 1]]^2 * (xMo1[[2, 1]] * εpface[[2, 1]] / (1 + a[[2, 1]])^2)^2 +
  σεpface[[2, 1]]^2 * (xMo1[[2, 1]] / (1 + a[[2, 1]]))^2;

σ2ℜTc1face[[2, 1]] = σx[[2, 1]]^2 * (εpface[[2, 1]] / (1 + a[[2, 1]]))^2 +
  σa[[2, 1]]^2 * (xTc1[[2, 1]] * εpface[[2, 1]] / (1 + a[[2, 1]])^2)^2 +
  σεpface[[2, 1]]^2 * (xTc1[[2, 1]] / (1 + a[[2, 1]]))^2;

σ2ℜTc1face[[3, 1]] = σx[[3, 1]]^2 * (εpface[[3, 1]] / (1 + a[[3, 1]]))^2 +
  σa[[3, 1]]^2 * (xTc1[[3, 1]] * εpface[[3, 1]] / (1 + a[[3, 1]])^2)^2 +
  σεpface[[3, 1]]^2 * (xTc1[[3, 1]] / (1 + a[[3, 1]]))^2 + σx[[3, 2]]^2 *
   (εpface[[3, 2]] / (1 + a[[3, 2]]) * xTc1[[2, 1]] * εpface[[2, 1]] / (1 + a[[2, 1]]))^2 + σa[[3, 2]]^2 *
   (xTc1[[3, 2]] * εpface[[3, 2]] / (1 + a[[3, 2]])^2 * xTc1[[2, 1]] * εpface[[2, 1]] / (1 + a[[2, 1]]))^2 +
  σεpface[[3, 2]]^2 *
   (xTc1[[3, 2]] / (1 + a[[3, 2]]) * xTc1[[2, 1]] * εpface[[2, 1]] / (1 + a[[2, 1]]))^2 + σx[[2, 1]]^2 *
   (xTc1[[3, 2]] * εpface[[3, 2]] / (1 + a[[3, 2]]) * εpface[[2, 1]] / (1 + a[[2, 1]]))^2 + σa[[2, 1]]^2 *
   (xTc1[[3, 2]] * εpface[[3, 2]] / (1 + a[[3, 2]]) * xTc1[[2, 1]] * εpface[[2, 1]] / (1 + a[[2, 1]])^2)^2 +
  σεpface[[2, 1]]^2 * (xTc1[[3, 2]] * εpface[[3, 2]] / (1 + a[[3, 2]]) * xTc1[[2, 1]] / (1 + a[[2, 1]]))^2;
```

$$\sigma 2\mathcal{R}\text{Mo1far}[[4,1]] = \sigma x[[4,1]]^2 * \left(\frac{\varepsilon\text{pface}[[4,1]]}{1+a[[4,1]]}\right)\text{^}2 +$$
$$\sigma a[[4,1]]^2 * \left(\frac{x\text{Mo1}[[4,1]] * \varepsilon\text{pface}[[4,1]]}{(1+a[[4,1]])^2}\right)\text{^}2 +$$
$$\sigma\varepsilon\text{pface}[[4,1]]^2 * \left(\frac{x\text{Mo1}[[4,1]]}{1+a[[4,1]]}\right)\text{^}2 + \sigma x[[4,2]]^2 *$$
$$\left(\frac{\varepsilon\text{pface}[[4,2]]}{1+a[[4,2]]} * \frac{x\text{Mo1}[[2,1]] * \varepsilon\text{pface}[[2,1]]}{1+a[[2,1]]}\right)\text{^}2 + \sigma a[[4,2]]^2 *$$
$$\left(\frac{x\text{Mo1}[[4,2]] * \varepsilon\text{pface}[[4,2]]}{(1+a[[4,2]])^2} * \frac{x\text{Mo1}[[2,1]] * \varepsilon\text{pface}[[2,1]]}{1+a[[2,1]]}\right)\text{^}2 +$$
$$\sigma\varepsilon\text{pface}[[4,2]]^2 *$$
$$\left(\frac{x\text{Mo1}[[4,2]]}{1+a[[4,2]]} * \frac{x\text{Mo1}[[2,1]] * \varepsilon\text{pface}[[2,1]]}{1+a[[2,1]]}\right)\text{^}2 + \sigma x[[2,1]]^2 *$$
$$\left(\frac{x\text{Mo1}[[4,2]] * \varepsilon\text{pface}[[4,2]]}{1+a[[4,2]]} * \frac{\varepsilon\text{pface}[[2,1]]}{1+a[[2,1]]}\right)\text{^}2 + \sigma a[[2,1]]^2 *$$
$$\left(\frac{x\text{Mo1}[[4,2]] * \varepsilon\text{pface}[[4,2]]}{1+a[[4,2]]} * \frac{x\text{Mo1}[[2,1]] * \varepsilon\text{pface}[[2,1]]}{(1+a[[2,1]])^2}\right)\text{^}2 +$$
$$\sigma\varepsilon\text{pface}[[2,1]]^2 * \left(\frac{x\text{Mo1}[[4,2]] * \varepsilon\text{pface}[[4,2]]}{1+a[[4,2]]} * \frac{x\text{Mo1}[[2,1]]}{1+a[[2,1]]}\right)\text{^}2;$$

$$\sigma 2\mathcal{R}\text{Mo1face}[[4,2]] = \sigma x[[4,2]]^2 * \left(\frac{\varepsilon\text{pface}[[4,2]]}{1+a[[4,2]]}\right)\text{^}2 +$$
$$\sigma a[[4,2]]^2 * \left(\frac{x\text{Mo1}[[4,2]] * \varepsilon\text{pface}[[4,2]]}{(1+a[[4,2]])^2}\right)\text{^}2 +$$
$$\sigma\varepsilon\text{pface}[[4,2]]^2 * \left(\frac{x\text{Mo1}[[4,2]]}{1+a[[4,2]]}\right)\text{^}2;$$

$$\sigma 2\mathcal{R}\text{Mo2face}[[5,3]] = \sigma x[[5,3]]^2 * \left(\frac{\varepsilon\text{pface}[[5,3]]}{1+a[[5,3]]}\right)\text{^}2 +$$
$$\sigma a[[5,3]]^2 * \left(\frac{x\text{Mo2}[[5,3]] * \varepsilon\text{pface}[[5,3]]}{(1+a[[5,3]])^2}\right)\text{^}2 +$$
$$\sigma\varepsilon\text{pface}[[5,3]]^2 * \left(\frac{x\text{Mo2}[[5,3]]}{1+a[[5,3]]}\right)\text{^}2;$$

```
σ2ℜMo2face[[6, 3]] = σx[[6, 3]]^2 * (epface[[6, 3]] / (1 + a[[6, 3]]))^2 +
  σa[[6, 3]]^2 * (xMo2[[6, 3]] * epface[[6, 3]] / (1 + a[[6, 3]])^2)^2 +
  σepface[[6, 3]]^2 * (xMo2[[6, 3]] / (1 + a[[6, 3]]))^2 + σx[[6, 5]]^2 *
   (epface[[6, 5]] / (1 + a[[6, 5]]) * xMo2[[5, 3]] * epface[[5, 3]] / (1 + a[[5, 3]]))^2 + σa[[6, 5]]^2 *
   (xMo2[[6, 5]] * epface[[6, 5]] / (1 + a[[6, 5]])^2 * xMo2[[5, 3]] * epface[[5, 3]] / (1 + a[[5, 3]]))^2 +
  σepface[[6, 5]]^2 *
   (xMo2[[6, 5]] / (1 + a[[6, 5]]) * xMo2[[5, 3]] * epface[[5, 3]] / (1 + a[[5, 3]]))^2 + σx[[5, 3]]^2 *
   (xMo2[[6, 5]] * epface[[6, 5]] / (1 + a[[6, 5]]) * epface[[5, 3]] / (1 + a[[5, 3]]))^2 + σa[[5, 3]]^2 *
   (xMo2[[6, 5]] * epface[[6, 5]] / (1 + a[[6, 5]]) * xMo2[[5, 3]] * epface[[5, 3]] / (1 + a[[5, 3]])^2)^2 +
  σepface[[5, 3]]^2 * (xMo2[[6, 5]] * epface[[6, 5]] / (1 + a[[6, 5]]) * xMo2[[5, 3]] / (1 + a[[5, 3]]))^2;

σ2ℜMo1face[[6, 4]] = σx[[6, 4]]^2 * (epface[[6, 4]] / (1 + a[[6, 4]]))^2 +
  σa[[6, 4]]^2 * (xMo1[[6, 4]] * epface[[6, 4]] / (1 + a[[6, 4]])^2)^2 +
  σepface[[6, 4]]^2 * (xMo1[[6, 4]] / (1 + a[[6, 4]]))^2;

σ2ℜMo1face[[6, 5]] = σx[[6, 5]]^2 * (epface[[6, 5]] / (1 + a[[6, 5]]))^2 +
  σa[[6, 5]]^2 * (xMo2[[6, 5]] * epface[[6, 5]] / (1 + a[[6, 5]])^2)^2 +
  σepface[[6, 5]]^2 * (xMo2[[6, 5]] / (1 + a[[6, 5]]))^2;

σ2ℳMo1face = Table[0, {i, 1, m}, {k, 1, m}];

σ2ℳMo2face = Table[0, {i, 1, m}, {k, 1, m}];

σ2ℳTc1face = Table[0, {i, 1, m}, {k, 1, m}];
```

$$\sigma 2\mathcal{M}\text{Mo1face}[[4,2]] = \sigma x[[2,1]]^2 * \left(1 - \frac{\varepsilon\text{tface}[[2,1]]}{1+a[[2,1]]}\right)\text{^}2 +$$
$$\sigma a[[2,1]]^2 * \left(x\text{Mo1}[[2,1]] * \frac{\varepsilon\text{tface}[[2,1]]}{(1+a[[1,2]])^2}\right)\text{^}2 +$$
$$\sigma\varepsilon\text{tface}[[2,1]]^2 * \left(x\text{Mo1}[[2,1]] * \frac{1}{1+a[[2,1]]}\right)\text{^}2;$$

$$\sigma 2\mathcal{M}\text{Mo1face}[[6,4]] = \sigma x[[2,1]]^2 *$$
$$\left(\left(1 - \frac{\varepsilon\text{tface}[[2,1]]}{1+a[[2,1]]}\right) * x\text{Mo1}[[4,2]] * \left(1 - \frac{\varepsilon\text{tface}[[4,2]]}{1+a[[4,2]]}\right)\right)\text{^}2 +$$
$$\sigma a[[2,1]]^2 * \left(\left(x\text{Mo1}[[2,1]] * \frac{\varepsilon\text{tface}[[2,1]]}{(1+a[[2,1]])^2}\right) *$$
$$x\text{Mo1}[[4,2]] * \left(1 - \frac{\varepsilon\text{tface}[[4,2]]}{1+a[[4,2]]}\right)\right)\text{^}2 +$$
$$\sigma\varepsilon\text{tface}[[2,1]]^2 *$$
$$\left(\left(x\text{Mo1}[[2,1]] * \frac{1}{1+a[[2,1]]}\right) * x\text{Mo1}[[4,2]] * \left(1 - \frac{\varepsilon\text{tface}[[4,2]]}{1+a[[4,2]]}\right)\right)\text{^}2 +$$
$$\sigma x[[4,2]]^2 *$$
$$\left(x\text{Mo1}[[2,1]] * \left(1 - \frac{\varepsilon\text{tface}[[2,1]]}{1+a[[2,1]]}\right) * \left(1 - \frac{\varepsilon\text{tface}[[4,2]]}{1+a[[4,2]]}\right)\right)\text{^}2 +$$
$$\sigma a[[4,2]]^2 * \left(x\text{Mo1}[[2,1]] *$$
$$\left(1 - \frac{\varepsilon\text{tface}[[2,1]]}{1+a[[1,2]]}\right) * x\text{Mo1}[[4,2]] * \frac{\varepsilon\text{tface}[[4,2]]}{(1+a[[4,2]])^2}\right)\text{^}2 +$$
$$\sigma\varepsilon\text{tface}[[4,2]]^2 *$$
$$\left(x\text{Mo1}[[2,1]] * \left(1 - \frac{\varepsilon\text{tface}[[2,1]]}{1+a[[2,1]]}\right) * x\text{Mo1}[[4,2]] * \frac{1}{1+a[[4,2]]}\right)\text{^}2;$$

$$\sigma 2\mathcal{M}\text{Mo2face}[[6,5]] = \sigma x[[5,3]]^2 * \left(1 - \frac{\varepsilon\text{tface}[[5,3]]}{1+a[[5,3]]}\right)\text{^}2 +$$
$$\sigma a[[5,3]]^2 * \left(x\text{Mo2}[[5,3]] * \frac{\varepsilon\text{tface}[[5,3]]}{(1+a[[5,3]])^2}\right)\text{^}2 +$$
$$\sigma\varepsilon\text{tface}[[5,3]]^2 * \left(x\text{Mo2}[[5,3]] * \frac{1}{1+a[[5,3]]}\right)\text{^}2;$$

$$\sigma\mathcal{S}\text{Mo1face} = (\text{Table}[\sigma 2\mathcal{B}\text{Mo1face}[[i,k]] * \mathcal{R}\text{Mo1face}[[i,k]]^2 * \mathcal{M}\text{Mo1face}[[k]]^2 +$$
$$\sigma 2\mathcal{R}\text{Mo1face}[[i,k]] * \mathcal{B}\text{Mo1face}[[i]]^2 * \mathcal{M}\text{Mo1face}[[k]]^2 +$$
$$\sigma 2\mathcal{M}\text{Mo1face}[[i,k]] * \mathcal{R}\text{Mo1face}[[i,k]]^2 * \mathcal{B}\text{Mo1face}[[i]]^2,$$
$$\{i,1,m\},\{k,1,m\}])\text{^}\frac{1}{2};$$

```
σSMo2face = (Table[σ2BMo2face[[i, k]] * AMo2face[[i, k]]^2 * MMo2face[[k]]^2 +
      σ2AMo2face[[i, k]] * BMo2face[[i]]^2 * MMo2face[[k]]^2 +
      σ2MMo2face[[i, k]] * AMo2face[[i, k]]^2 * BMo2face[[i]]^2,
     {i, 1, m}, {k, 1, m}])^
   1/2;

σSTc1face = (Table[σ2BTc1face[[i, k]] * ATc1face[[i, k]]^2 * MTc1face[[k]]^2 +
      σ2ATc1face[[i, k]] * BTc1face[[i]]^2 * MTc1face[[k]]^2 +
      σ2MTc1face[[i, k]] * ATc1face[[i, k]]^2 * BTc1face[[i]]^2,
     {i, 1, m}, {k, 1, m}])^
   1/2;

σSface = σSMo1face + σSMo2face + σSTc1face;

MatrixForm[σSface]
```

$$\begin{pmatrix} 0 & 0 & 0 & 0 & 0 & 0 \\ 0.00984221 & 0 & 0 & 0 & 0 & 0 \\ 7.55002\times10^{-6} & 0 & 0 & 0 & 0 & 0 \\ 0.000486691 & 0.0000222138 & 0 & 0 & 0 & 0 \\ 0 & 0 & 0.000519062 & 0 & 0 & 0 \\ 0 & 0 & 0.000180138 & 0.000288601 & 2.42517\times10^{-7} & 0 \end{pmatrix}$$

```
percentσSfacelist =
 100 * {σSface[[6, 3]] / Sface[[6, 3]], σSface[[6, 4]] / Sface[[6, 4]],
   σSface[[6, 5]] / Sface[[6, 5]], σSface[[5, 3]] / Sface[[5, 3]],
   σSface[[4, 1]] / Sface[[4, 1]], σSface[[3, 1]] / Sface[[3, 1]],
   σSface[[2, 1]] / Sface[[2, 1]], σSface[[4, 2]] / Sface[[4, 2]]};

TableForm[Table[
  {Mo99gammas[[i]], Sfacelist[[i]], percentσSfacelist[[i]]}, {i, 1, 8}],
 TableHeadings -> {None, {"Gamma (Mev)", "Peak Prob, Face", "% Dev"}},
 TableAlignments -> Center]
```

Gamma (Mev)	Peak Prob, Face	% Dev
0.777921	0.0024665	7.3034
0.7395	0.00521012	5.53923
0.411491	0.0000125654	1.93004
0.366421	0.00133364	38.9206
0.181068	0.00998895	4.87229
0.142675	0.0000666706	11.3244
0.140511	0.185865	5.29535
0.0405845	0.000275118	8.07427

```
AFTACεpfacelist = {0.053555, 0.041723, 0, 0.098674, 0.14925, 0, 1, 0};
```

```
AFTACintensitylist = {0.0424, 0.1200, 0, 0.0119, 0.0604, 0, 0.8245, 0};

AFTACSlist = AFTACεpfacelist * AFTACintensitylist;

RelDiff = Table[100 * (Sfacelist[[i]] - AFTACSlist[[i]]) / AFTACSlist[[i]], {i, 1, 8}];

TableForm[Table[{Mo99gammas[[i]], AFTACSlist[[i]],
   Sfacelist[[i]], RelDiff[[i]]}, {i, 1, 5}], TableHeadings -> {None,
   {"Gamma (Mev)", "AFTAC Face Prob", "AFIT Face Prob", "Rel. % Diff"}},
 TableAlignments -> Center]
```

Gamma (Mev)	AFTAC Face Prob	AFIT Face Prob	Rel. % Diff
0.777921	0.00227073	0.0024665	8.62127
0.7395	0.00500676	0.00521012	4.06175
0.411491	0	0.0000125654	ComplexInfinity
0.366421	0.00117422	0.00133364	13.5769
0.181068	0.0090147	0.00998895	10.8074

Appendix D: Analytical Method Code for Cs-136

```
Off[General::spell1]
```

AFTAC Canberra Detector 120 peak efficiency was characterized using a NIST source 10 cm above the detector. This distance is large enough to ensure that the solid angle subtended makes the contribution from correlated cascading gammas negligible by a factor of Ω shown below.

The following are the dimensions for a Cs-136 disk source and Det#120 to calculate the solid angle subtended. The reference is Equation 8.10, pg. 254, in **(Tsoulfanidis, 1983)**.

Cs-136 disk source radius in cm. The precipitate area on the planchet is as follows:
1.667 cm^2 for Y, Ce, Nd, Sm, Eu, Tb
3.125 cm^2 for Sr, Zr, Mo, Ag, Cd, Cs, Ba
2.381 cm^2 for U, Np

$$\text{Rsource} = \sqrt{\frac{3.125}{\pi}};$$

Det#120 crystal radius minus the Li contact in cm:

```
Lidepth = 0.05;
```

```
Rcrystal = 6.0 / 2 - Lidepth;
```

The thickness of the Al end cap in cm:

```
Aldepth = 0.16;
```

The spacing between the end cap and lithium contact in cm:

```
gap = 0.5;
```

Source to detector distance in cm:

```
sourceheight = 9.7;
```

$$z = \frac{\text{sourceheight} + \text{Aldepth} + \text{gap} + \text{Lidepth}}{\text{Rsource}};$$

```
s = Rcrystal / Rsource;
```

```
Ωfar = s * NIntegrate[Exp[-ρ * z] * BesselJ[1, (ρ * s)] * BesselJ[1, ρ] / ρ,
    {ρ, 0, 10}]
```

```
0.0188295
```

Thus, summing contributions are about two percent of the total counts of the correlated energy peaks.

The following are the efficiency function coefficients for Detector 120 with the disk source at 10cm. The efficiency is calibrated only between 0.059 and 1.836 MeV. The error in the peak efficiencies for the calibrated range is no larger than 1.5% as Capt Weimer, AFTAC/TOD, stated on 25 Jul 97.

```
c1 = -5.927;

c2 = -0.8438;

c3 = -0.02031;

c4 = -.00007080;

c5 = .02496;

c6 = .01560;
```

The following is the peak efficiency function with the disk source at 10 cm.

```
εpds5sfar[e_] =
 Exp[c1 + c2 * Log[e] + c3 * (Log[e]) ^ 2 + c4 * (Log[e]) ^ 3 +
   c5 * (Log[e]) ^ 4 + c6 * (Log[e]) ^ 5];
```

```
Plot[εpds5sfar[e], {e, .02, 2.}, PlotRange -> All,
 Frame -> True, GridLines -> Automatic, PlotLabel ->
  "Det#120 Absolute Peak Efficiency with Disk Source 10cm Above",
 FrameLabel -> {"Energy (MeV)", "ε peak"}]
```

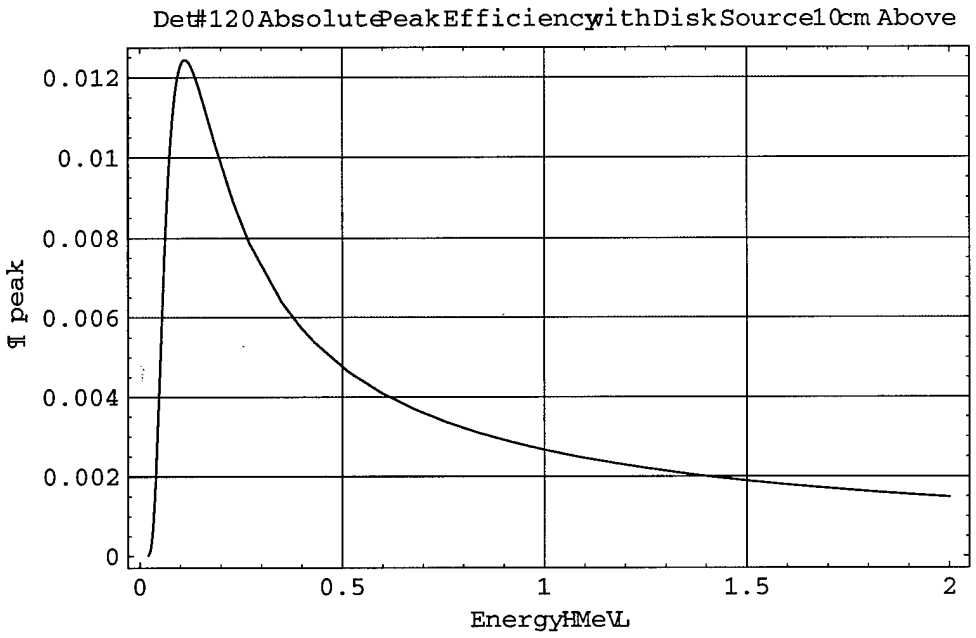

- Graphics -

The following are the Mo-99 gamma energies of interest with their corresponding peak efficiencies.

```
Cs136gammas = {1.235362, 1.048073, .818514, .507188, .340547,
   .319911, .273646, .187285, .176602, .166576, .163920,
   .153246, .109681, .08636, .066881};

εpds5sfarlist = Table[εpds5sfar[Cs136gammas[[i]]], {i, 1, 15}];
```

The row and column numbers of the matrix element represent the transition from level i to k.

```
εpfar =
 {{0, 0, 0, 0, 0, 0, 0, 0}, {εpds5sfarlist[[3]], 0, 0, 0, 0, 0, 0, 0},
  {0, εpds5sfarlist[[2]], 0, 0, 0, 0, 0, 0},
  {0, 0, εpds5sfarlist[[11]], 0, 0, 0, 0, 0}, {0, εpds5sfarlist[[1]],
   εpds5sfarlist[[8]], 0, 0, 0, 0, 0}, {0, 0, εpds5sfarlist[[7]],
   εpds5sfarlist[[13]], εpds5sfarlist[[14]], 0, 0, 0}, {0, 0,
   εpds5sfarlist[[5]], εpds5sfarlist[[9]], εpds5sfarlist[[12]],
   εpds5sfarlist[[15]], 0, 0}, {0, 0, εpds5sfarlist[[4]],
   0, εpds5sfarlist[[6]], 0, εpds5sfarlist[[10]], 0}};
```

The density (g/cm^3) at 300K is assumed to be similar to actual conditions of 77K for Ge and Li. The reference is **(Turner, 1995)**.

```
Gedensity = 5.32;

Aldensity = 2.70;

Lidensity = 0.53;
```

The atomic weight is in atoms per gram. The reference is **(Turner, 1995)**.

$$\text{Geatomicweight} = \frac{6.022 * 10^{23}}{72.59};$$

```
Geatomden = Gedensity * Geatomicweight;
```

$$\text{Alatomicweight} = \frac{6.022 * 10^{23}}{26.98154};$$

```
Alatomden = Aldensity * Alatomicweight;
```

$$\text{Liatomicweight} = \frac{6.022 * 10^{23}}{6.941};$$

```
Liatomden = Lidensity * Liatomicweight;
```

The following is a table of the compton scattering, photoelectric, and pair production cross sections in Ge, Al, and Li which will be turned into an interpolation function for use in computing total efficiencies. The reference is the Brookhaven National Laboratory website at TELNET bnlnd2.dne.bnl.gov, 23 Jul 1997. The gamma energies are in MeV and the cross sections in cm^2.

```
Gedata = Table[{{.02, (12.38 + 4996.) * 10^-24 * Geatomden},
    {.03, (14.00 + 1610.) * 10^-24 * Geatomden},
    {.04, (14.75 + 704.5) * 10^-24 * Geatomden},
    {.05, (15.05 + 367.0) * 10^-24 * Geatomden},
    {.06, (15.12 + 214.0) * 10^-24 * Geatomden},
    {.08, (14.94 + 90.61) * 10^-24 * Geatomden},
    {.10, (14.59 + 46.24) * 10^-24 * Geatomden},
    {.15, (13.57 + 13.56) * 10^-24 * Geatomden},
    {.20, (12.63 + 5.706) * 10^-24 * Geatomden},
    {.30, (11.13 + 1.733) * 10^-24 * Geatomden},
    {.40, (10.03 + .7731) * 10^-24 * Geatomden},
    {.50, (9.188 + .4270) * 10^-24 * Geatomden},
    {.60, (8.516 + .2699) * 10^-24 * Geatomden},
    {.80, (7.497 + .1379) * 10^-24 * Geatomden},
    {1.0, (6.747 + .08585) * 10^-24 * Geatomden},
    {1.022, (6.676 + .08158) * 10^-24 * Geatomden},
    {1.25, (6.038 + .05512 + .01073) * 10^-24 * Geatomden},
    {1.5, (5.490 + .03968 + .05320) * 10^-24 * Geatomden},
    {2.0, (4.687 + .02437 + .1971) * 10^-24 * Geatomden},
    {2.044, (4.629 + .02353 + .2116) * 10^-24 * Geatomden},
    {3.0, (3.689 + .01314 + .5378) * 10^-24 * Geatomden}}];

ΣGe = Interpolation[Gedata];
```

The macroscopic cross sections (in 1/cm) of Ge for the Cs-136 gamma energies are below:

```
ΣGelist = Table[ΣGe[Cs136gammas[[i]]], {i, 1, 15}];

ΣGem = {{0, 0, 0, 0, 0, 0, 0, 0}, {ΣGelist[[3]], 0, 0, 0, 0, 0, 0, 0},
  {0, ΣGelist[[2]], 0, 0, 0, 0, 0, 0},
  {0, 0, ΣGelist[[11]], 0, 0, 0, 0, 0},
  {0, ΣGelist[[1]], ΣGelist[[8]], 0, 0, 0, 0, 0},
  {0, 0, ΣGelist[[7]], ΣGelist[[13]], ΣGelist[[14]], 0, 0, 0}, {0, 0,
   ΣGelist[[5]], ΣGelist[[9]], ΣGelist[[12]], ΣGelist[[15]], 0, 0},
  {0, 0, ΣGelist[[4]], 0, ΣGelist[[6]], 0, ΣGelist[[10]], 0}};
```

```
Aldata = Table[{{.02, (6.142 + 138.9) * 10^-24 * Alatomden},
   {.03, (6.561 + 39.08) * 10^-24 * Alatomden},
   {.04, (6.695 + 15.70) * 10^-24 * Alatomden},
   {.05, (6.702 + 7.696) * 10^-24 * Alatomden},
   {.06, (6.645 + 4.285) * 10^-24 * Alatomden},
   {.08, (6.447 + 1.695) * 10^-24 * Alatomden},
   {.10, (6.218 + .8254) * 10^-24 * Alatomden},
   {.15, (5.678 + .2237) * 10^-24 * Alatomden},
   {.20, (5.233 + .08970) * 10^-24 * Alatomden},
   {.30, (4.573 + .02573) * 10^-24 * Alatomden},
   {.40, (4.105 + .01111) * 10^-24 * Alatomden},
   {.50, (3.752 + .006021) * 10^-24 * Alatomden},
   {.60, (3.474 + .003764) * 10^-24 * Alatomden},
   {.80, (3.053 + .001905) * 10^-24 * Alatomden},
   {1.0, (2.746 + .001184) * 10^-24 * Alatomden},
   {1.022, (2.717 + .001115) * 10^-24 * Alatomden},
   {1.25, (2.456 + .0007562 + .001404) * 10^-24 * Alatomden},
   {1.5, (2.232 + .0005476 + .007652) * 10^-24 * Alatomden},
   {2.0, (1.905 + .0003420 + .03023) * 10^-24 * Alatomden},
   {2.044, (1.882 + .0003307 + .03258) * 10^-24 * Alatomden},
   {3.0, (1.499 + .00031892 + .08595) * 10^-24 * Alatomden}}];

ΣAl = Interpolation[Aldata];
```

The macroscopic cross sections (in 1/cm) of Al for the Cs-136 gamma energies are below:

```
ΣAllist = Table[ΣAl[Cs136gammas[[i]]], {i, 1, 15}];

ΣAlm = {{0, 0, 0, 0, 0, 0, 0, 0}, {ΣAllist[[3]], 0, 0, 0, 0, 0, 0, 0},
  {0, ΣAllist[[2]], 0, 0, 0, 0, 0, 0},
  {0, 0, ΣAllist[[11]], 0, 0, 0, 0, 0},
  {0, ΣAllist[[1]], ΣAllist[[8]], 0, 0, 0, 0, 0},
  {0, 0, ΣAllist[[7]], ΣAllist[[13]], ΣAllist[[14]], 0, 0, 0}, {0, 0,
   ΣAllist[[5]], ΣAllist[[9]], ΣAllist[[12]], ΣAllist[[15]], 0, 0},
  {0, 0, ΣAllist[[4]], 0, ΣAllist[[6]], 0, ΣAllist[[10]], 0}};
```

```
Lidata = Table[{{.02, (1.702 + .1516) * 10^-24 * Liatomden},
    {.03, (1.718 + .03841) * 10^-24 * Liatomden},
    {.04, (1.692 + .01445) * 10^-24 * Liatomden},
    {.05, (1.656 + .006770) * 10^-24 * Liatomden},
    {.06, (1.617 + .003645) * 10^-24 * Liatomden},
    {.08, (1.540 + .001373) * 10^-24 * Liatomden},
    {.10, (1.471 + .0006464) * 10^-24 * Liatomden},
    {.15, (1.328 + .0001666) * 10^-24 * Liatomden},
    {.20, (1.218 + .00006481) * 10^-24 * Liatomden},
    {.30, (1.060 + .00001796) * 10^-24 * Liatomden},
    {.40, (.9499 + 7.615 * 10^-6) * 10^-24 * Liatomden},
    {.50, (.8676 + 4.081 * 10^-6) * 10^-24 * Liatomden},
    {.60, (.8027 + 2.533 * 10^-6) * 10^-24 * Liatomden},
    {.80, (.7053 + 1.276 * 10^-6) * 10^-24 * Liatomden},
    {1.0, (.6341 + 7.939 * 10^-7) * 10^-24 * Liatomden},
    {1.022, (.6274 + 7.038 * 10^-7) * 10^-24 * Liatomden},
    {1.25, (.5670 + 4.788 * 10^-7 + 7.052 * 10^-5) * 10^-24 * Liatomden},
    {1.5, (.5154 + 3.486 * 10^-7 + .0003953) * 10^-24 * Liatomden},
    {2.0, (.4398 + 2.212 * 10^-7 + .001583) * 10^-24 * Liatomden},
    {2.044, (.4344 + 2.141 * 10^-7 + .001707) * 10^-24 * Liatomden},
    {3.0, (.3460 + 1.250 * 10^-7 + .004545) * 10^-24 * Liatomden}}];

ΣLi = Interpolation[Lidata];
```

The macroscopic cross sections (in 1/cm) of Li for the Mo-99 gamma energies are below:

```
ΣLilist = Table[ΣLi[Cs136gammas[[i]]], {i, 1, 15}];

ΣLim = {{0, 0, 0, 0, 0, 0, 0, 0}, {ΣLilist[[3]], 0, 0, 0, 0, 0, 0, 0},
  {0, ΣLilist[[2]], 0, 0, 0, 0, 0, 0},
  {0, 0, ΣLilist[[11]], 0, 0, 0, 0, 0},
  {0, ΣLilist[[1]], ΣLilist[[8]], 0, 0, 0, 0, 0},
  {0, 0, ΣLilist[[7]], ΣLilist[[13]], ΣLilist[[14]], 0, 0, 0}, {0, 0,
   ΣLilist[[5]], ΣLilist[[9]], ΣLilist[[12]], ΣLilist[[15]], 0, 0},
  {0, 0, ΣLilist[[4]], 0, ΣLilist[[6]], 0, ΣLilist[[10]], 0}};
```

To review and compare the macroscopic cross sections of the elements involved:

```
TableForm[Table[{Cs136gammas[[i]], ΣGelist[[i]],
   ΣAllist[[i]], ΣLilist[[i]]}, {i, 1, 15}], TableHeadings ->
  {None, {"Mev", "ΣGe (1/cm)", "ΣAl (1/cm)", "ΣLi (1/cm)"}},
 TableAlignments -> Center]
```

Mev	ΣGe (1/cm)	ΣAl (1/cm)	ΣLi (1/cm)
1.235362	0.270967	0.149026	0.026236
1.048073	0.294437	0.161784	0.0284955
0.818514	0.333168	0.182133	0.0320856
0.507188	0.421267	0.22511	0.0396563
0.340547	0.519014	0.263977	0.0464761
0.319911	0.541161	0.270399	0.0475881
0.273646	0.783189	0.291284	0.0504276
0.187285	1.06751	0.333599	0.0571857
0.176602	1.15798	0.341143	0.058227
0.166576	1.18203	0.346728	0.0592544
0.16392	1.18355	0.348101	0.0595353
0.153246	1.19032	0.353753	0.0607041
0.109681	2.44549	0.413162	0.0662532
0.08636	4.06767	0.471788	0.0698017
0.066881	7.30136	0.572063	0.073228

To better simulate the response of the detector, the Al end cap and Li contact will be included to account for their attenuation.

The path length of a gamma through the end cap and contact in cm. Since the end cap and contact extend beyond the crystal, there are no vertical edges affecting the path length for this simplified approach.

```
xAl[ξ_] = Aldepth / ξ;
```

```
xLi[ξ_] = Lidepth / ξ;
```

The following is the equation to compute the total efficiency of the five-sided detector crystal with a point source. The references are **(Camp and Van Lehn, 1969)**, pg. 237-238, **(McCallum and Coote, 1975)**, pg. 192, and **(Heath, 1964)**, pg. 21.

The radial depth of the five-sided crystal in cm:

```
Rdd = (6.0 - 0.8 - 2 * Lidepth) / 2;
```

The axial depth of the five sided crystal in cm:

```
Add = 5.1 - 3.65 - Lidepth;
```

The crystal length in cm:

```
Lcrystal = 5.1 - Lidepth;
```

The limits of integration for the five-sided cylinder:

```
Array[Aps5sfar, 4];

Array[Bps5sfar, 4];

Array[xps5sfar, 4];

Bps5sfar[4] = Cos[0];

Aps5sfar[4] = Cos[ArcTan[(Rcrystal - Rdd) /
    (sourceheight + Aldepth + gap + Lidepth + Lcrystal)]];

xps5sfar[4][ξ_] = Add / ξ;

Bps5sfar[3] = Aps5sfar[4];

Aps5sfar[3] =
 Cos[ArcTan[(Rcrystal - Rdd) / (sourceheight + Aldepth + gap + Lidepth + Add)]];

xps5sfar[3][ξ_] =
 (sourceheight + Aldepth + gap + Lidepth + Lcrystal + Add) / ξ -
  (Rcrystal - Rdd) / Sqrt[1 - ξ^2];

Bps5sfar[2] = Aps5sfar[3];

Aps5sfar[2] = Cos[ArcTan[
   Rcrystal / (sourceheight + Aldepth + gap + Lidepth + Lcrystal)]];

xps5sfar[2][ξ_] = Lcrystal / ξ;

Bps5sfar[1] = Aps5sfar[2];

Aps5sfar[1] =
 Cos[ArcTan[Rcrystal / (sourceheight + Aldepth + gap + Lidepth)]];

xps5sfar[1][ξ_] =
 Rcrystal / Sqrt[1 - ξ^2] - (sourceheight + Aldepth + gap + Lidepth) / ξ;

εtps5sfar[e_] :=
 1/2 * Sum[NIntegrate[(1 - Exp[-ΣGe[e] * xps5sfar[i][ξ]]) *
     Exp[-ΣAl[e] * xAl[ξ] - ΣLi[e] * xLi[ξ]],
    {ξ, Aps5sfar[i], Bps5sfar[i]}], {i, 1, 4}]
```

The total efficiency for the five-sided cylinder with a point source 10 cm above for the Cs-136 gamma energies:

```
εtps5sfarlist = Table[εtps5sfar[Cs136gammas[[n]]], {n, 1, 15}];

εtps5sfarm =
 {{0, 0, 0, 0, 0, 0, 0, 0}, {εtps5sfarlist[[3]], 0, 0, 0, 0, 0, 0, 0},
  {0, εtps5sfarlist[[2]], 0, 0, 0, 0, 0, 0},
  {0, 0, εtps5sfarlist[[11]], 0, 0, 0, 0, 0}, {0, εtps5sfarlist[[1]],
   εtps5sfarlist[[8]], 0, 0, 0, 0, 0}, {0, 0, εtps5sfarlist[[7]],
   εtps5sfarlist[[13]], εtps5sfarlist[[14]], 0, 0, 0}, {0, 0,
   εtps5sfarlist[[5]], εtps5sfarlist[[9]], εtps5sfarlist[[12]],
   εtps5sfarlist[[15]], 0, 0}, {0, 0, εtps5sfarlist[[4]],
   0, εtps5sfarlist[[6]], 0, εtps5sfarlist[[10]], 0}};
```

The following is the equation to compute the total efficiency of the solid cylindrical detector crystal with a point source 10cm above. The references is **(Heath, 1964)**, pg. 21.

The limits of integration for the solid cylinder with a point source:

```
Array[Aps3sfar, 2];

Array[Bps3sfar, 2];

Array[xps3sfar, 2];

Bps3sfar[2] = 1;

Aps3sfar[2] = Cos[ArcTan[
   Rcrystal / (sourceheight + Aldepth + gap + Lidepth + Lcrystal)]];

xps3sfar[2][ξ_] = Lcrystal / ξ;

Bps3sfar[1] = Aps3sfar[2];

Aps3sfar[1] =
 Cos[ArcTan[Rcrystal / (sourceheight + Aldepth + gap + Lidepth)]];

xps3sfar[1][ξ_] =
 Rcrystal / √(1 - ξ²) - (sourceheight + Aldepth + gap + Lidepth) / ξ;

εtps3sfar[e_] :=
 1/2 * Σ_{i=1}^{2} NIntegrate[(1 - Exp[-ΣGe[e] * xps3sfar[i][ξ]]) *
    Exp[-ΣAl[e] * xAl[ξ] - ΣLi[e] * xLi[ξ]],
   {ξ, Aps3sfar[i], Bps3sfar[i]}];
```

```
εtps3sfarlist = Table[εtps3sfar[Cs136gammas[[n]]], {n, 1, 15}];

εtps3sfarm =
 {{0, 0, 0, 0, 0, 0, 0, 0}, {εtps3sfarlist[[3]], 0, 0, 0, 0, 0, 0, 0},
  {0, εtps3sfarlist[[2]], 0, 0, 0, 0, 0, 0},
  {0, 0, εtps3sfarlist[[11]], 0, 0, 0, 0, 0}, {0, εtps3sfarlist[[1]],
   εtps3sfarlist[[8]], 0, 0, 0, 0, 0}, {0, 0, εtps3sfarlist[[7]],
   εtps3sfarlist[[13]], εtps3sfarlist[[14]], 0, 0, 0}, {0, 0,
   εtps3sfarlist[[5]], εtps3sfarlist[[9]], εtps3sfarlist[[12]],
   εtps3sfarlist[[15]], 0, 0}, {0, 0, εtps3sfarlist[[4]],
   0, εtps3sfarlist[[6]], 0, εtps3sfarlist[[10]], 0}};
```

The following is the equation to compute the total efficiency of the solid cylindrical detector crystal with a disk source 10 cm above. The references is Scintillation Spectrometry 2nd Ed., Heath, R., 1964, pg. 21.

The limits of integration for the solid cylinder with a disk source:

```
A1ds3sfar = Cos[0];

B1ds3sfar[ϕ_, ρ_] =

 Cos[ArcTan[(-ρ * Sin[ϕ] + Sqrt[ρ^2 * (Sin[ϕ])^2 - (ρ^2 - Rcrystal^2)])/
    (sourceheight + Aldepth + gap + Lidepth + Lcrystal)]];

x1ds3sfar[ξ_] = Lcrystal / ξ;

A2ds3sfar[ϕ_, ρ_] =

 Cos[ArcTan[(-ρ * Sin[ϕ] + Sqrt[ρ^2 * (Sin[ϕ])^2 - (ρ^2 - Rcrystal^2)])/
    (sourceheight + Aldepth + gap + Lidepth + Lcrystal)]];

B2ds3sfar[ϕ_, ρ_] =

 Cos[ArcTan[(-ρ * Sin[ϕ] + Sqrt[ρ^2 * (Sin[ϕ])^2 - (ρ^2 - Rcrystal^2)])/
    (sourceheight + Aldepth + gap + Lidepth)]];

x2ds3sfar[ξ_, ϕ_, ρ_] =

 (-ρ * Sin[ϕ] + Sqrt[ρ^2 * (Sin[ϕ])^2 - (ρ^2 - Rcrystal^2)])/
  Sqrt[1 - ξ^2] -
 (sourceheight + Aldepth + gap + Lidepth)/ξ;
```

```
εtds3sfar1[e_] := 1/(π (Rsource)^2) (NIntegrate[
    NIntegrate[
      NIntegrate[
         (1 - Exp[-ΣGe[e] * xlds3sfar[ξ]]) *
        Exp[-ΣAl[e] * xAl[ξ] - ΣLi[e] * xLi[ξ]],
       {ξ, B1ds3sfar[ϕ, ρ], A1ds3sfar}] , {ϕ, -π/2, π/2}] * ρ,
    {ρ, 0, Rsource}])

εtds3sfar1list = Table[εtds3sfar1[Cs136gammas[[n]]], {n, 1, 15}];

εtds3sfar2[e_] := 1/(π (Rsource)^2) (NIntegrate[
    NIntegrate[
      NIntegrate[
         (1 - Exp[-ΣGe[e] * x2ds3sfar[ξ, ϕ, ρ]]) *
        Exp[-ΣAl[e] * xAl[ξ] - ΣLi[e] * xLi[ξ]],
       {ξ, B2ds3sfar[ϕ, ρ], A2ds3sfar[ϕ, ρ]}] , {ϕ, -π/2, π/2}] * ρ,
    {ρ, 0, Rsource}])

εtds3sfar2list = Table[εtds3sfar2[Cs136gammas[[n]]], {n, 1, 15}];

εtds3sfarlist = εtds3sfar1list + εtds3sfar2list;

εtds3sfarm =
 {{0, 0, 0, 0, 0, 0, 0, 0}, {εtds3sfarlist[[3]], 0, 0, 0, 0, 0, 0, 0},
  {0, εtds3sfarlist[[2]], 0, 0, 0, 0, 0, 0},
  {0, 0, εtds3sfarlist[[11]], 0, 0, 0, 0, 0}, {0, εtds3sfarlist[[1]],
   εtds3sfarlist[[8]], 0, 0, 0, 0, 0}, {0, 0, εtds3sfarlist[[7]],
   εtds3sfarlist[[13]], εtds3sfarlist[[14]], 0, 0, 0}, {0, 0,
   εtds3sfarlist[[5]], εtds3sfarlist[[9]], εtds3sfarlist[[12]],
   εtds3sfarlist[[15]], 0, 0}, {0, 0, εtds3sfarlist[[4]],
   0, εtds3sfarlist[[6]], 0, εtds3sfarlist[[10]], 0}};
```

The following table shows the contribution of each zone to the total efficiency of the three-sided cylinder with a disk source.

```
TableForm[Table[{εtds3sfar1list[[i]],
   εtds3sfar2list[[i]], εtds3sfarlist[[i]]}, {i, 1, 15}],
 TableHeadings -> {None, {"Inner Cone Total Eff.",
    "Outer Wedge Total Eff.", "Sum Total Eff."}},
 TableAlignments -> Center];
```

The following is the equation to compute the total efficiency of the five-sided cylindrical detector crystal with a disk source 10 cm above. It is assumed the ratio of the five-sided to three-sided crystal total efficiencies using a point source at a given distance is the same for using a disk source at the same distance.

$$\varepsilon\text{tds5sfarlist} = \frac{\varepsilon\text{tps5sfarlist}}{\varepsilon\text{tps3sfarlist}} * \varepsilon\text{tds3sfarlist};$$

```
εtfar =
 {{0, 0, 0, 0, 0, 0, 0, 0}, {εtds5sfarlist[[3]], 0, 0, 0, 0, 0, 0, 0},
  {0, εtds5sfarlist[[2]], 0, 0, 0, 0, 0, 0},
  {0, 0, εtds5sfarlist[[11]], 0, 0, 0, 0, 0}, {0, εtds5sfarlist[[1]],
   εtds5sfarlist[[8]], 0, 0, 0, 0, 0}, {0, 0, εtds5sfarlist[[7]],
   εtds5sfarlist[[13]], εtds5sfarlist[[14]], 0, 0, 0}, {0, 0,
   εtds5sfarlist[[5]], εtds5sfarlist[[9]], εtds5sfarlist[[12]],
   εtds5sfarlist[[15]], 0, 0}, {0, 0, εtds5sfarlist[[4]],
   0, εtds5sfarlist[[6]], 0, εtds5sfarlist[[10]], 0}};
```

The following is the peak to total efficiency ratio which is presumed to be independent of distance. This ratio will allow finding the peak efficiency from the calculated total efficiency with a disk source on the face of the detector. The reference is Equation 11 and text, **(McCallum and Coote, 1975)**, pg. 192.

$$\text{PKtoTTLds5slist} = \frac{\varepsilon\text{pds5sfarlist}}{\varepsilon\text{tds5sfarlist}};$$

```
TableForm[Table[{Cs136gammas[[i]], εtds5sfarlist[[i]],
   εpds5sfarlist[[i]], PKtoTTLds5slist[[i]]}, {i, 1, 15}],
 TableHeadings -> {None, {"Mev", "εtds5s", "εpds5s", "P/T"}},
 TableAlignments -> Center]
```

Mev	εtds5s	εpds5s	P/T
1.235362	0.0101983	0.002229	0.218565
1.048073	0.0106328	0.00256278	0.241024
0.818514	0.0112624	0.00315491	0.280127
0.507188	0.0123716	0.00469878	0.379804
0.340547	0.0132356	0.00653519	0.493757
0.319911	0.0133956	0.00687769	0.513429
0.273646	0.0146551	0.00779652	0.532001
0.187285	0.0153411	0.0102609	0.668851
0.176602	0.0154929	0.0106358	0.686494
0.166576	0.0155193	0.0109936	0.708381
0.16392	0.0155181	0.0110884	0.714546
0.153246	0.0155142	0.0114644	0.738966
0.109681	0.0164054	0.0124301	0.757679
0.08636	0.0166731	0.0115871	0.694961
0.066881	0.0166939	0.00896527	0.53704

```
TableForm[Table[{Cs136gammas[[i]], εtds3sfarlist[[i]],
   εtps5sfarlist[[i]], εtps3sfarlist[[i]]}, {i, 1, 15}],
 TableHeadings -> {None, {"Mev", "εtds3s", "εtps5s", "εtps3s"}},
 TableAlignments -> Center]
```

Mev	εtds3s	εtps5s	εtps3s
1.235362	0.0102858	0.0102377	0.0103256
1.048073	0.0107211	0.0106746	0.0107632
0.818514	0.0113509	0.0113078	0.0113965
0.507188	0.012457	0.0124239	0.0125097
0.340547	0.0133146	0.0132941	0.0133734
0.319911	0.0134729	0.0134553	0.0135329
0.273646	0.0147133	0.0147253	0.0147838
0.187285	0.0153802	0.0154187	0.015458
0.176602	0.0155273	0.0155723	0.0156068
0.166576	0.0155524	0.015599	0.0156324
0.16392	0.0155512	0.0155979	0.0156312
0.153246	0.0155469	0.015594	0.0156269
0.109681	0.0164108	0.0164973	0.0165026
0.08636	0.0166736	0.01677	0.0167706
0.066881	0.0166939	0.0167939	0.0167939

Next, the total efficiency of the three-sided crystal with the disk source on the detector face is shown below. (The procedure of using the ratios of the efficiencies is repeated to find the total efficiency for the five-sided crystal.) The distance in cm between

the detector's face and crystal includes the thickness of the Al can, the axial space (vacuum), and the Li contact.

```
sourceheight = 0;
```

The limits of integration for the five-sided cylinder:

```
Array[Aps5sface, 4];

Array[Bps5sface, 4];

Array[xps5sface, 4];

Bps5sface[4] = Cos[0];

Aps5sface[4] = Cos[ArcTan[(Rcrystal - Rdd) /
    (sourceheight + Aldepth + gap + Lidepth + Lcrystal)]];

xps5sface[4][ξ_] = Add / ξ;

Bps5sface[3] = Aps5sface[4];

Aps5sface[3] = Cos[ArcTan[
   (Rcrystal - Rdd) / (sourceheight + Aldepth + gap + Lidepth + Add)]];

xps5sface[3][ξ_] =
 (sourceheight + Aldepth + gap + Lidepth + Lcrystal + Add) / ξ -
  (Rcrystal - Rdd) / Sqrt[1 - ξ^2];

Bps5sface[2] = Aps5sface[3];

Aps5sface[2] = Cos[ArcTan[
   Rcrystal / (sourceheight + Aldepth + gap + Lidepth + Lcrystal)]];

xps5sface[2][ξ_] = Lcrystal / ξ;

Bps5sface[1] = Aps5sface[2];

Aps5sface[1] =
 Cos[ArcTan[Rcrystal / (sourceheight + Aldepth + gap + Lidepth)]];

xps5sface[1][ξ_] =
 Rcrystal / Sqrt[1 - ξ^2] - (sourceheight + Aldepth + gap + Lidepth) / ξ;

εtps5sface[e_] :=
 1/2 * Sum[NIntegrate[(1 - Exp[-ΣGe[e] * xps5sface[i][ξ]]) *
     Exp[-ΣAl[e] * xAl[ξ] - ΣLi[e] * xLi[ξ]],
    {ξ, Aps5sface[i], Bps5sface[i]}], {i, 1, 4}];
```

```
εtps5sfacelist = Table[εtps5sface[Cs136gammas[[n]]], {n, 1, 15}];
```

The limits of integration for the solid cylinder with a point source:

```
Array[Aps3sface, 2];

Array[Bps3sface, 2];

Array[xps3sface, 2];

Bps3sface[2] = Cos[0];

Aps3sface[2] = Cos[ArcTan[
   Rcrystal / (sourceheight + Aldepth + gap + Lidepth + Lcrystal)]];

xps3sface[2][ξ_] = Lcrystal / ξ;

Bps3sface[1] = Aps3sface[2];

Aps3sface[1] =
 Cos[ArcTan[Rcrystal / (sourceheight + Aldepth + gap + Lidepth)]];

xps3sface[1][ξ_] =
 Rcrystal / √(1 - ξ^2) - (sourceheight + Aldepth + gap + Lidepth) / ξ;

εtps3sface[e_] :=
 1/2 * Σ_{i=1}^{2} NIntegrate[(1 - Exp[-ΣGe[e] * xps3sface[i][ξ]]) *
    Exp[-ΣAl[e] * xAl[ξ] - ΣLi[e] * xLi[ξ]],
   {ξ, Aps3sface[i], Bps3sface[i]}];

εtps3sfacelist = Table[εtps3sface[Cs136gammas[[n]]], {n, 1, 15}];
```

The limits of integration for the solid cylinder with a disk source:

```
A1ds3sface = Cos[0];

B1ds3sface[ϕ_, ρ_] =

 Cos[ArcTan[(-ρ * Sin[ϕ] + √(ρ^2 * (Sin[ϕ])^2 - (ρ^2 - Rcrystal^2))
    / (sourceheight + Aldepth + gap + Lidepth + Lcrystal)]];

x1ds3sface[ξ_] = Lcrystal / ξ;

A2ds3sface[ϕ_, ρ_] =

 Cos[ArcTan[(-ρ * Sin[ϕ] + √(ρ^2 * (Sin[ϕ])^2 - (ρ^2 - Rcrystal^2))
    / (sourceheight + Aldepth + gap + Lidepth + Lcrystal)]];
```

```
B2ds3sface[ϕ_, ρ_] =
 Cos[ArcTan[(-ρ * Sin[ϕ] + Sqrt[ρ^2 * (Sin[ϕ])^2 - (ρ^2 - Rcrystal^2)]) /
     (sourceheight + Aldepth + gap + Lidepth)]];

x2ds3sface[ξ_, ϕ_, ρ_] =
 (-ρ * Sin[ϕ] + Sqrt[ρ^2 * (Sin[ϕ])^2 - (ρ^2 - Rcrystal^2)]) /
   Sqrt[1 - ξ^2] -
  (sourceheight + Aldepth + gap + Lidepth) / ξ;

εtds3sface1[e_] := 1 / (π (Rsource)^2) (NIntegrate[
    NIntegrate[
      NIntegrate[
        (1 - Exp[-ΣGe[e] * x1ds3sface[ξ]]) *
         Exp[-ΣAl[e] * xAl[ξ] - ΣLi[e] * xLi[ξ]],
        {ξ, B1ds3sface[ϕ, ρ], A1ds3sface}], {ϕ, -π/2, π/2}] * ρ,
    {ρ, 0, Rsource}])

εtds3sface1list = Table[εtds3sface1[Cs136gammas[[n]]], {n, 1, 15}];

εtds3sface2[e_] := 1 / (π (Rsource)^2) (NIntegrate[
    NIntegrate[
      NIntegrate[
        (1 - Exp[-ΣGe[e] * x2ds3sface[ξ, ϕ, ρ]]) *
         Exp[-ΣAl[e] * xAl[ξ] - ΣLi[e] * xLi[ξ]],
        {ξ, B2ds3sface[ϕ, ρ], A2ds3sface[ϕ, ρ]}], {ϕ, -π/2, π/2}] * ρ,
    {ρ, 0, Rsource}])

εtds3sface2list = Table[εtds3sface2[Cs136gammas[[n]]], {n, 1, 15}];

εtds3sfacelist = εtds3sface1list + εtds3sface2list;
```

The following table shows the contribution of each zone to the total efficiency of the three-sided cylinder with a disk source.

```
TableForm[Table[{εtds3sface1list[[i]],
   εtds3sface2list[[i]], εtds3sfacelist[[i]]}, {i, 1, 15}],
 TableHeadings -> {None, {"Inner Cone Total Eff.",
    "Outer Wedge Total Eff.", "Sum Total Eff."}},
 TableAlignments -> Center];
```

The following is the equation to compute the total efficiency of the five-sided cylindrical detector crystal with a disk source at the face. It is assumed the ratio of the five-sided to three-sided crystal total efficiencies using a point source is the same for using a disk source at the same distance.

$$\varepsilon\text{tds5sfacelist} = \frac{\varepsilon\text{tps5sfacelist}}{\varepsilon\text{tps3sfacelist}} * \varepsilon\text{tds3sfacelist};$$

Using the peak-to-total efficiency ratio calculated above, the peak efficiency of the five-sided crystal with a disk source at the face is shown below:

```
εpds5sfacelist = εtds5sfacelist * PKtoTTLds5slist;
```

To summarize the results up to present, a table is provided below.

```
TableForm[Table[{Cs136gammas[[i]],
   εtds5sfacelist[[i]], εpds5sfacelist[[i]]}, {i, 1, 15}],
 TableHeadings -> {None, {"Gamma (Mev)",
    "Total Face Efficiency", "Peak Face Efficiency"}},
 TableAlignments -> Center]
```

Gamma (Mev)	Total Face Efficiency	Peak Face Efficiency
1.235362	0.176704	0.0386214
1.048073	0.185113	0.0446167
0.818514	0.19754	0.0553363
0.507188	0.220298	0.0836701
0.340547	0.239085	0.11805
0.319911	0.242711	0.124615
0.273646	0.273449	0.145475
0.187285	0.291161	0.194743
0.176602	0.295126	0.202602
0.166576	0.295752	0.209505
0.16392	0.295703	0.211293
0.153246	0.29552	0.218379
0.109681	0.315647	0.239159
0.08636	0.317962	0.220971
0.066881	0.312915	0.168048

```
TableForm[Table[{Cs136gammas[[i]], εtds3sfacelist[[i]],
   εtps5sfacelist[[i]], εtps3sfacelist[[i]]}, {i, 1, 15}],
 TableHeadings -> {None, {"Mev", "εtds3s", "εtps5s", "εtps3s"}},
 TableAlignments -> Center]
```

Mev	εtds3s	εtps5s	εtps3s
1.235362	0.177835	0.180888	0.182046
1.048073	0.186242	0.189519	0.190675
0.818514	0.198652	0.202275	0.203414
0.507188	0.221331	0.22563	0.226688
0.340547	0.24	0.244882	0.245819
0.319911	0.243599	0.248592	0.249501
0.273646	0.274058	0.279919	0.280542
0.187285	0.291536	0.297713	0.298096
0.176602	0.295447	0.301649	0.301977
0.166576	0.29606	0.302256	0.302571
0.16392	0.29601	0.302203	0.302517
0.153246	0.295823	0.302006	0.302316
0.109681	0.315689	0.321184	0.321227
0.08636	0.317966	0.322721	0.322725
0.066881	0.312915	0.317029	0.317029

The next step is to place the various coefficients for the summing correction equations in matrix form. The reference is **(Andreev and others, 1972)**, pg. 1358-1360.

The internal conversion coefficients for Cs-136 are shown below. The reference is **(Tuli, 1987)**, pg. 311. Due to *Mathematica*'s indexing, the ground state is level 1.

```
a = {{0, 0, 0, 0, 0, 0, 0, 0}, {0.00282, 0, 0, 0, 0, 0, 0, 0},
  {0, 0, 0, 0, 0, 0, 0, 0}, {0, 0, 2.26, 0, 0, 0, 0, 0},
  {0, 0, 0.190, 0, 0, 0, 0, 0}, {0, 0, 0.016, 1.47, 0.343, 0, 0, 0, 0},
  {0, 0, 0.0305, 0.094, 0.433, 0.694, 0, 0},
  {0, 0, 0.0112, 0, 0.0393, 0, 0.245, 0}};

MatrixForm[a];
```

The following are branch ratios for cascading Cs-136 gammas . The reference is **(Tuli, 1987)**, pg. 311. Due to Mathematica's indexing, the ground state is level 1.

```
x = {{0, 0, 0, 0, 0, 0, 0, 0},
  {1, 0, 0, 0, 0, 0, 0, 0}, {0, 1, 0, 0, 0, 0, 0, 0},
  {0, 0, 1, 0, 0, 0, 0, 0}, {0, 0.982, 0.018, 0, 0, 0, 0, 0},
  {0, 0, 0.671, 0.014, 0.315, 0, 0, 0},
  {0, 0, 0.673, 0.159, 0.092, 0.076, 0, 0},
  {0, 0, 0.527, 0, 0.272, 0, 0.201, 0}};

MatrixForm[x];
```

The peak face efficiencies are placed in a matrix according to their level transitions.

```
εpface =
 {{0, 0, 0, 0, 0, 0, 0, 0}, {εpds5sfacelist[[3]], 0, 0, 0, 0, 0, 0, 0},
  {0, εpds5sfacelist[[2]], 0, 0, 0, 0, 0, 0},
  {0, 0, εpds5sfacelist[[11]], 0, 0, 0, 0, 0},
  {0, εpds5sfacelist[[1]], εpds5sfacelist[[8]], 0, 0, 0, 0, 0},
  {0, 0, εpds5sfacelist[[7]],
   εpds5sfacelist[[13]], εpds5sfacelist[[14]], 0, 0, 0}, {0, 0,
   εpds5sfacelist[[5]], εpds5sfacelist[[9]], εpds5sfacelist[[12]],
   εpds5sfacelist[[15]], 0, 0}, {0, 0, εpds5sfacelist[[4]],
   0, εpds5sfacelist[[6]], 0, εpds5sfacelist[[10]], 0}};

MatrixForm[εpface];

MatrixForm[εpfar];
```

The total face efficiencies are placed in a matrix according to their level transitions.

```
εtface =
 {{0, 0, 0, 0, 0, 0, 0, 0}, {εtds5sfacelist[[3]], 0, 0, 0, 0, 0, 0, 0},
  {0, εtds5sfacelist[[2]], 0, 0, 0, 0, 0, 0},
  {0, 0, εtds5sfacelist[[11]], 0, 0, 0, 0, 0},
  {0, εtds5sfacelist[[1]], εtds5sfacelist[[8]], 0, 0, 0, 0, 0},
  {0, 0, εtds5sfacelist[[7]],
   εtds5sfacelist[[13]], εtds5sfacelist[[14]], 0, 0, 0}, {0, 0,
   εtds5sfacelist[[5]], εtds5sfacelist[[9]], εtds5sfacelist[[12]],
   εtds5sfacelist[[15]], 0, 0}, {0, 0, εtds5sfacelist[[4]],
   0, εtds5sfacelist[[6]], 0, εtds5sfacelist[[10]], 0}};

MatrixForm[εtface];

MatrixForm[εtfar];
```

The Mo-99 β- decay branch ratios are listed below in the array. The reference is **(Tuli, 1987)**, pg. 311.

```
β = {0, 0, 0.0198, 0, 0.0178, 0.00790, 0.00128, 0.929, 0.0226};

MatrixForm[β];
```

The following method determines the fraction of counts underneath an observed energy peak. The peak represents the sum of direct and true coincidence gamma rays depositing the given energy. The true activity has been normalized to one. This method does not include the angular correlation coefficient W since this was shown to be a negligible factor in analyzing Mo-99. The reference is **(Andreev and others, 1972)**, pg. 1359.

The number of energy levels in Cs-136 in the simplified decay scheme is eight (seven plus ground state). However due to Mathematica's automatic indexing at one, m =8. The terms are decoupled along the decay chains in order to calculate their contributions. They will be summed at the end.

```
m = 8;

afar = Table[ x[[i, k]] * εpfar[[i, k]] / (1 + a[[i, k]]), {i, 1, m}, {k, 1, m}];

aface = Table[ x[[i, k]] * εpface[[i, k]] / (1 + a[[i, k]]), {i, 1, m}, {k, 1, m}];

MatrixForm[aface];

MatrixForm[afar];

bface = Table[x[[i, k]] * (1 - εtface[[i, k]] / (1 + a[[i, k]])), {i, 1, m}, {k, 1, m}];

bfar = Table[x[[i, k]] * (1 - εtfar[[i, k]] / (1 + a[[i, k]])), {i, 1, m}, {k, 1, m}];

MatrixForm[bface];

MatrixForm[bfar];

ℬface = {0, 0, 0, 0, 0, 0, 0, 0};

ℬfar = {0, 0, 0, 0, 0, 0, 0, 0};

Do[ℬface[[i]] = β[[i]] + Sum[ℬface[[n]] * bface[[n, i]], {n, i+1, m}], {i, m, 1, -1}]

Do[ℬfar[[i]] = β[[i]] + Sum[ℬfar[[n]] * bfar[[n, i]], {n, i+1, m}], {i, m, 1, -1}]
```

```
MatrixForm[ℬface];

MatrixForm[ℬfar];

ℳface = {1, 1, 1, 1, 1, 1, 1, 0};

ℳfar = {1, 1, 1, 1, 1, 1, 1, 0};

mm = m - 1;

Do[ℳface[[k]] = Sum[bface[[k, j]] * ℳface[[j]], {j, 1, k-1}], {k, 2, mm}]

Do[ℳfar[[k]] = Sum[bfar[[k, j]] * ℳfar[[j]], {j, 1, k-1}], {k, 2, mm}]

MatrixForm[ℳface];

MatrixForm[ℳfar];

𝒜face = Table[0, {i, 1, m}, {j, 1, m}];

𝒜far = Table[0, {i, 1, m}, {j, 1, m}];

Do[Do[𝒜face[[i, k]] =
    aface[[i, k]] + Sum[aface[[i, j]] * 𝒜face[[j, k]], {j, k+1, i-1}], {k, 1, i}],
 {i, 2, m}]

Do[Do[𝒜far[[i, k]] =
    afar[[i, k]] + Sum[afar[[i, j]] * 𝒜far[[j, k]], {j, k+1, i-1}], {k, 1, i}],
 {i, 2, m}]

MatrixForm[𝒜face];

MatrixForm[𝒜far];

𝒮face =
 Table[ℬface[[i]] * 𝒜face[[i, k]] * ℳface[[k]], {i, 1, m}, {k, 1, m}];

𝒮facelist = {𝒮face[[5, 2]], 𝒮face[[3, 2]], 𝒮face[[2, 1]],
  𝒮face[[8, 3]], 𝒮face[[7, 3]], 𝒮face[[8, 5]], 𝒮face[[6, 3]],
  𝒮face[[5, 3]], 𝒮face[[7, 4]], 𝒮face[[8, 7]], 𝒮face[[4, 3]],
  𝒮face[[7, 5]], 𝒮face[[6, 4]], 𝒮face[[6, 5]], 𝒮face[[7, 6]]};
```

```
Sfar =
 Table[Bfar[[i]] * Afar[[i, k]] * Mfar[[k]], {i, 1, m}, {k, 1, m}];

Sfarlist = {Sfar[[5, 2]], Sfar[[3, 2]], Sfar[[2, 1]],
  Sfar[[8, 3]], Sfar[[7, 3]], Sfar[[8, 5]], Sfar[[6, 3]],
  Sfar[[5, 3]], Sfar[[7, 4]], Sfar[[8, 7]], Sfar[[4, 3]],
  Sfar[[7, 5]], Sfar[[6, 4]], Sfar[[6, 5]], Sfar[[7, 6]]};

MatrixForm[Sface]
```

$$\begin{pmatrix} 0 & 0 & 0 & 0 & 0 \\ 0.0327291 & 0 & 0 & 0 & 0 \\ 0.00123994 & 0.0180442 & 0 & 0 & 0 \\ 2.69419\times10^{-6} & 0.0000392072 & 0.000716087 & 0 & 0 \\ 0.000474625 & 0.00690696 & 0.000435644 & 0 & 0 \\ 5.80632\times10^{-6} & 0.0000844963 & 0.0010589 & 0.0000135511 & 0.000573064 \\ 0.0000325451 & 0.000473611 & 0.00749862 & 0.00251773 & 0.00136239 \\ 0.00017048 & 0.00248091 & 0.0282069 & 0.000550729 & 0.0202376 \end{pmatrix}$$

```
MatrixForm[Sfar]
```

$$\begin{pmatrix} 0 & 0 & 0 & 0 & 0 \\ 0.00299268 & 0 & 0 & 0 & 0 \\ 5.44753\times10^{-6} & 0.00171211 & 0 & 0 & 0 \\ 8.06516\times10^{-10} & 2.5348\times10^{-7} & 0.0000978567 & 0 & 0 \\ 2.00382\times10^{-6} & 0.000629781 & 0.0000441729 & 0 & 0 \\ 1.31752\times10^{-9} & 4.14082\times10^{-7} & 0.00011019 & 1.50033\times10^{-6} & 0.0000581638 \\ 7.34319\times10^{-9} & 2.30789\times10^{-6} & 0.000776609 & 0.000279451 & 0.00013392 \\ 2.99246\times10^{-8} & 9.40502\times10^{-6} & 0.00223265 & 2.48152\times10^{-6} & 0.00163735 \end{pmatrix}$$

The following is to show an estimate of the uncorrected values ignoring summing-in and -out effects.

```
Bunface = Table[0, {i, 1, m}, {k, 1, m}];

Bunfar = Table[0, {i, 1, m}, {k, 1, m}];

Do[Do[Bunface[[i, k]] =
   β[[i]] + Sum[Bunface[[n, k]] * x[[n, i]], {i, m, 1, -1}],
 {k, 1, mm}]
```

```
Do[Do[Bunfar[[i, k]] =
    β[[i]] + Sum[Bunfar[[n, k]] * x[[n, i]], {i, m, 1, -1}],
  {k, 1, mm}]

Aunface = Table[0, {i, 1, m}, {j, 1, m}];

Aunfar = Table[0, {i, 1, m}, {j, 1, m}];

Do[Do[Aunface[[i, k]] = x[[i, k]] * epface[[i, k]] / (1 + a[[i, k]]), {k, 1, i}],
  {i, 2, m}]

Do[Do[Aunfar[[i, k]] = x[[i, k]] * epfar[[i, k]] / (1 + a[[i, k]]), {k, 1, i}],
  {i, 2, m}]

Munface = Table[1, {i, 1, m}, {k, 1, m}];

Munfar = Table[1, {i, 1, m}, {k, 1, m}];

Sunface = Table[Bunface[[i, k]] * Aunface[[i, k]] * Munface[[i, k]],
  {i, 1, m}, {k, 1, m}];

Sunfacelist = {Sunface[[5, 2]], Sunface[[3, 2]], Sunface[[2, 1]],
  Sunface[[8, 3]], Sunface[[7, 3]], Sunface[[8, 5]],
  Sunface[[6, 3]], Sunface[[5, 3]], Sunface[[7, 4]],
  Sunface[[8, 7]], Sunface[[4, 3]], Sunface[[7, 5]],
  Sunface[[6, 4]], Sunface[[6, 5]], Sunface[[7, 6]]};

Sunfar = Table[Bunfar[[i, k]] * Aunfar[[i, k]] * Munfar[[i, k]],
  {i, 1, m}, {k, 1, m}];

Sunfarlist = {Sunfar[[5, 2]], Sunfar[[3, 2]], Sunfar[[2, 1]],
  Sunfar[[8, 3]], Sunfar[[7, 3]], Sunfar[[8, 5]], Sunfar[[6, 3]],
  Sunfar[[5, 3]], Sunfar[[7, 4]], Sunfar[[8, 7]], Sunfar[[4, 3]],
  Sunfar[[7, 5]], Sunfar[[6, 4]], Sunfar[[6, 5]], Sunfar[[7, 6]]};
```

```
MatrixForm[Sunface]
```

0	0	0	0	0	0
0.0538442	0	0	0	0	0
0	0.030621	0	0	0	0
0	0	0.00195764	0	0	0
0	0.0111797	0.000868316	0	0	0
0	0	0.00213181	0.000030078	0.00115001	0
0	0	0.0144948	0.00553609	0.00263591	0.00141746
0	0	0.0405098	0	0.030298	0

```
MatrixForm[Sunfar]
```

0	0	0	0	0
0.00306984	0	0	0	0
0	0.00175886	0	0	0
0	0	0.000102735	0	0
0	0.000645226	0.0000457509	0	0
0	0	0.000114251	1.56328×10^{-6}	0.0000603035
0	0	0.000802424	0.000290621	0.00013838
0	0	0.00227496	0	0.00167219

The tables below compare the corrected and uncorrected peak count fraction--the fraction of decays that result in gamma rays depositing their full energy in the detector crystal and causing a count in the full energy peak.

```
Ratiofarlist = Sfarlist / Sunfarlist;
```

```
TableForm[Table[{Cs136gammas[[i]], Sunfarlist[[i]],
   Sfarlist[[i]], Ratiofarlist[[i]]}, {i, 1, 15}],
 TableHeadings -> {None, {"Gamma (Mev)",
    "Far, Uncrtd Peak Count", "Far, Crtd Peak Count", "Ratio"}},
 TableAlignments -> Center]
```

Gamma (Mev)	Far, Uncrtd Peak Count	Far, Crtd Peak Count
1.235362	0.000645226	0.000629781
1.048073	0.00175886	0.00171211
0.818514	0.00306984	0.00299268
0.507188	0.00227496	0.00223265
0.340547	0.000802424	0.000776609
0.319911	0.00167219	0.00163735
0.273646	0.000114251	0.00011019
0.187285	0.0000457509	0.0000441729
0.176602	0.000290621	0.000279451
0.166576	0.00164885	0.00158977
0.16392	0.000102735	0.0000978567
0.153246	0.00013838	0.00013392
0.109681	1.56328×10^{-6}	1.50033×10^{-6}
0.08636	0.0000603035	0.0000581638
0.066881	0.0000756209	0.0000720608

```
Ratiofacelist = Sfacelist / Sunfacelist;
```

```
TableForm[Table[{Cs136gammas[[i]], Sunfacelist[[i]],
   Sfacelist[[i]], Ratiofacelist[[i]]}, {i, 1, 15}],
 TableHeadings -> {None, {"Gamma (Mev)",
    "Face, Uncrtd Peak Count", "Face, Crtd Peak Count", "Ratio"}},
 TableAlignments -> Center]
```

Gamma (Mev)	Face, Uncrtd Peak Count	Face, Crtd Peak Count
1.235362	0.0111797	0.00690696
1.048073	0.030621	0.0180442
0.818514	0.0538442	0.0327291
0.507188	0.0405098	0.0282069
0.340547	0.0144948	0.00749862
0.319911	0.030298	0.0202376
0.273646	0.00213181	0.0010589
0.187285	0.000868316	0.000435644
0.176602	0.00553609	0.00251773
0.166576	0.0314223	0.0152555
0.16392	0.00195764	0.000716087
0.153246	0.00263591	0.00136239
0.109681	0.000030078	0.0000135511
0.08636	0.00115001	0.000573064
0.066881	0.00141746	0.000526783

```
AFTACεpds5sface =
 Table[εpds5sfacelist[[i]] * Ratiofacelist[[i]], {i, 1, 15}];
```

The table below shows the adjusted face peak efficiency that AFTAC could use in its ananlysis.

```
TableForm[Table[{Cs136gammas[[i]], εpds5sfacelist[[i]],
   Ratiofacelist[[i]], AFTACεpds5sface[[i]]}, {i, 1, 15}],
 TableHeadings -> {None, {"Gamma (Mev)",
    "Face Peak Eff.", "Ratio", "Adjusted Face Peak Eff."}},
 TableAlignments -> Center]
```

Gamma (Mev)	Face Peak Eff.	Ratio	Adjusted Face Peak
1.235362	0.0386214	0.617815	0.0238609
1.048073	0.0446167	0.589276	0.0262915
0.818514	0.0553363	0.607849	0.0336361
0.507188	0.0836701	0.696299	0.0582594
0.340547	0.11805	0.517333	0.0610711
0.319911	0.124615	0.667952	0.0832367
0.273646	0.145475	0.496714	0.0722595
0.187285	0.194743	0.501711	0.0977049
0.176602	0.202602	0.454786	0.0921407
0.166576	0.209505	0.485498	0.101714
0.16392	0.211293	0.36579	0.077289
0.153246	0.218379	0.516858	0.112871
0.109681	0.239159	0.450531	0.107749
0.08636	0.220971	0.498312	0.110113
0.066881	0.168048	0.371639	0.062453

```
AFTACεpfacelist = {.022025, .026148, .033183, 0, .074673, 0,
  .077396, 0, .18784, 0, .13263, .14242, 0, .11149, .071853};

RelDiff = Table[100 * (AFTACεpds5sface[[i]] - AFTACεpfacelist[[i]]) /
    AFTACεpfacelist[[i]],
  {i, 1, 15}];
```

```
TableForm[Table[{Cs136gammas[[i]], AFTACεpfacelist[[i]],
   AFTACεpds5sface[[i]], RelDiff[[i]]}, {i, 1, 15}],
 TableHeadings -> {None, {"Gamma (Mev)", "AFTAC Face Peak Eff.",
    "AFIT Face Peak Eff.", "Rel. % Diff"}},
 TableAlignments -> Center]
```

Gamma (Mev)	AFTAC Face Peak Eff.	AFIT Face Peak Eff.
1.235362	0.022025	0.0238609
1.048073	0.026148	0.0262915
0.818514	0.033183	0.0336361
0.507188	0	0.0582594
0.340547	0.074673	0.0610711
0.319911	0	0.0832367
0.273646	0.077396	0.0722595
0.187285	0	0.0977049
0.176602	0.18784	0.0921407
0.166576	0	0.101714
0.16392	0.13263	0.077289
0.153246	0.14242	0.112871
0.109681	0	0.107749
0.08636	0.11149	0.110113
0.066881	0.071853	0.062453

The following section is the error in the internal conversion coefficients and gamma-ray intensities. Unfortunately, the reference **(Tuli, 1979)** is missing a large portion of them and precludes a meaningful error analysis.

```
σa = {{0, 0, 0, 0, 0, 0, 0, 0}, {0, 0, 0, 0, 0, 0, 0, 0},
   {0, 0, 0, 0, 0, 0, 0, 0}, {0, 0, 0, 0, 0, 0, 0, 0},
   {0, 0, 0.016, 0, 0, 0, 0, 0}, {0, 0, 0.004, 0.07, 0, 0, 0, 0, 0},
   {0, 0, 0, 0.046, 0, 0.002, 0, 0}, {0, 0, 0.0017, 0, 0.0022, 0, 0, 0}};

σi = {{0, 0, 0, 0, 0, 0, 0, 0},
   {0, 0, 0, 0, 0, 0, 0, 0}, {0, 0.03, 0, 0, 0, 0, 0, 0},
   {0, 0, 0.0012, 0, 0, 0, 0, 0}, {0, 0.007, 0.0004, 0, 0, 0, 0, 0},
   {0, 0, 0.004, 0.0003, 0.002, 0, 0, 0},
   {0, 0, 0.013, 0.004, 0.0018, 0.002, 0, 0},
   {0, 0, 0.0003, 0, 0.0005, 0, 0.004, 0}};
```

Appendix E: AFIT Experimental Data

In an attempt to quantify what percentage of gamma-rays that are scattered into the detector due to the presence of the planchet, measurements were made at the AFIT Nuclear Engineering Laboratory using Cs-137 in the form of a thin disk source. The isotope is a single gamma-ray emitter of 662 keV. Because of this property, the isotope is ideal for determining the peak-to-total (P/T) efficiency ratio for energies near 662 keV. Since the analytical method uses the P/T ratio in determining summing events, a change in the P/T ratio will have a direct affect on the results. Even though the scattered gamma-rays will not register counts in their full energy peaks, they can add to total detection efficiency. The increased total efficiency would then lower the P/T ratio.

The intent is to get a rough estimate in the change of the face peak efficiency for the key Mo-99 gamma-ray, the 740 keV one. So, noting the change in the P/T ratios from Appendix C between 662 and 740 keV is minor, the reduction in the 662 keV P/T ratio suggests a similar reduction in the 740 keV P/T ratio—ergo, a reduction in the AFIT face peak efficiency. See the experimental data in Table E.1.

Table E.1 AFIT Experimental Data

			Measure-ment without planchet			
Source	**Serial Number**	**Height above Det #01**	**Date**	**Dead Time**	**Live Time**	**Real Time**
Cs-137	1S811	30 cm	5 Sep 97	5.48%	120 sec	126 sec
	662 keV peak				**Total Spectrum**	
Left Margin	**Right Margin**	**Peak Center**	**Total Peak Counts**	**Left Margin**	**Right Margin**	**Total Counts**
1797	1718	1807	42045	47	1817	160413
P/T =	$\frac{42045}{160413}$		**Error =**	0.00144		
	=.2621					
			Measure-ment with planchet			
Source	**Serial Number**	**Height above Det #01**	**Date**	**Dead Time**	**Live Time**	**Real Time**
Cs-137	1S811	30 cm	5 Sep 97	5.62%	120 sec	127 sec
	662 keV peak				**Total Spectrum**	
Left Margin	**Right Margin**	**Peak Center**	**Total Peak Counts**	**Left Margin**	**Right Margin**	**Total Counts**
1797	1817	1807	42372	48	1817	165432
P/T =	$\frac{42372}{165432}$		**Error =**	0.00139		
	=.2561					
ratio:	$\frac{w/pcht}{w/o}$	= $\frac{.2561}{.2622}$	= 0.977		**Error =**	0.0075

From the analysis of the experiment, a 2 to 3% reduction appears in the peak-to-total counts when placing the planchet above the source. Thus, there should be a reduction in the adjusted AFIT face peak efficiency. The errors were found using Equations E-1 through E-3.

$$P/T = \frac{\text{PeakCounts(CP)}}{\text{TotalCounts(CT)}} \qquad \text{(E-1)}$$

$$\sigma^2_{p/t} = \left(\frac{\partial P/T}{\partial CP}\right)^2 \sigma^2_{cp} + \left(\frac{\partial P/T}{\partial CT}\right)^2 \sigma^2_{ct} \qquad \text{(E-2)}$$

$$\sigma_{p/t} = \left[\frac{CP}{CT^2} + \frac{CP^2}{CT^3}\right]^{1/2} \qquad \text{(E-3)}$$

Appendix F: Bibliography

AFTAC. "Technical Memorandum 96-12: Face Efficiencies Calibrated from Galaxy Thermal Calibrations 95-20 and 96-20." 9 January 1997.

Andreev, D.S., K.I. Erokhina, V.S. Zvonov, and I.Kh. Lemberg. "Consideration of Cascade Transitions in Determining the Absolute Yield of Gamma Rays," Instruments and Experimental Techniques, 15: 1358-1360 (1972).

Bailar, J.C. Jr. and others. Comprehensive Inorganic Chemistry. New York: Pergamon Press. pp.735-738. 1973.

Brookhaven National Laboratory. "XRAY Database." n. pag. TELNET bnlnd2.dne.bnl.gov. 23 July 1997.

Camp, D.C., and A.L. Van Lehn. "Finite Solid-Angle Corrections for Ge(Li) Detectors," Nuclear Instruments and Methods, 76: 192-240 (1969).

Canberra, Inc.. Canberra Nuclear Products. (Ninth Edition). pp. 91. 1992.

Canberra, Inc.. Detector #120 Specification and Performance Data. 1995.

Evans, R.D.. The Atomic Nucleus. New York: McGraw Hill. pp. 232-243. 1967.

Ferguson, A.J.. Angular Correlation Methods in Gamma-Ray Spectroscopy. New York: North-Holland. 1965.

Friedlander, G. and others. Nuclear and Radiochemistry. (Third Edition). New York: John Wiley & Sons. pp. 476-478 (1981).

Gardulski, P.L., and M.L. Wiedenbeck. "Multipole Mixing Ratios of Transitions in Tc-99," Physical Review C, 9 (1): 262-265 (1974).

Heath, R.L.. Scintillation Spectrometry: Gamma-Ray Spectrum Catalogue, Vol. 1. (Second Edition). 1964.

ICRP. Publication 38, Radionuclide Transformations: Energy and Intensity of Emissions. New York: Pergamon Press. 1983.

Kolotov, V.P. and others. "Testing of Different True Coincidence Correction Approaches for Gamma-Ray Spectrometry of Voluminous Sources." MARC IV Conference. Log No. 97-62. April 1997.

Knoll, G.F.. Radiation Detection and Measurement. (Second Edition). New York: John Wiley & Sons. pp. 402. 1989.

McCallum, G.J. and G.E. Coote. "Influence of Source-Detector Distance on Relative Intensity and Angular Correlation Measurements with Ge(Li) Spectrometers," Nuclear Instruments and Methods, 130: 189-197 (1975).

Peker, L.K., Editor. "Nuclear Data Sheets Update for A = 99," Nuclear Data Sheets, 73 (1): 34-43 (1994).

Singh, M.. "An Electronically Collimated Gamma Camera for Single Photon Emission Computed Tomography. Part 1: Theoretical Considerations and Design Criteria," Medical Physics, 10 (4): 421-427 (1983).

Tuli, J.K., Editor. "Nuclear Data Sheets for A = 136," Nuclear Data Sheets, 52 (2): 311 (1987).

Turner, J.E.. Atoms, Radiation, and Radiation Protection. (Second Edition). New York: John Wiley & Sons. pp.524. 1995.

Tsoulfanidis, N.. Measurement and Detection of Radiation. New York: Hemisphere Publishing Corporation. pp. 149. 1983.

Appendix G: Vita

Anthony P. Popovich graduated from the University of Florida receiving a Bachelor of Science in Nuclear Engineering in 1988. He started his first assignment at the Oklahoma City Air Logistics Center, Tinker AFB, serving as a Survivability/Vulnerability engineer. He developed the Single Point Excitation for Hardness Surveillance (SPEHS) device currently testing the E-4 and AF-1. His work has been published in the Defense Nuclear Agency's Nuclear Survivability Journal. During this first assignment, Capt. Popovich attended classes at and graduated from the University of Oklahoma in 1993 receiving a Masters of Public Administration. He then moved to his next assignment at Holloman AFB, NM serving as the Deputy Branch Chief of Plans and Programs of the 46th Test Group. There Capt. Popovich assisted the commander and staff in managing test facility, financial, and human resources. Capt. Popovich was directly in charge of the Group's T&E Base Realignment And Closure (BRAC) response team, the Major Range and Test Facility Base (MRTFB) program, the Small Business Innovation Research (SBIR) program, and the Quality Air Force program. In 1996, he departed Holloman AFB to pursue a Master's of Nuclear Engineering degree at the Air Force Institute of Technology, Wright-Patterson AFB, OH.

REPORT DOCUMENTATION PAGE

Form Approved
OMB No. 0704-0188

1. AGENCY USE ONLY *(Leave blank)*	2. REPORT DATE	3. REPORT TYPE AND DATES COVERED
	December 1997	Master's Thesis

4. TITLE AND SUBTITLE
AN ANALYTICAL METHOD TO CALCULATE ACTIVITY FROM MEASUREMENTS AFFECTED BY COINCIDENCE SUMMING

5. FUNDING NUMBERS

6. AUTHOR(S)
Anthony P. Popovich, Captain, USAF

7. PERFORMING ORGANIZATION NAME(S) AND ADDRESS(ES)
Air Force Instittute of Technology
2750 P Street
WPAFB OH 45433-7765

8. PERFORMING ORGANIZATION REPORT NUMBER
AFIT/GAP/ENP/97D-09

9. SPONSORING/MONITORING AGENCY NAME(S) AND ADDRESS(ES)
AFTAC/TOD
6000 Patrol Road
McClellan AFB CA 95652-6437
POC: Captain Nathan Wimer

10. SPONSORING/MONITORING AGENCY REPORT NUMBER

11. SUPPLEMENTARY NOTES

12a. DISTRIBUTION AVAILABILITY STATEMENT
Approved for public release; distribution unlimited

12b. DISTRIBUTION CODE

13. ABSTRACT *(Maximum 200 words)*

An analytical method is developed and applied to find the activities of two radioisotopes based on measurements influenced by true coincidence summing. The method incorporates the solid angle subtended by the detector, the macroscopic cross sections of the materials present, the absolute peak and total efficiencies of the detector, and the modes and probabilities of decay of the radioisotope. With this information, the method corrects for both summing-in and summing-out events. Summing events affect peak counts and cause the calculated activity to differ from the true activity.

Thin disk sources of Mo-99 and Cs-136 on the face of a closed-end, coaxial high purity germanium detector have been studied. For Mo-99, the analytical method shows there is a 29% reduction in the 740 keV peak counts due to summing events. This factor adjusts the no-coincidence-assumed activity to within 4.0% of the correct value. As for Cs-136, the analytical method shows a 41% reduction in the 1048 keV peak counts. This factor corrects the simplistic activity to within 0.5% of the correct value. Hence, the results indicate that coincidence summing is the primary cause of activity discrepancies for the given configuration.

14. SUBJECT TERMS	15. NUMBER OF PAGES
COINCIDENCE COUNTING	198
	16. PRICE CODE

17. SECURITY CLASSIFICATION OF REPORT	18. SECURITY CLASSIFICATION OF THIS PAGE	19. SECURITY CLASSIFICATION OF ABSTRACT	20. LIMITATION OF ABSTRACT
UNCLASSIFIED	UNCLASSIFIED	UNCLASSIFIED	UL